DISSERTATION

# SALT TRANSPORT AND LOADING IN TILE-DRAINED WATERSHEDS: OBSERVATIONS, MODELING, AND MANAGEMENT

Submitted by

Haider Addab

Department of Civil and Environmental Engineering

In partial fulfillment of the requirements

For the Degree of Doctor of Philosophy

Colorado State University

Fort Collins, Colorado

Spring 2022

Doctoral Committee:

Advisor: Ryan T. Bailey

Neil Grigg
Mazdak Arabi
Jordan Suter

ABSTRACT

SALT TRANSPORT AND LOADING IN TILE-DRAINED WATERSHEDS: OBSERVATIONS, MODELING, AND MANAGEMENT

Salinity in soil water, groundwater, and surface water is a critical issue for food security worldwide. Approximately 20% of total cultivated lands and 33% of irrigated lands worldwide are affected by high salinity, and increasing in many regions of the world, such as the western United States, eastern Australia, the Middle East, China, and north and east Africa. To combat this issue, artificial subsurface drains often are used to remove excess soil water, groundwater, and associated salt from waterlogged, saline-affected cultivated fields. However, the benefits of removing salt from these cultivated areas are often tempered by negative impacts on the water quality of receiving waters, leading to poor growing conditions downstream, as downstream users divert the saline water for irrigation purposes. Increased downstream salinity can also be a detriment to environmental systems and receiving water bodies due to eutrophication. Due to these secondary effects of subsurface drainage, there is a need to study the storage, transport, and transformation of salt species in artificially drained systems and quantify the relative effects on downstream areas. This assessment should be performed within the context of potential management practices (e.g. drainage depth, drainage material conductance) and climate extremes (drought, wet periods).

The overall objective of this dissertation is to understand the impact of subsurface drainage systems `on salt movement and loading in an irrigated, drained stream-aquifer system. This objective is accomplished by a suite of numerical modeling experiments applied to the stream-aquifer system that encompasses the Fairmont Drainage District (FDD; 385-ha) tile drain network within the Lower Arkansas River Valley, Colorado, USA. The numerical models used in this dissertation simulate the reactive

transport of major salt ions ($SO_4$, Ca, Na, Cl, Mg, K, $CO_3$, and $HCO_3$) in soils, groundwater, tile drain water, and streams.

This dissertation first presents the use of the SWAT-Salt model, a new version of the SWAT model that includes a salinity reactive transport module and modified in this study to include salt ion transport in tile drain water, applied it to a 732 $km^2$ salinity-impaired irrigated region within the Lower Arkansas River Valley. The tool, tested against tile drain salt ion concentrations in the FDD, is used to assess the impact of region-wide implementation of subsurface tile drainage on in-stream salt ion concentrations, in-stream salt ion loading, and total salt export from the watershed. Results indicate that implementing region-wide tile drainage increases total salt yield from the watershed by only 1% during a long simulation period (2000-2018). The increase in salt loaded from the landscape to stream via tile drains is balanced by the decrease in groundwater loading, as the salt mass that would be transported in the aquifer is instead intercepted by the tile drains.

To provide a more realistic simulation of salt transport in tile drained stream-aquifer systems, the second study uses the groundwater flow model MODFLOW and the groundwater reactive transport model RT3D-Salt, modified in this study to include salt ion mass exchange between the aquifer and the tile drains, at grid cells designated as drainage cells. Model results are tested against measured groundwater levels, groundwater salt ion concentrations, and estimated tile outflow and tile salt ion loading. Results indicate the following: i) the model tracks groundwater levels and tile drain outflow well; however, groundwater levels were available for 2015-2018 whereas tile drain outflow rates were available only for 3 months during the 2018 growing season, due to equipment failure. Additional tile drain outflow rate measurements are needed to perform a thorough audit of the MODFLOW model; and ii) including tile drainage in this area only slightly improved soil salinity and crop yield conditions; however, export loading from the drains has a strong negative impact on the water quality of receiving waters. Timpas Creek, a tributary to the Arkansas River, experiences an overall increase of approximately

200 mg/L in the areas immediately downstream of the tile drain outflow point. If the tile drains loaded to the Arkansas River, the downstream concentration increase would be approximately 85 mg/L. These increases can have detrimental impacts on downstream crop yield, if river water is diverted and used as irrigation water, and ecosystem health.

In the third study, the calibrated and tested MODFLOW/RT3D-Salt modeling system for the FDD region is used to quantify the impacts of climate extremes and management strategies on salt transport and consequent system variables in the FDD. These impacts include direct model results: water table depth, groundwater discharge to tile drains, groundwater salt loading to tile drains, and soil salinity; and impacts derived from model output: 1) relative yield and 2) the salt concentration of waters receiving tile outflow. Climate extremes include periodic drought and periodic wet conditions; drainage management features include drainage depth (shallow, deep) and drain material conductance (high, low). Combined climate-management scenarios also are run. Results indicate that i) drainage depth has a much stronger impact on drainage outflow volumes and salt loading mass than extreme climate conditions or drain material conductance; ii) climate conditions (drought, wet conditions) have a much stronger impact on soil salinity and crop yield than drainage management schemes (drainage depth, drain material conductance). Therefore, future climate extremes likely will play a larger role in the viability of tile drain systems than will the specific characteristics (e.g., depth) of the tile drain network; and iii) scenarios with high drainage outflow volumes and salt loading mass (e.g. deep drains, deep drains + wet conditions) result in lower downstream salinity concentrations than scenarios with low outflow volumes and salt loading mass, due to the dilution effect of higher water volumes on salt mass in the tile drainage water. Therefore, if new tile drain networks are being installed, we recommend using a deep drainage scheme (1.52 m) as opposed to the regular depth of 1.22 m, to minimize the effect on downstream salinity concentration.

Results of this dissertation can be used in other tile drained landscapes to guide tile network design. Methods used herein can be adopted for other tile drain studies that use numerical models as experimental tools. In general, the modeling system (MODFLOW/RT3D-Salt) introduced in this dissertation can be used to assist with salinity management schemes in saline-affected tile drained regions, to balance crop yield sustainability and downstream water quality needs.

TABLE OF CONTENTS

ABSTRACT ........ ii

CHAPTER 1 - INTRODUCTION AND OBJECTIVES ........ 1

1.1 Introduction ........ 1

1.2 Dissertation objectives ........ 3

REFERENCES ........ 5

CHAPTER 2 - SIMULATING THE EFFECT OF SUBSURFACE TILE DRAINAGE ON WATERSHED SALINITY USING SWAT ........ 8

2.1 Introduction ........ 8

2.2 Swat-salt model with tile drainage ........ 10

2.2.1 Overview of the swat model ........ 10

2.2.2 Overview of the swat-salt model ........ 11

2.2.3 Modifying swat-salt to include tile drain salinity transport ........ 13

2.3. Swat-salt application to a saline tile drained region ........ 14

2.3.1 Study region: lower Arkansas river valley, Colorado ........ 14

2.3.2 Study site and data collection: fairmont drainage district ........ 15

2.3.3 Simulating salinity transport in the Fairmont drainage district ........ 17

2.3.4 Simulating effects of region-wide implementation of tile drainage ........ 20

2.3.5 Results and discussion ........ 20

2.3.5.1 Tile drain network ........ 20

2.3.5.2 Impacts of tile drains on region-wide salinity transport ........ 22

2.4. Limitations of using swat-salt for salt transport in tile drained regions ........ 28

2.5 Summary and conclusions ........ 29

REFERENCES ........ 32

CHAPTER 3 – QUANTIFYING THE IMPACT OF TILE DRAINS ON SALINITY TRANSPORT IN IRRIGATED SEMI-ARID REGIONS ........ 36

3.1 Introduction ........ 36

3.2 Methods ........ 38

3.2.1 Study region ........ 39

3.2.2 Field data collection ........ 41

3.2.2.1 Groundwater levels and salt concentration ........ 41

3.2.2.2 Tile drain outflow and concentration....42
3.2.3 Simulating salinity transport in an aquifer-drain system....42
3.2.3.1 Groundwater storage and interactions: MODFLOW....43
3.2.3.2 Salt ion fate and transport: RT3D-salt....45
3.2.3.3 Aquifer-drain salt ion mass exchange....47
3.2.4 Simulation overview....48
3.2.5 System analysis and scenarios....48
3.3. Results and discussion....49
3.3.1 Hydrologic results....49
3.3.1.1 Groundwater levels....49
3.3.1.2 Tile flow....52
3.3.1.3 Comparison without drains....54
3.3.2 Salt ion results....55
3.3.3 The influence of tile drains....59
3.3.3.1 Within system: crop yield....59
3.3.3.2 Outside of system: impact on downstream water quality....61
3.3.4 Limitations of this study....62
3.3.5 Comparison between swat-salt and rt3d -salt....64
3.4. Summary and Conclusions....65
REFERENCES....67
CHAPTER 4 - QUANTIFYING THE IMPACT OF CLIMATE EXTREMES AND LAND MANAGEMENT PRACTICES ON CROP YIELD AND SALT LOADING WITHIN A TILE DRAINED CATCHMENT....71
4.1 Introduction....71
4.2 Methods....72
4.3 Quantifying impact of climate extremes and management strategies....72
4.4 Results and Discussion....75
4.5 Groundwater discharge and salt loading to tile drains....76
4.6 System effects: relative yield, concentration of receiving waters....79
4.7 Summary of climate and management impacts: assessment of metrics....84
4.8 Study limitations....86
4.9 Summary and Conclusions....87
REFERENCES....89
CHAPTER 5 – SUMMARY AND CONCLUSIONS....91

5.1 Summary and major findings....................91
5.2 Filling method gaps and future research....................95

# CHAPTER 1 - INTRODUCTION AND OBJECTIVES

## 1.1 Introduction

Salinity in soil water, groundwater, and surface water is a critical issue for food security worldwide. Approximately 20% of total cultivated lands and 33% of irrigated lands worldwide are affected by high salinity (Ghassemi et al., 1995, Shirvastava et al., 2014), and increasing in many regions of the world, such as the western United States, eastern Australia, the Middle East, China, and north and east Africa (Abbas et al., 2013; Ivushkin et al., 2019). Within irrigated regions, elevated levels of soil salinity often result from dissolution of salt minerals, salt loading from irrigation water application, upflux of saline shallow groundwater into the soil profile and root zone, and, within arid and semi-arid regions, overall inadequate drainage that leads to evapo-concentration (Morway and Gates, 2012). These elevated salinity levels often lead to a reduction in plant transpiration and seasonal crop yield.

Artificial subsurface drains often are used to remove excess soil water, groundwater, and associated salt from waterlogged, saline-affected cultivated fields (Hornbuckle et al., 2007; Rhoades et al., 1997; Ritzema et al., 2008; Hopkins et al., 2012; Feng et al., 2017; Tiwari et al., 2017). However, the benefits of removing salt from these cultivated areas are often tempered by negative impacts on the water quality of receiving waters, leading to poor growing conditions downstream, as downstream users divert the saline water for irrigation purposes (Cristen et al., 2001; Gill et al., 2015). Increased downstream salinity can also be a detriment to environmental systems and receiving water bodies due to eutrophication. Due to these secondary effects of subsurface drainage, there is a need to study the storage, transport, and transformation of salt species, e.g. major salt ions (sulfate $SO_4$, calcium Ca, sodium Na, chloride Cl, magnesium Mg, potassium K, carbonate $CO_3$, bicarbonate $HCO_3$) in artificially drained systems and quantify the relative effects on downstream areas. This assessment should be performed within the context of potential management practices (e.g. drainage depth, drainage material conductance) and climate extremes (drought, wet periods). As discussed by Qian et al. (2021), while many studies have addressed studying and optimizing drain parameters for water outflow, relatively few studies have investigated parameters for salinity discharge.

While many field studies have been performed to investigate the influence of drains on soil salinity, salt loading, and crop yield (Cristen et al., 2001; Horbuckle et al., 2005; Jafari-Talukolaee et al., 2015; Okuda et al., 2020; El-Ghannam et al., 2021), spatially distributed, physically based hydrological and contaminant transport models can be valuable tools to 1) quantify salt movement within artificially drained landscapes that include surface-soil interactions, soil-groundwater interactions, groundwater-surface water interactions, and groundwater-drain interactions; and 2) explore the impact of management practices and climate extremes on these interactions. Furthermore, temporally-refined models (e.g. daily time steps) can be used to quantify water and salt yield from the drained catchments over long time periods. Many studies have investigated the influence of drainage and drainage parameters on soil salinity and salt loading, using either hypothetical systems or existing drainage layouts (Yao et al., 2017; Lu et al., 2019; Qian et al., 2021; Liu et al., 2021). These studies, however, focus on field-scale effects of drains on soil water, soil salinity, and crop yield. There is a need to employ models at larger spatial scales to include system-wide salt storage, transport, groundwater-drain salt loading, and salt loading to downstream receiving waters, exploring the balance between beneficial within-system impacts (i.e. decrease soil salinity → improve crop yield) and negative downstream effects (i.e. increased salt loading in surface water).

### 1.2 Dissertation objectives

The overall objective of this dissertation is to understand the impact of subsurface drainage systems on salt movement and loading in an irrigated, drained stream-aquifer system. This objective is accomplished by the following three sub-objectives, with each sub-objective comprising a dissertation chapter. Each sub-objective uses as a study region the Lower Arkansas River Valley (LARV) in southeastern Colorado, and specifically the Fairmont Drainage District (FDD) near the town of Swink, Colorado.

1. **Chapter 2**: Investigate the impact of subsurface tile drains on watershed-wide salinity loading in a semi-arid region. This is accomplished by modifying the SWAT-Salt model to include tile drain salt loading and applying it to a 732 $km^2$ region of the LARV, part of which is tile drained. The model is tested against tile drain outflow salt ion concentrations.
2. **Chapter 3**: Assess spatially refined transport and mass balance of salt ions in a tile drained catchment and the influence of salt loading on receiving waters. This is accomplished by applying the MODFLOW and UZF-RT3D groundwater flow and transport models to a 17 $km^2$ tile drainage district in the LARV. The model is tested against a suite of groundwater and tile drainage flow and salt ion concentration data.
3. **Chapter 4**: Quantify the impact of climate extreme and drain management practices on soil salinity, crop yield, and salt loading from a tile drained catchment. The MODFLOW and UZF-RT3D models from Chapter 3 will be used in conjunction with climate scenarios to explore the impact of drain management schemes (drain depths, drain material conductance) on tile outflow, tile salinity loading, soil salinity, and crop yield, to quantify the ratio between beneficial aspects (increase in crop yield) and negative aspects (salt concentration of receiving waters).

**Chapter 5** provides a summary of results, conclusions, and future work. Chapter 2 has been published in *Agricultural Water Management*: "Simulating the effect of subsurface tile drainage on watershed salinity using SWAT" (Addab and Bailey, 2022). Chapters 3 and 4 will be combined into a single journal article and submitted to *Journal of Hydrology*.

REFERENCES


Addab, H. and Bailey, R. T. (2022), Simulating the effect of subsurface tile drainage on watershed salinity using SWAT", Agriculture Water Management, 262. https://doi.org/10.1016/j.agwat.2021.107431.

Abbas, G., Saqib, M., Rafique, Q., Rahman, A. U., Akhtar, J., Haq, M. A. U., & Nasim, M. (2013). Effect of salinity on grain yield and grain quality of wheat (Triticum aestivum L.). Pak J Bot, 50, 185-189.

Christen EW, Ayars JE, Hornbuckle JW. Subsurface drainage design and management in irrigated areas of Australia. Irrigation Science. 2001 Dec 1;21(1):35-43.

El-Ghannam, M., Aiad, M. and Abdallah, A., 2021. Irrigation efficiency, drain outflow and yield responses to drain depth in the Nile delta clay soil, Egypt. Agricultural Water Management, 246, p.106674.

Feng, G., Zhang, Z., Wan, C., Lu, P. and Bakour, A., 2017. Effects of saline water irrigation on soil salinity and yield of summer maize (Zea mays L.) in subsurface drainage system. Agricultural water management, 193, pp.205-213.

Ghassemi, F., Jakeman, A.J., and Nix, H.A. Salinisation of Land and Water Resources. University of New South Wales Press Ltd, Canberra, Australia. (1995)

Gill BC, Terry AD. 'Keeping salt on the farm'—Evaluation of an on-farm salinity management system in the Shepparton irrigation region of South-East Australia. Agricultural Water Management. 2016 Jan 31;164:291-303.

Hopkins, D., Chambers, K., Fraase, A., He, Y., Larson, K., Malum, L., Sande, L., Schulte, J., Sebesta, E., Strong, D. and Viall, E., 2012. Evaluating salinity and sodium levels on soils before drain tile installation: A case study. Soil Horizons, 53(4), pp.24-29.

Hornbuckle, J.W., Christen, E.W., Ayars, J.E. and Faulkner, R.D., 2005. Controlled water table management as a strategy for reducing salt loads from subsurface drainage under perennial agriculture in semi-arid Australia. Irrigation and Drainage Systems, 19(2), pp.145-159.

Hornbuckle, J.W., Christen, E.W. and Faulkner, R.D., 2007. Evaluating a multi-level subsurface drainage system for improved drainage water quality. Agricultural water management, 89(3), pp.208-216.

Ivushkin, K., Bartholomeus, H., Bregt, A.K., Pulatov, A., Kempen, B. and De Sousa, L., 2019. Global mapping of soil salinity change. Remote sensing of environment, 231, p.111260.

Jafari-Talukolaee M, Shahnazari A, Ahmadi MZ, Darzi-Naftchali A. Drain discharge and salt load in response to subsurface drain depth and spacing in paddy fields. Journal of Irrigation and Drainage Engineering. 2015 Nov 1;141(11):04015017.

Liu, Y., Ao, C., Zeng, W., Kumar Srivastava, A., Gaiser, T., Wu, J. and Huang, J., 2021. Simulating water and salt transport in subsurface pipe drainage systems with HYDRUS-2D. Journal of Hydrology, 592, p.125823.

Lu, P., Zhang, Z., Sheng, Z., Huang, M. and Zhang, Z., 2019. Assess Effectiveness of Salt Removal by a Subsurface Drainage with Bundled Crop Straws in Coastal Saline Soil Using HYDRUS-3D. Water, 11(5), p.943.

Morway, E. D. and Gates, T. K.: Regional assessment of soil water salinity across an intensively irrigated river valley, J. Irrig. Drain. E., 138, 5, 393–405, https://doi.org/10.1061/(ASCE)IR.1943-4774.0000411, 2012.

Okuda, Y., Onishi, J., Shirokova, Y., Kitagawa, I., Kitamura, Y. and Fujimaki, H., 2020. Water and Salt Balance in Agricultural Lands under Leaching with Shallow Subsurface Drainage Used in Combination with Cut-Drains. Water, 12(11), p.3207.

Qian, Y., Zhu, Y., Ye, M., Huang, J. and Wu, J., 2021. Experiment and numerical simulation for designing layout parameters of subsurface drainage pipes in arid agricultural areas. Agricultural Water Management, 243, p.106455.

Rhoades, J.D., Lesch, S.M., LeMert, R.D. and Alves, W.J., 1997. Assessing irrigation/drainage/salinity management using spatially referenced salinity measurements. Agricultural Water Management, 35(1-2), pp.147-165.

Ritzema, H.P., Satyanarayana, T.V., Raman, S. and Boonstra, J., 2008. Subsurface drainage to combat waterlogging and salinity in irrigated lands in India: Lessons learned in farmers' fields. Agricultural water management, 95(3), pp.179-189.

Shrivastava, P., & Kumar, R. (2015). Soil salinity: A serious environmental issue and plant growth promoting bacteria as one of the tools for its alleviation. Saudi journal of biological sciences, 22(2), 123–131. https://doi.org/10.1016/j.sjbs.2014.12.001

Tiwari, P. and Goel, A., 2017. An overview of impact of subsurface drainage project studies on salinity management in developing countries. Applied Water Science, 7(2), pp.569-580.

Yao, R., Yang, J., Wu, D., Xie, W., Wang, X. and Zhang, X., 2017. Scenario Simulation of Field Soil Water and Salt Balances Using SahysMod for Salinity Management in a Coastal Rainfed Farmland. Irrigation and Drainage, 66(5), pp.872-883.

# CHAPTER 2 - SIMULATING THE EFFECT OF SUBSURFACE TILE DRAINAGE ON WATERSHED SALINITY USING SWAT

## 2.1 Introduction

Salinity in soil water, groundwater, and surface water is a critical issue for food security worldwide. Approximately 20% of total cultivated lands and 33% of irrigated lands worldwide are affected by high salinity (Ghassemi et al., 1995, Shirvastava et al., 2014), and remain threatened in many regions of the world, such as the western United States, eastern Australia, the Middle East, China, and north and east Africa (Abbas et al., 2013). For irrigated regions, high soil salinity and associated decrease in crop yield are typically a result of Osmotic effect and toxicity effects, poor natural drainage, shallow water tables and waterlogging, and evapo-concentration in the root zone of crops (Morway and Gates, 2012). Salt minerals (e.g. gypsum $CaSO_4.2H_2O$, and calcite $CaCO_3$) in soils and parent rock are the origin of dissolved salt ions (Harrington et al., 2014), but then are transported through a watershed system, often concentrating in shallow soil zones in irrigated regions.

To combat rising water tables and associated evapo-concentration of salt ions in root zones, artificial subsurface drains often are installed to drain away excess soil water and groundwater (Hornbuckle et al., 2007; Rhoades et al., 1997; Ritzema et al., 2008; Hopkins et al., 2012; Feng et al., 2017; Tiwari et al., 2017). However, tile drains also serve as an artificial route of salt mass from the landscape to receiving water bodies, thereby increasing salt export from the drained areas (Christen et al., 2001; Okuda et al., 2020). While salt removal is beneficial for the tiled area, salt loads exported via the tile drains to streams can lead to poor growing conditions downstream, as downstream users divert the saline water for irrigation purposes (Christen et al., 2001; Gill et al., 2015). Increased downstream salinity can also be a detriment to environmental systems and receiving water bodies due to eutrophication. Due to these secondary effects of subsurface drainage, there is a growing need to study the storage, transport, and transformation of major salt ions (sulfate $SO_4$, calcium Ca, sodium Na, chloride Cl, magnesium Mg, potassium K, carbonate $CO_3$, bicarbonate $HCO_3$) in a tile drained system as it relates to salt export, salinity in receiving water bodies, and effects on downstream areas. This assessment should be performed within the context of potential management practices (e.g. drain diameter, distance between drains, depth to drains) and a changing climate.

Many studies have investigated the influence of subsurface drainage and subsurface drainage system parameters (spacing, depth, pipe size) on soil salinity and salt loading. Several studies use existing tile drain layouts, while others explore hypothetical scenarios of drain implementation. Study methods include field experiments, laboratory experiments, numerical modeling experiments, and combinations of these. Field studies (Cristen et al., 2001; Horbuckle et al., 2005; Jafari-Talukolaee et al., 2015; Okuda et al., 2020; El-Ghannam et al., 2021) have focused on the effect of system design (drain spacing, drain depth, controlled drainage) on soil salinity build-up, crop yield, and tile drain salt loading, demonstrating the effect of tile drains on increasing salt loading from tile drained areas.

Modeling studies have mainly focused on field-scale experiments of subsurface drainage and its relation to soil salinity. Yao et al. (2017) used a water and salt balance model, SahysMod, to simulate salt balances and field soil water under various scenarios and derive appropriate field management practices based upon the simulation results for a farmland in a coastal region of eastern China. Lu et al. (2019) used field experiments and HYDRUS-3D to simulate soil water flow and salt transport under the application of a drainage module in a field planted with maize straw, under a variety of leaching scenarios. Feng et al. (2019) using HYDRUS-2D to quantify the effect of irrigation water salinity and subsurface drainage depth on soil water-salt content and crop yield in an experimental field plot. Qian et al. (2021) used SWMS-2D, based on the HYDRUS model, to simulate salinity transport in a 2D cross-section of a subsurface drain system. The model size was 5 m depth, with a width equal to the spacing between two subsurface drains.

Liu et al. (2021) used HYDRUS-2D to test various boundary treatment for small-scale subsurface pipe drainage. Similar to Qian et al. (2021), they used a cross-section layout of a small-scale drained field. While these modeling studies have focused on field-scale effects of tile drains on soil water, soil salinity, and crop yield, there remains a need to quantify the influence of subsurface tile drains on system-wide salt storage, transport, and loading in a tile drained system, where the system is a network of tile drains. The system-wide assessment includes groundwater salinity, soil salinity, and tile drain salt loading. In addition, salinity should be decomposed into individual salt ions, to determine the relative magnitude of each and quantify their relative fate and transport as each are subject to distinct chemical reactions (e.g. precipitation-dissolution, complexation, cation exchange).

The objectives of this paper are to first, introduce a version of SWAT-Salt that simulates salt ion fate and transport in a tile drained, irrigated watershed; second, apply and test the model to an irrigated area with a network of connected tile drains; and third, use the model to investigate the impact of subsurface tile drains on watershed-wide salinity loading in a semi-arid region. The second objective is accomplished for the Fairmont Drainage District (15 $km^2$), located in the Lower Arkansas River Valley (LARV), Colorado. The third objective is accomplished for a salinity-impaired 732 $km^2$ region that encompasses the Fairmont Drainage District. The LARV has high salt concentration in soils, groundwater, irrigation canals, and river water, leading to a decrease in crop yield in recent decades (Morway and Gates, 2002). Previous studies (Xiaolu et al., 2018; Bailey et al., 2019) have constructed and tested SWAT and SWAT-Salt models in this region.

### 2.2 Swat-salt model with tile drainage

#### 2.2.1 Overview of the swat model

The SWAT (Soil and Water Assessment Tool) model (Arnold et al. 1998) is a physically based, comprehensive hydrologic simulation model for long-term predictions of water quality and hydrological impacts of alternative land management practices. SWAT offers a range of capabilities to address issues in agriculture, water, and environmental management, including water supply, irrigation systems, subsurface drainage systems, nutrient management, crop yield and food production, and climate change impacts. The model simulates water budgets, nutrient mass budgets, and sediment mass budgets at the watershed scale by considering climate, soil, topography, and land use. To prepare a SWAT model, the watershed is delineated into smaller subbasins, with each subbasin containing one surface water stream. Each subbasin is divided into multiple hydrologic response units (HRUs), with each HRU a unique combination of soil type, topographic slope class, and land use type within the subbasin. For each daily time step of the simulation, the water volume, nutrient mass, and sediment mass generated from each HRU via surface runoff, soil lateral flow, tile drain flow, and groundwater flow is calculated and routed to the subbasin stream. Each constituent is then routed through the watershed stream network towards the watershed outlet.

### 2.2.2 Overview of the swat-salt model

Whereas SWAT simulates the fate and transport of nutrient (nitrogen and phosphorus) species, pesticides, and sediment, the original code does not simulate the transport of salinity species, which in many semi-arid and arid regions of the world are the chemical species of concern in relation to soil health, crop growth, and general environmental health. Bailey et al. (2019) developed SWAT-Salt, a modified version of SWAT that includes a salinity module that simulates the fate and transport of eight major salt ions (sulfate $SO_4$, calcium Ca, magnesium Mg, sodium Na, potassium K, chloride Cl, carbonate $CO_3$, and bicarbonate $HCO_3$) in an irrigated watershed system. Equilibrium precipitation-dissolution reactions are included for five salt minerals ($CaCO_3$, $MgCO_3$, $CaSO_4$, $MgSO_4$, NaCl), which are simulated for each HRU soil layer and each HRU aquifer unit. Detailed salt ion equilibrium chemistry equations are provided in Bailey et al. (2019). The mass fate and transport of each salt ion in the soil system (i.e. HRU soil layers) and the aquifer system (HRU aquifer) is shown in the following equations. Using SO4 as an example, the mass balance (kg ha-1) in an HRU soil layer for a daily time step is formulated as:

$$\frac{dM_{SO_4,soil}}{dt} = M_{irrig,sw} + M_{irrig,gw} + M_{diss} - M_{precip} - M_{ro} - M_{lat} - M_{perc} + M_{revap} \qquad (1)$$

where M represents salt ion mass, irrig,sw represents salt ion mass in surface water irrigation; irrig,gw represents salt ion mass in groundwater irrigation; diss represents dissolution of salt minerals into salt ion mass (e.g. $CaSO_4 \rightarrow Ca + SO_4$); precip represents precipitation of salt minerals from dissolved salt ion mass; ro represents salt ion mass removed via surface runoff; lat represents salt ion mass removed via soil lateral flow; perc represents salt ion mass removed via percolation from the bottom of the soil layer; and revap represents salt ion mass added to the soil layer via upflux from the shallow aquifer. Salt ion mass removal in surface runoff occurs only for the top soil layer, whereas salt ion mass addition in upflux occurs only for the bottom soil layer. Equation (1) is repeated for each salt ion, for each soil layer, for each HRU in the watershed. Again, using $SO_4$ as an example, the mass balance (kg $ha^{-1}$) in the aquifer for each HRU on a daily time step is formulated as:

$$\frac{dM_{SO_4,gw}}{dt} = M_{perc} - M_{revap} + M_{diss} - M_{precip} - M_{gwflow} \qquad (2)$$

where *gwflow* represents the salt ion mass removed from the aquifer via groundwater discharge to the subbasin stream. From Equations (1) and (2), salt ion mass loading to the subbasin streams, and therefore salt loading (i.e. export) from the watershed, occurs via surface runoff ($M_{ro}$), soil lateral flow ($M_{lat}$), and groundwater discharge ($M_{gwflow}$).

Figure 2-1 shows a schematic of hydrologic and salinity transport processes simulated by SWAT-Salt, with equilibrium chemistry reactions (precipitation-dissolution, complexation, cation exchange) simulated in the soil profile and unconfined aquifer. The inclusion of salinity transport in tile drains is explained in the next section (Section 2.3). The salinity module is imbedded in the SWAT code

(FORTRAN), with new subroutines added for salt equilibrium chemistry, salinity percolation and leaching, salt irrigation loading from surface water and groundwater irrigation, and salt groundwater transport and loading to streams. Other subroutines within SWAT were also modified to incorporate salt ion transport and effects, such as lagging solutes in surface runoff and groundwater flow and routing salt ions through the stream network (Bailey et al., 2019). The code writes files containing HRU-specific, subbasin-specific, and watershed-wide salt ion concentrations and fluxes to determine transport and storage of salt within the watershed system. The source files of SWAT and the accompanying salinity module are available on GitHub (https://github.com/rtbailey8/SWAT_Salinity).

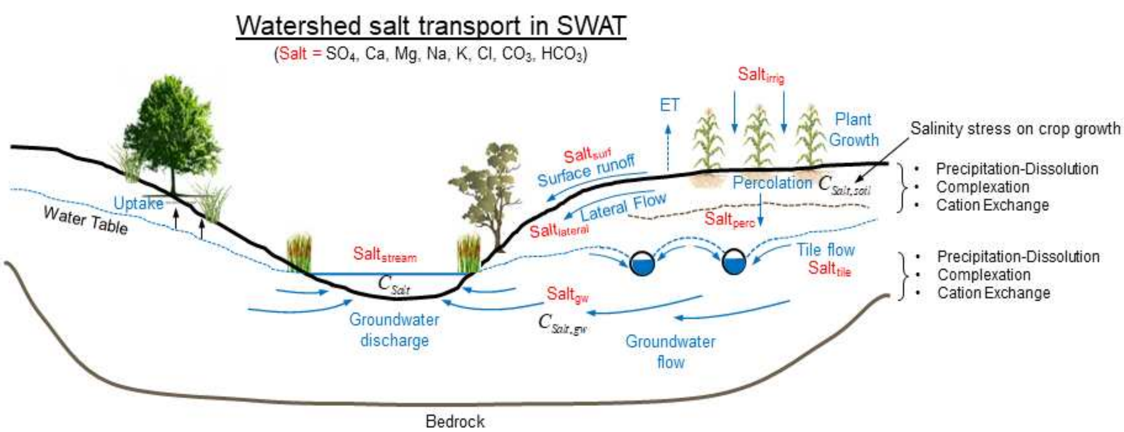


**Figure 2-1.** Schematic showing hydrologic flow and salinity transport in an irrigated watershed system, as simulated by the SWAT-Salt model (Bailey et al., 2019). Salinity consists of the eight major salt ions ($SO_4$, Ca, Mg, Na, K, Cl, $CO_3$, and $HCO_3$). The current study adds the transport of salt ion mass in subsurface tile drains.

### 2.2.3 Modifying swat-salt to include tile drain salinity transport

As part of this study the SWAT salinity module was modified to include the transport of the 8 salt ions ($SO_4$, Ca, Mg, Na, K, Cl, $CO_3$, and $HCO_3$) in subsurface tile drains and their loading to subbasin streams. The SWAT model simulates water flow in subsurface tile drains for tile-designated HRUs using a basic tile flow equation (Neitsch et al., 2011) or incorporating DRAINMOD equations (Moriasi et al., 2012), with the latter using the physically based Hooghoudt and Kirkham tile drain equations. The main tile drain parameter for the original equation is the time required to drain the soil to field capacity dtime (hr), whereas the tile drain parameters for DRAINMOD include drain radius drad (mm), distance between drains ddist (mm), depth to the tile drains ddepth (mm), and saturated soil hydraulic conductivity ksat (mm/hr). For each day of the simulation, and for HRUs specified as containing a subsurface tile drain, a tile drain flow rate qtile (mm) is calculated. This volume of water (depth * HRU area) is added to the corresponding subbasin stream using a lagging equation (see SWAT documentation in Neitsch et al., 2011).

To include salt ion transport and loading in tile drains, the salt ion balance in the HRU soil layers (Equation 1) was modified to include salt removal via tile drains, Mtile (kg $ha^{-1}$), here again using $SO_4$ as an example ion:

$$\frac{dM_{SO_4,soil}}{dt} = M_{irrig,sw} + M_{irrig,gw} + M_{diss} - M_{precip} - M_{ro} - M_{lat} - M_{tile} - M_{perc} + M_{revap}$$

(3)

$M_{tile}$ (kg $ha^{-1}$) is calculated for each salt ion as the product of salt ion concentration in the HRU soil water (kg salt / mm water) and tile flow *qtile* (mm of water), which is then subtracted from the salt ion mass in the soil profile. Salt mass removed by tile drains is output for HRUs, subbasins, and the entire watershed, as part of the general salt mass budget.

### 2.3. Swat-salt application to a saline tile drained region

This section provides a demonstration of the modified SWAT-Salt code for salt ion transport in a tile drain network. The study region is described first, followed by the model application.

#### 2.3.1 Study region: lower Arkansas river valley, Colorado

The general study region (Figure 2-2) is located within the Lower Arkansas River Valley (LARV), (38°01′ 39″ N, 103°48′ 11″ W), a productive agricultural region in southeastern Colorado, located downstream of Pueblo Reservoir and upstream of John Martin Reservoir. The region spans 732 $km^2$ between the towns of Manzanola and Las Animas, encompassing 26,400 ha of irrigated land. The region has a semi-arid climate. The average annual temperature is 13.6 °C, with the monthly average temperature ranging from -13 °C in January to 36 °C in July. Average annual precipitation is 375 mm (14.5 in), necessitating irrigation to sustain crop growth. Irrigation, begun in the late 19th century, is provided by earthen canals that divert water from the Arkansas River, or from a network of wells that pump groundwater from the alluvial aquifer (see Figure 2-2B, C). Main crop types include wheat, sorghum, corn, alfalfa, legumes, melons, and vegetables. The region has experienced high salinity in soils, groundwater, the surface water (Arkansas River and tributaries) during the past few decades (Gates et al., 2002; Morway and Gates, 2012).

Salinity in the stream-aquifer system of the LARV is due to salt mineral dissolution and extended irrigation practices (Konikow and Person, 1985; Gates et al., 2016), with the latter causing high water tables and associated salinization of soil profiles due to a lack of adequate natural drainage. As reported by Gates et al. (2002) and Morway and Gates (2012), about 70% of the region experiences crop yield decrease due to high soil salinity levels, which range from 2 dS/m to over 10 dS/m, leading to a mean yield reduction of approximately 6%. During the 2006-2010 period for the region shown in Figure 2-2B, which coincides with the boundary of the SWAT model used in this study, average groundwater salinity concentration was approximately 3,300 mg/L (443 samples from groundwater monitoring wells); average soil salinity was 4.1 dS/m; and average surface water salinity in the Arkansas River and its tributaries was 1,145 mg/L.

### 2.3.2 Study site and data collection: fairmont drainage district

The specific area investigated in this study for model testing is the Fairmont Drainage District (FDD) (Figure 2-2C), a network of tile drains located within the Timpas Creek watershed. The free drainage system is approximately 2 km south of the Arkansas River. The diameter of the tile drains in the field are

(4,6,7,8,10,14, and 15 inches). while the average depth of these drains is about 4 feet (1.22 m) and the horizontal distance between two drains is about 100 m. The FDD has been well maintained and is operating in a very good condition, with substantial outflow and effect on surrounding groundwater levels. As seen in Figure 2-3, the drains from outlying fields are connected to main lines, which then drain to a main tile drain trunk (northernmost line in Figure 2-2C). The water that leaves the outlet of the tile drain trunk mixes with surface water runoff and then discharges to Timpas Creek. The water at the outlet of the drainshed was sampled for salt ion concentration 27 times approximately every 3 months between June 10, 2014, and August 25, 2018. All samples were collected using a peristaltic pump. A QED multiparameter sonde was used for in-situ readings, consisting of electrical conductivity (specific conductance at 25 $^{o}$C), temperature, oxidation-reduction potential (ORP), pH, and dissolved oxygen (DO). Samples were shipped in a cooler with ice to Ward Laboratories Inc. (Kearney, Nebraska) for salt ion analysis.

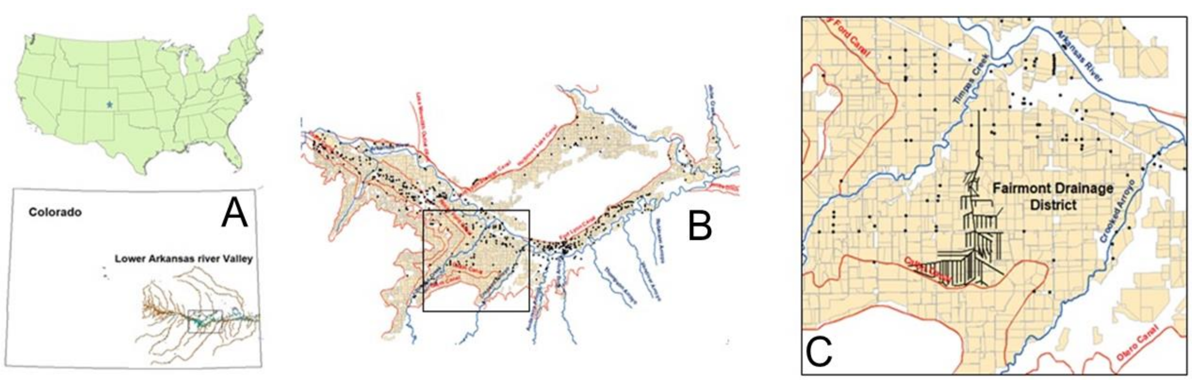


**Figure 2-2.** Maps of the study region, showing (A) the stream network of the Lower Arkansas River Valley in Colorado, (B) the 732 km$^2$ region modeled by SWAT-Salt, and (C) the tile drain network of the Fairmont Drainage, with its location shown by the black hollow box in (B). Red lines in (B) and (C) indicate irrigation canals. Black dots in (C) indicate locations of groundwater pumping wells, used for irrigation.

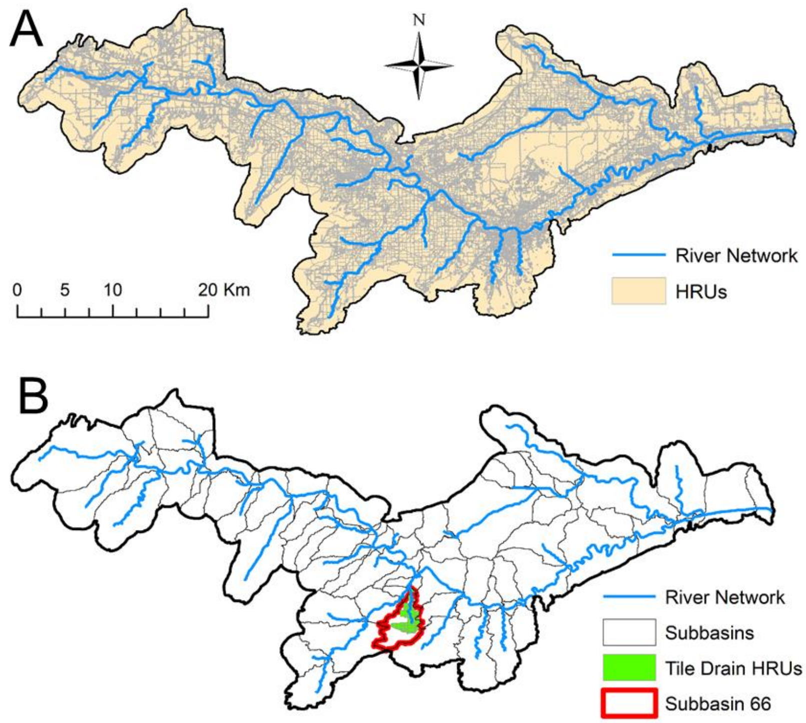


**Figure 2-3.** Computational units of the SWAT-Salt model, showing (A) hydrologic response units and the river network, and (B) subbasins. (B) shows the outline of Subbasin 66, which encompasses the FDD tile drain network. The HRUs that contain tile drains are colored in green.

### 2.3.3 Simulating salinity transport in the Fairmont drainage district

The SWAT-Salt model, with the added routines for tile drainage salt ion transport, is applied to the FDD and tested against results from the water quality samples. A previously tested SWAT hydrologic model (Wei et al., 2018) of the 732 $km^2$ region (Figure 2-2B), which encompasses the FDD, is used to drive the hydrologic fluxes in the FDD area. The region was divided into 72 subbasins and 5270 HRUs (Figure 2-4), determined from a digital elevation model, stream network, soil map, and land use map. Each cultivated field is represented by a unique HRU (Wei et al., 2018). Including canal seepage in the modeling process required a change to the SWAT code (Wei et al., 2018). Within the code, estimated daily seepage from earthen canals was added to the aquifer unit of adjacent HRUs, with values obtained from an input file. The model, however, did not include tile drainage for any HRUs. The model was run for the 1999–2009 time period and tested against measured streamflow at three gages along the Arkansas River and two tributaries. For this study, the model was extended to run through 2018, to coincide with the time period of collected water samples in the FDD. This extension required processing climate data (rainfall, temperature) and land use for each year between 2010 and 2018. Climate data were included in the appropriate SWAT input files, and the management file of each HRU was extended to include crop type and associated irrigation routines for these years.

The tested SWAT-Salt model for this region (Bailey et al., 2019) is used as the base salinity transport model. The model requires initial soil water and groundwater salt ion concentrations, initial soil and aquifer salt mineral fractions, and salinity loading in the Arkansas River in the upstream end of the modeled region as a source input. The original model was tested against soil salinity, groundwater salt ion concentrations, and in-stream salt ion concentrations (Bailey et al., 2019).

For this study, tile flow was included for the 41 HRUs that correspond to the cultivated fields within the FDD. These HRUs are shown in Figure 2-3B, within Subbasin 66 of the SWAT model. Only the DRAINMOD routines of Moriasi et al. (2012) were used within the SWAT drainage routines. Tile drain parameters include the effective drain radius (RE), set to 20 mm; the horizontal distance between two drains (SDRAIN), set to 100 m, based on the actual map distance (see Figure 2-2C); and the drainage coefficient (DRAIN_CO), which signifies the maximum allowable daily drainage depth for a given HRU, set to 15 mm. As most of the groundwater within these HRUs drains to the tile drains rather than discharges to Timpas Creek, groundwater discharge to streams was negated for these 41 HRUs by changing aquifer parameters to values that prevents the simulation of groundwater discharge. Groundwater delay (GW_DELAY) was set to 10,000 days, and the baseflow alpha factor (ALPHA_BF) was set to 0.00.

As seen in Figure 2-3B, the FDD resides within Subbasin 66 of the original SWAT model, which has 160 HRUs. The outlet of this subbasin, i.e. the discharge location to Timpas Creek, coincides with the location of water quality sampling. Therefore, the model was tested by comparing simulated salt ion concentrations at the outlet of subbasin 66 with the measured salt ion concentrations from the water quality samples (see Section 3.2). Salt budgets are then used for Subbasin 66 to determine the relative salinity yield of surface runoff, soil lateral flow, groundwater discharge, and tile drainage, to provide context for the effect of tile flow on salt mass export from the tile drained area. Model testing results are shown in Section 3.5.

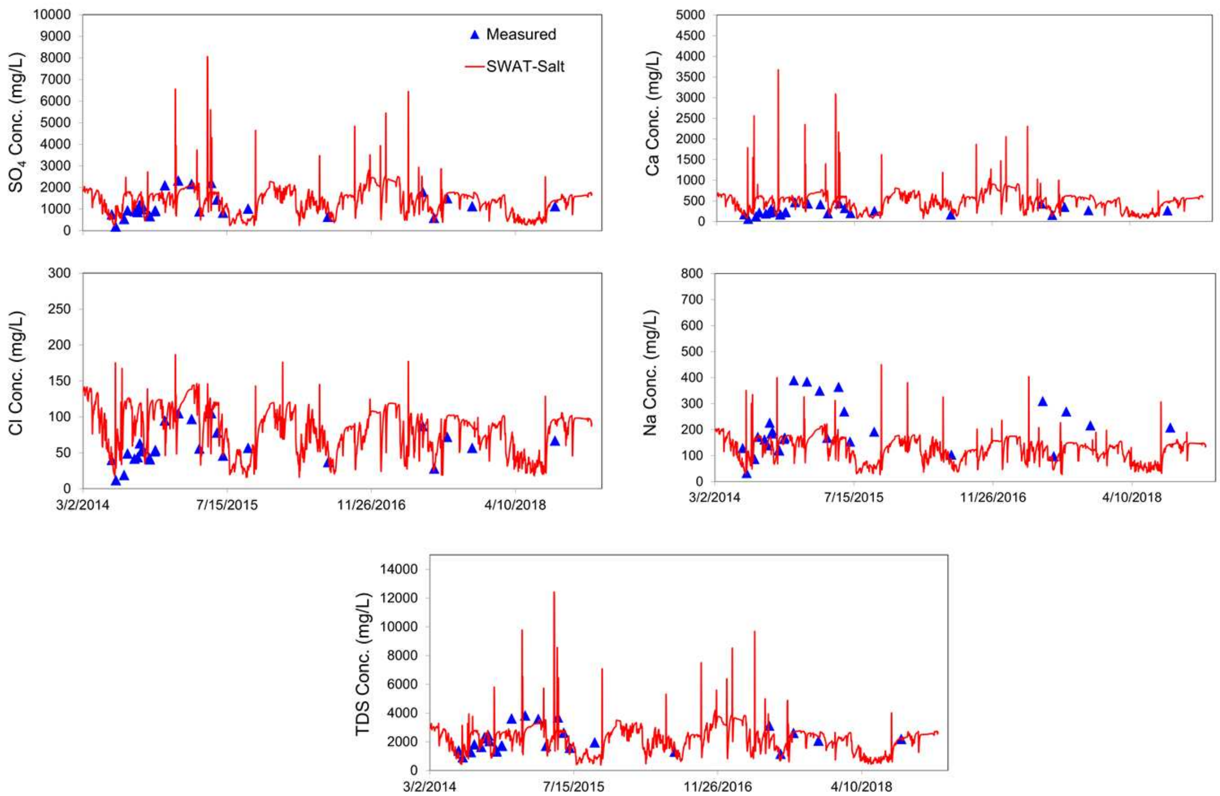


**Figure 2-4.** Time series of measured and simulated concentration (mg/L) of $SO_4$, Ca, Cl, Na, and TDS (summation of all 8 ions) at the outlet of Subbasin 66, which contains the FDD tile drain network.

### 2.3.4 Simulating effects of region-wide implementation of tile drainage

With the model tested against salt export data in the tile drained area, the model for the entire 732 $km^2$ region is used to investigate the effects of region-wide implementation of tile drains on watershed salinity, specifically analyzing in-stream salt loading in the Arkansas River and tributaries, and the change in the watershed salt budget. Region-wide implementation of tile drains is achieved by activating tile drainage for each cultivated HRU in the region-wide SWAT-Salt model.

### 2.3.5 Results and discussion

#### 2.3.5.1 Tile drain network

Simulated and observed salt ion concentrations (mg/L) at the subbasin outlet are shown in Figure 2-4 for $SO_4$, Ca, Cl, Na, and the summation ∑ of all 8 salt ions. Overall, the model tracks the temporal variation of measured concentrations successfully. $R^2$ values are 0.58, 0.65, 0.62, 0.70, and 0.54, for SO4, Na, Cl, and ∑, respectively. However, the model underpredicts Na concentration, particularly during the winter of 2014-2015 and the summer of 2017. Simulating Na and Cl in this area is problematic. The SWAT-Salt model requires salt mineral soil fractions as inputs for each HRU. The soil maps used to populate these data contained $CaSO_4$ (gypsum) and $CaCO_3$ (calcite) fractions but did not contain NaCl fractions. Therefore, there is a high degree of uncertainty in initial NaCl mineral content, which drives the resulting Na and Cl concentration in soil water, groundwater, resulting tile water and irrigation water. Several model scenarios were run (see Figure 2-5) to investigate the influence of varying NaCl initial soil fractions. In general, comparing simulated and measured solute concentrations on a daily basis is a difficult challenge for watershed modelling. In general, however, we conclude from these results that the model performs adequately well in simulating salt ion export from a subbasin that contains extensive tile drainage.

Daily and annual salt fluxes (kg/ha) are shown in Figure 2-6 for lateral flow, surface runoff, groundwater flow, and tile drain flow in Subbasin 66. Although 70% of the total salt loaded from Subbasin 66 is via groundwater discharge, tile drainage has high daily salt fluxes (Figure 2-6A) and contributes 22% of the total salt flux from the subbasin. Surface runoff (6%) and lateral flow (2%) are minor contributors to salt loading. Salt export in 2002-2003 and 2012-2013 are relatively low due to drought conditions, when rainfall, recharge, and groundwater storage were all low compared to other years. The dominant salt ion in tile drainage water is $SO_4$ (Figure 2-6D), due to the prevalence of the salt mineral gypsum ($CaSO_4$) in the region's soils. This is true of soil water, groundwater, and surface water in the LARV in general (Gates et al., 2009; Bailey et al., 2019).

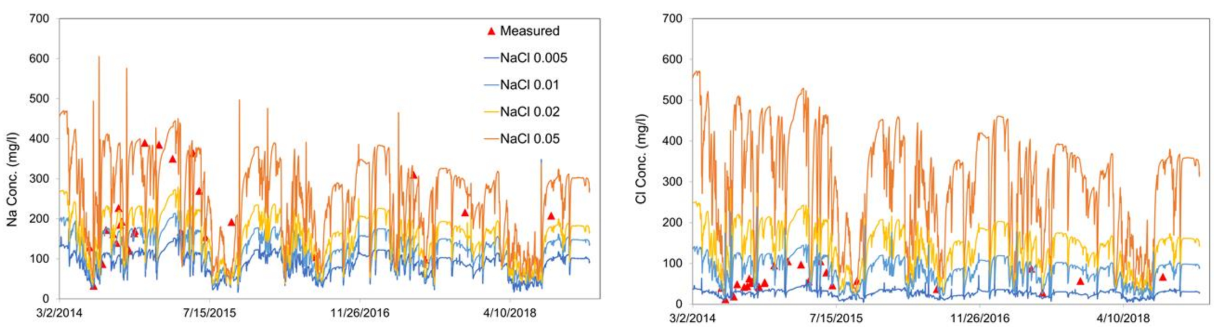


**Figure 2-5.** Time series of measured and simulated concentration of Na and Cl (mg/L), for four scenarios of varied initial NaCl soil fraction in the HRUs.

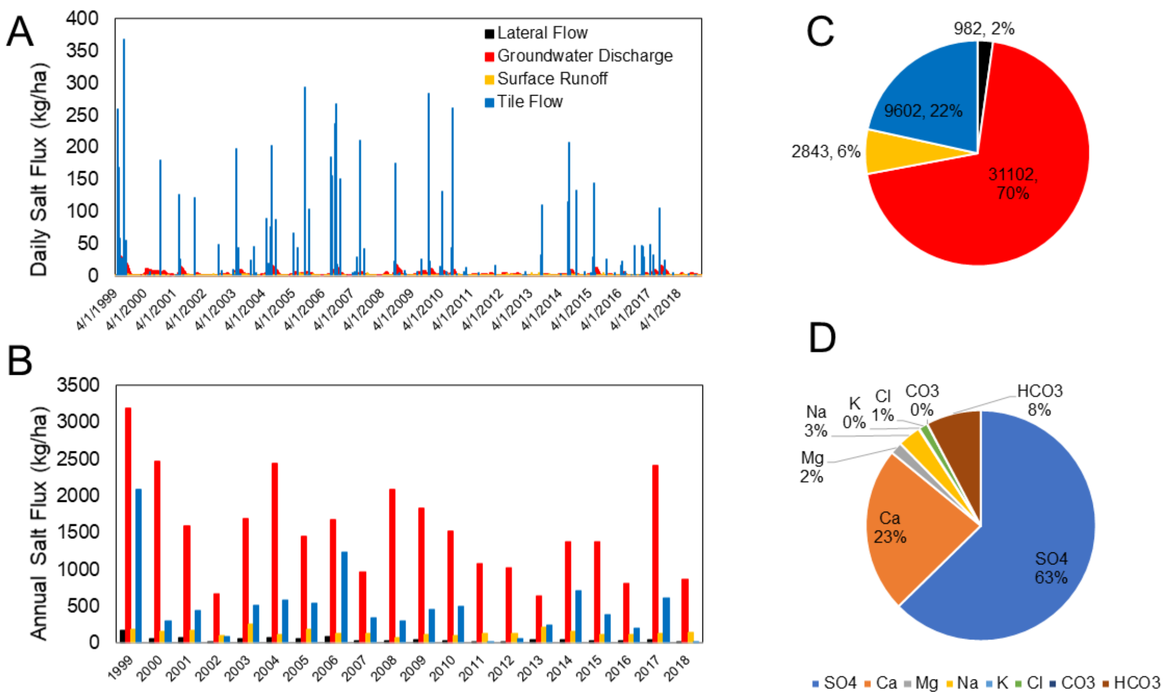


**Figure 2-6.** Results for Subbasin 66: (A) time series of daily salt fluxes for the period 1999-2018, (B) time series of annual salt fluxes, (C) pie chart showing the total salt flux contributed by lateral flow, groundwater discharge, surface runoff, and tile flow, and (D) the percentage of tile drain salt export attributed to each of the 8 salt ions.

### 2.3.5.2 Impacts of tile drains on region-wide salinity transport

Results for the region-wide implementation of tile drainage in the study region are shown in Figures 2-7 through 2-11. Figure 2-7 shows the region-wide average annual water flux (mm) and salt flux (kg/ha) in surface runoff, soil lateral flow, groundwater discharge to streams (from shallow aquifer), groundwater discharge to streams (from deep aquifer), and tile drain flow, for conditions with and without tile drainage. For water flux (Figure 2-7A), tile flow increases from 0.1 mm to 14 mm (the 0.1 mm corresponds to the tile drainage in the FDD, in subbasin 66) under the tile drain scenario. However, total water yield in the river system (runoff + lateral flow + groundwater discharge + tile flow) is approximately the same (103 mm vs. 102 mm), as groundwater discharge from the shallow aquifer decreases from 77 mm to 63 mm, with the water that typically would recharge the aquifer and move towards streams instead being intercepted by the tile drains. ET decreases from 217 mm to 207 mm, and recharge to deep aquifers decreases from 6.4 mm to 5.6 mm. Therefore, results show that implementing region-wide tile drainage does not change the overall water yield from the watershed, but likely changes the timing of flow due to the difference in travel time between groundwater flow and tile drain flow.

A similar relationship between groundwater and tile drains occurs for salt transport (Figure 2-7B), as the increase in salt loading to streams via tile drains (6 kg/ha → 359 kg/ha; $\Delta$ = 353 kg/ha) causes a decrease in salt loading via groundwater discharge (1,603 kg/ha → 1,281 kg/ha; $\Delta$ = 322 kg/ha), with a net increase in total salt yield of 32 kg/ha (1,619 kg/ha → 1,651 kg/ha). Again, the salt that would have leached to the water table and then been transported diffusely to nearby streams is intercepted and routed quickly to the streams via the tile drains. The timing of loading via groundwater discharge and tile drain flow is demonstrated in Figure 2-8 with daily time series (kg/ha). Whereas groundwater salt loading occurs relatively consistently throughout each growing season, tile drainage provides high magnitude loads periodically, often during large irrigation and/or rainfall events that increase soil water flow to the tile drains. Therefore, although region-wide implementation of tile drains only slightly changes the overall salt yield from the watershed system on multi-year basis, pulses of high salt loading from tile drains do occur. Notice that the portion of total salt yield contributed by surface runoff is small (see Figure 2-7B) compared to its portion of water yield (see Figure 2-7A), due to lower salt ion concentrations in rainfall and irrigation water as compared to soil water and groundwater. Also notice that, even with tile drains installed in every cultivated field in the region, groundwater discharge is still the dominant pathway for salt to load to streams, with annual salt fluxes of 1,280 kg/ha and 360 kg/ha for groundwater and tile drains, respectively (see Figure 2-7B).

The interplay between long-term magnitude and short-term pulses (i.e. loads that occur over a short time span of 1-2 days) is also seen in the time series of in-stream loads (kg/day) of $SO_4$, Ca, and summation of the 8 ions in the Arkansas River at the outlet of the watershed, shown in Figure 2-9. For $SO_4$, the total mass export from the watershed is 1,337 x $10^6$ kg over the 19-year period of 2000-2018 with region-wide tile drainage, compared to 1,315 x $10^6$ kg in the baseline scenario, an increase of only 1.6%. However, as seen in Figure 2-9A, there are days in which the $SO_4$ loads are double or triple the baseline value, due to pulses from tile drain outflow. These pulses can change the in-stream concentration of $SO_4$ in the Arkansas River, as shown in Figure 2-9D. These higher concentrations can have a detrimental impact on crop yield and general soil health in downstream irrigated regions. This result has been documented in Australia (Hornbuckle et al., 2005), with local benefits in tile drained areas tempered by high-saline water in downstream consumptive areas. Similar temporal patterns of in-stream loading and concentrations occur for Ca (Figure 2-9B,E) and the summation of the 8 ions (Figure 2-9C,F).

The spatial patterns of salt loading via groundwater and tile drains are shown by subbasin and HRU in Figures 2-10 and 2-11, respectively. Providing a spatial analogue to the overall salt flux changes shown in Figure 2-7B, groundwater salt loading at the subbasin level decreases when tile drains are implemented (Figure 2-10A, B), due to the increase in tile drain salt loading (Figure 2-10C, D), due to tile drains intercepting water and salt ion mass that otherwise would leach to the aquifer and be transported to streams via groundwater flow. Notice that the majority of salt flux occurs in the central area of the region, due to the localized intensive cultivation practices in this area. A similar spatial pattern is seen in groundwater concentration (mg/L) at the HRU level (Figure 2-11.). For many of the cultivated fields in the central area of the study region, the $SO_4$ concentration in the underlying aquifer decreases (orange color in Figure 2-11A changes to yellow color in Figure 2-11B) when tile drains are implemented, as $SO_4$ mass is intercepted by the tile drains. Region-wide average $SO_4$ concentration in the aquifer decreases from 2,040 mg/L to 1,800 mg/L (12% decrease) when tile drains are implemented. The same pattern occurs for the other 7 salt ions. This can impact salt loading by groundwater irrigation: if tile drains are implemented at a large scale, and thereby decrease groundwater salt ion concentrations, salt loading to field surfaces via groundwater pumping will be decreased, leading to improved crop production and soil health. Again, however, these local benefits must be balanced with the potential of increased salinity concentrations in downstream river water, leading to negative impacts on crop yield and soil health in those areas.

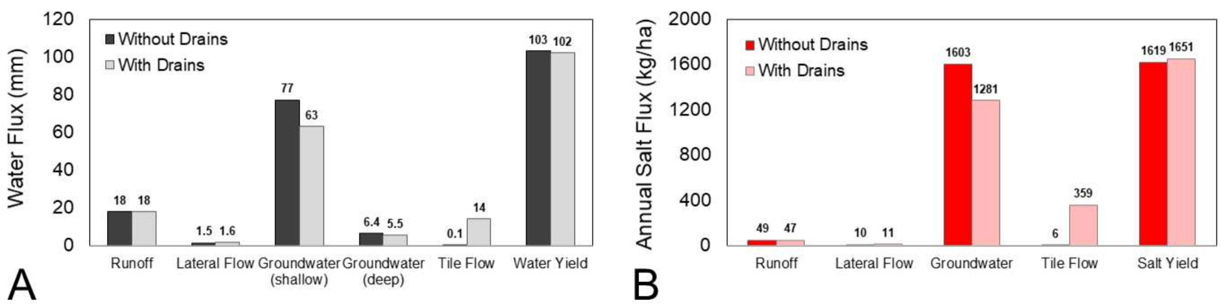


**Figure 2-7.** Results of region-wide tile drain analysis, showing average annual (A) region-wide water fluxes and (B) region-wide salt fluxes, with and without tile drain implementation.

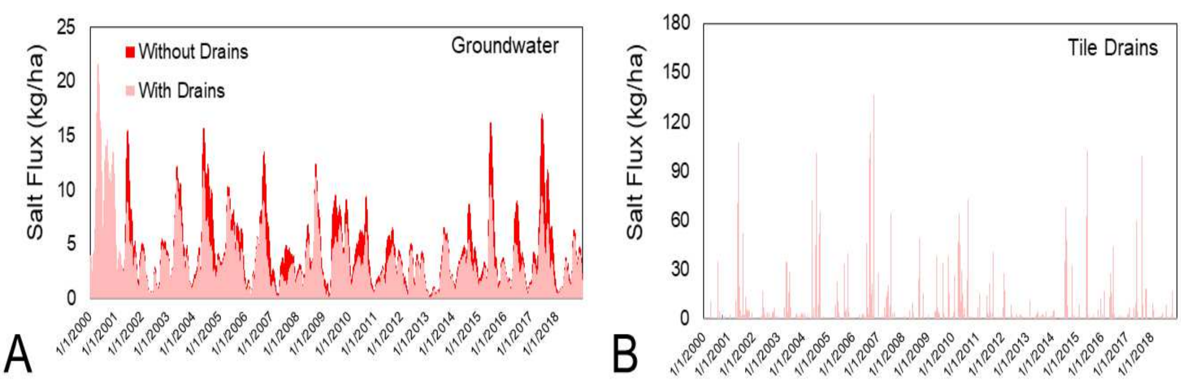


**Figure 2-8.** Salt flux of (A) groundwater and (B) tile drains with and without tile drain implementation

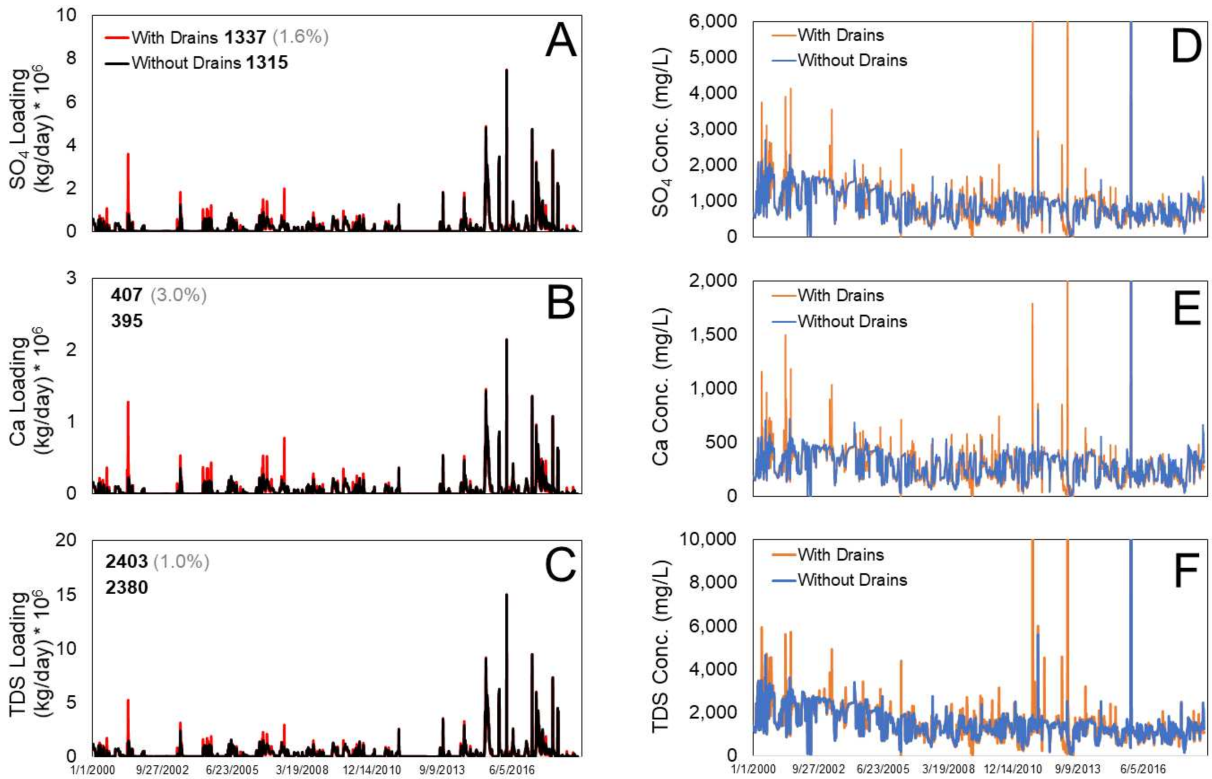


**Figure 2-9.** Daily in-stream salt loading in millions of kg per day at the watershed outlet, with and without region-wide implementation of tile drains, for (A) $SO_4$, (B), Ca, and (C) TDS. Daily in-stream concentrations (mg/L) at the watershed outlet, with and without region-wide implementation of tile drains, for (D) $SO_4$, (E) Ca, and (F) TDS.

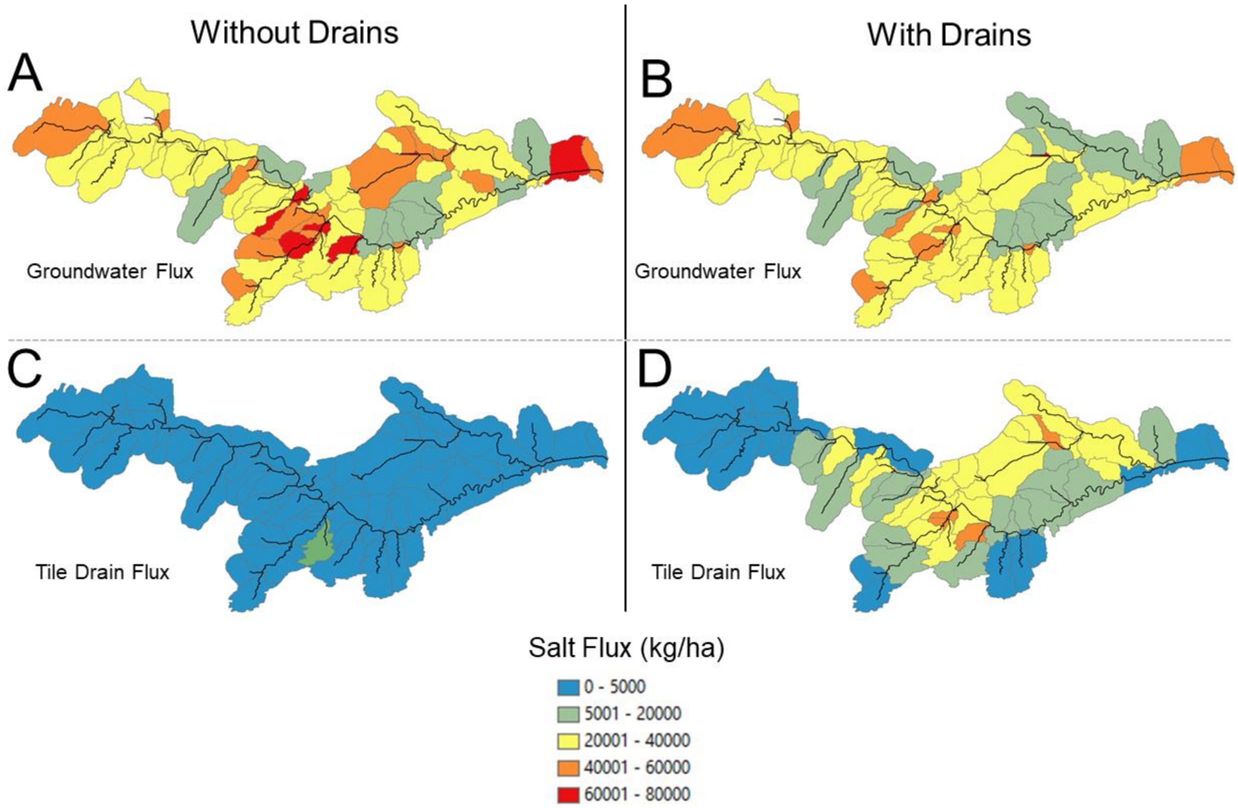


**Figure 2-10.** Simulated salt loadings to streams at the subbasin level for groundwater discharge (A) without drains and (B) with drains, and for tile drain flow (C) without drains and (D) with drains. The scenario without drains still includes the actual tile drain network in subbasin 66, and therefore shows tile drain flux in (C).

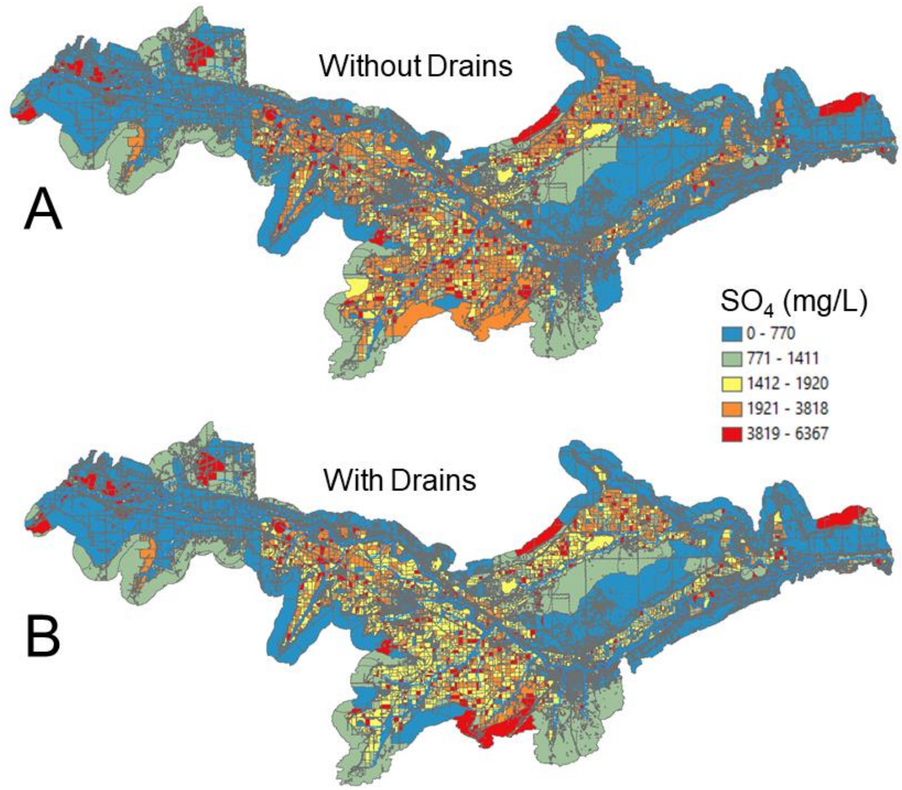


**Figure 2-11.** Simulated concentration (mg/L) of $SO_4$ in groundwater for each HRU during the spring of 2010, for (A) without drains and (B) with drains implemented in each cultivated field HRU.

### 2.4. Limitations of using swat-salt for salt transport in tile drained regions

The salinity tile drain module of SWAT differs from other salinity models in that it accounts for salt loading for each major hydrologic pathway in a watershed setting (stream, groundwater, lateral flow, surface runoff, tile drain flow), for each major salt ion, subject to chemical equilibrium reactions (precipitation–dissolution, complexation, cation exchange). As such, it can be used to estimate baseline salt loading within a watershed and also explore the impact of land management and water management scenarios to mitigate soil salinity, groundwater salinity, and surface water salinity. However, there are limitations in the processes simulated by SWAT-Salt. In general, the movement of salinity in the groundwater system is simulated in a simplistic manner at the HRU level, due to the use of steady-state and lumped equations in SWAT's groundwater module. A more accurate approach would be the use of SWAT-MODFLOW-RT3D (Wei et al., 2019), which uses physically based spatially distributed flow and reactive transport modeling for groundwater and associated solutes. However, a salinity module has not yet been included in the modeling code. Specific to tile drainage, tile drain flow as simulated by the incorporated tile drain equations in SWAT occurs as pulses at the HRU level, rather than diffuse transport of water from the soil/aquifer into individual tile drains. This shortcoming can be remedied by simulating groundwater storage, flow, and groundwater-tile drain interactions in a physically based spatially distributed manner, such as with SWAT-MODFLOW (Bailey et al., 2016). Again, however, the salinity module would need to be incorporated into the modeling code. Therefore, the modeling procedures used in this study are the best available for regional scale investigations and quantifying the interplay between various salt transport pathways.

Specifically for this study, the model was unable to capture the trends in sodium Na (see Figure 2-4), with the model underpredicting concentrations in the outlet water as compared to the measured concentrations. Likely this is due to the lack of NaCl mineral data for the region, i.e. the fraction of salt that is NaCl, which conversely is readily available for $CaCO_3$ and $CaSO_4$ from NRCS soil maps.

Also, this study does not include the effect of tile drainage on crop yield. The export of salinity via tile drains to downstream regions is detrimental to downstream irrigation practices, but tile drained areas result in less waterlogging and soil salinity build-up, leading to improved crop yield in the long-term. This balance between improved crop yield and decreased downstream water quality will be explored in future studies.

### 2.5 Summary and conclusions

This paper introduces a new version of SWAT-Salt (Bailey et al., 2019) that simulates the fate and transport of salt ions in irrigated watersheds drained by artificial subsurface tile drains. The model simulates transport of major cations and anions in groundwater, soil percolation, surface runoff, lateral flow, streams, and equilibrium chemistry reactions in soil layers and the aquifer. Model results are tested against salt ion concentrations in effluent from a tile drained area in the Arkansas River Valley, Colorado, whereupon the model is used to assess the impact of region-wide tile drain implementation on salt fluxes (surface runoff, lateral flow, groundwater discharge, tile drain outflow) and watershed salt export. General conclusions from the hypothetical region-wide tile drain analysis include:

1. Implementing region-wide tile drainage increases total salt yield from the watershed by only 1% during a long simulation period (2000-2018) (see Figure 2-9C). The increase in salt loaded from the landscape to stream via tile drains is balanced by the decrease in groundwater loading, as the salt mass that would be transported in the aquifer is instead intercepted by the tile drains.
2. Even with tile drains installed in every cultivated field in the region, groundwater discharge is still the dominant pathway for salt to load to streams, with annual salt fluxes of 1,280 kg ha-1 and 360 kg ha-1 for groundwater and tile drains, respectively (see Figure 2-7B).
3. Although the long-term watershed salt yield is approximately the same under tile drained conditions, the timing of salt loading to streams changes to higher daily pulse loadings as opposed to long-term diffuse loading from groundwater (see Figure 2-8). These higher daily loadings result in high in-stream concentrations (see Figure 2-9D,E,F), which can lead to negative impacts on crop growth and overall soil health in downstream irrigated areas.
4. Groundwater salt ion concentrations can be decreased significantly in tile drained areas (see Figures 2-10 and 2-11), resulting in improved crop yield for areas that pump groundwater for irrigation. See Figure 2-2B for the locations of pumping wells in the study region.

These results provide insights into the impact of tile drains on watershed-wide salinity transport and loading and can be used to help guide salinity management in irrigated, drained landscapes. Appropriate management at the regional scale must balance the derived local benefits (crop yield, soil health, groundwater quality) with downstream environmental conditions, for instream ecosystems and water users. In general, the model can be a useful tool in simulating salinity transport in tile drained watersheds, either irrigated or non-irrigated, and investigating salinity best management practices in watersheds of varying spatial scales.

REFERENCES

Arnold, J., Srinivasan, R., Muttiah, R., and Williams, J., 1998. Large Area Hydrologic Modeling and Assessment Part I: Model Development. JAWRA Journal of the American Water Resources Association, 34(1), pp.73-89.

Ayars JE, Christen EW, Hornbuckle JW. Controlled drainage for improved water management in arid regions irrigated agriculture. Agricultural Water Management. 2006 Nov 16;86(1-2):128-39.

Bailey, R. T., Wible, T. C., Arabi, M., Records, R. M., and Ditty, J.: Assessing regional-scale spatio-temporal patterns of groundwater-surface water interactions using a coupled SWAT-MODFLOW model, Hydrol. Process., 30, 4420–4433, https://doi.org/10.1002/hyp.10933, 2016.

Bailey, R. T., Tavakoli-Kivi, S., and Wei, X.: A salinity module for SWAT to simulate salt ion fate and transport at the watershed scale, Hydrol. Earth Syst. Sci., 23, 3155–3174, https://doi.org/10.5194/hess-23-3155-2019, 2019.

Bailey, R.: SWAT-Salt: Source code for original SWAT model and new salt transport subroutines, available at: https://github.com/ rtbailey8/SWAT_Salinity, last access: 22 July 2019.

Christen EW, Ayars JE, Hornbuckle JW. Subsurface drainage design and management in irrigated areas of Australia. Irrigation Science. 2001 Dec 1;21(1):35-43.

El-Ghannam, M., Aiad, M. and Abdallah, A., 2021. Irrigation efficiency, drain outflow and yield responses to drain depth in the Nile delta clay soil, Egypt. Agricultural Water Management, 246, p.106674.

Feng, G., Zhang, Z., Wan, C., Lu, P. and Bakour, A., 2017. Effects of saline water irrigation on soil salinity and yield of summer maize (Zea mays L.) in subsurface drainage system. Agricultural water management, 193, pp.205-213.

Gates, T. K., Burkhalter, J. P., Labadie, J. W., Valliant, J. C., and Broner, I.: Monitoring and modeling flow and salt transport in a salinity-threatened irrigated valley, J. Irrig. Drain. E., 128, 88– 99, https://doi.org/10.1061/(ASCE)0733-9437(2002)128:2(87), 2002.

Gates, T. K., Steed, G. H., Niemann, J. D., and Labadie, J.W.: Data for Improved Water Management in Colorado's Arkansas River Basin, Hydrological and Water Quality Studies, Colorado State University, USA, 2016.

Ghassemi, F., Jakeman, A.J., and Nix, H.A. Salinisation of Land and Water Resources. University of New South Wales Press Ltd, Canberra, Australia. (1995)

Gill BC, Terry AD. 'Keeping salt on the farm'—Evaluation of an on-farm salinity management system in the Shepparton irrigation region of South-East Australia. Agricultural Water Management. 2016 Jan 31;164:291-303.

Hopkins, D., Chambers, K., Fraase, A., He, Y., Larson, K., Malum, L., Sande, L., Schulte, J., Sebesta, E., Strong, D. and Viall, E., 2012. Evaluating salinity and sodium levels on soils before drain tile installation: A case study. Soil Horizons, 53(4), pp.24-29.

Hornbuckle, J.W., Christen, E.W., Ayars, J.E. and Faulkner, R.D., 2005. Controlled water table management as a strategy for reducing salt loads from subsurface drainage under perennial agriculture in semi-arid Australia. Irrigation and Drainage Systems, 19(2), pp.145-159.

Hornbuckle, J.W., Christen, E.W. and Faulkner, R.D., 2007. Evaluating a multi-level subsurface drainage system for improved drainage water quality. Agricultural Water Management, 89(3), pp.208-216.

Jafari-Talukolaee M, Shahnazari A, Ahmadi MZ, Darzi-Naftchali A. Drain discharge and salt load in response to subsurface drain depth and spacing in paddy fields. Journal of Irrigation and Drainage Engineering. 2015 Nov 1;141(11):04015017.

Kirkham, D. (1957). Theory of land drainage. In J. N. Luthin (Ed.), Drainage of Agricultural Lands (pp. 139-181). Madison, WI: ASA

Konikow, L. F. and Person, M.: Assessment of long-term salinity changes in an irrigated stream aquifer system, Water Resour. Res., 21, 1611–1624, https://doi.org/10.1029/WR021i011p01611, 1985.

Liu, Y., Ao, C., Zeng, W., Kumar Srivastava, A., Gaiser, T., Wu, J. and Huang, J., 2021. Simulating water and salt transport in subsurface pipe drainage systems with HYDRUS-2D. Journal of Hydrology, 592, p.125823.

Lu, P., Zhang, Z., Sheng, Z., Huang, M. and Zhang, Z., 2019. Assess Effectiveness of Salt Removal by a Subsurface Drainage with Bundled Crop Straws in Coastal Saline Soil Using HYDRUS-3D. Water, 11(5), p.943.

Moriasi, D. N., C. G. Rossi, J. G. Arnold, and M. D. Tomer. 2012. Evaluating hydrology of SWAT with new tile drain equations. J. Soil Water Cons.

Moriasi, D. N., Gowda, P. H., Arnold, J. G., Mulla, D. J., Ale, S., Steiner, J. L., & Tomer, M. D. (2013b). Evaluation of the Hooghoudt and Kirkham tile drain equations in the Soil and Water Assessment Tool to simulate tile flow and nitrate-nitrogen. J. Environ. Qual., 42(6), 1699-1710.http://dx.doi.org/10.2134/jeq2013.01.0018

Morway, E. D. and Gates, T. K.: Regional assessment of soil water salinity across an intensively irrigated river valley, J. Irrig. Drain. E., 138, 5, 393–405, https://doi.org/10.1061/(ASCE)IR.1943-4774.0000411, 2012.

Morway, E. D., Gates, T. K., and Niswonger, R. G.: Appraising options to reduce shallow groundwater tables and enhance flow conditions over regional scales in an irrigated alluvial aquifer system, J. Hydrol., 495, 216–237, https://doi.org/10.1016/j.jhydrol.2013.04.047, 2013.

Neitsch, S.L., Arnold, J.G., Kiniry, J.R. and Williams, J.R., 2011. Soil and water assessment tool theoretical documentation version 2009. Texas Water Resources Institute.

Okuda, Y., Onishi, J., Shirokova, Y., Kitagawa, I., Kitamura, Y. and Fujimaki, H., 2020. Water and Salt Balance in Agricultural Lands under Leaching with Shallow Subsurface Drainage Used in Combination with Cut-Drains. Water, 12(11), p.3207.

Qi H, Qi Z, Zhang TQ, Tan CS, Sadhukhan D. Modeling Phosphorus Losses through Surface Runoff and Subsurface Drainage Using ICECREAM. J Environ Qual. 2018;47(2):203-211. doi:10.2134/jeq2017.02.0063

Qian, Y., Zhu, Y., Ye, M., Huang, J. and Wu, J., 2021. Experiment and numerical simulation for designing layout parameters of subsurface drainage pipes in arid agricultural areas. Agricultural Water Management, 243, p.106455.

Rhoades, J.D., Lesch, S.M., LeMert, R.D. and Alves, W.J., 1997. Assessing irrigation/drainage/salinity management using spatially referenced salinity measurements. Agricultural Water Management, 35(1-2), pp.147-165.

Ritzema, H.P., Satyanarayana, T.V., Raman, S. and Boonstra, J., 2008. Subsurface drainage to combat waterlogging and salinity in irrigated lands in India: Lessons learned in farmers' fields. Agricultural water management, 95(3), pp.179-189.

Šimùnek, J., M.T. Van Genuchten and M. Sejna, 2005.The hydrus-1d software package for simulating the one-dimensional movement of water, heat and multiple solutes in variably-saturated media. Univ.Calif. Riverside Res. Rep., 3: 1-240

Schoups, G., Hopmans, J. W., and Tanji, K. K.: Evaluation of model complexity and space–time resolution on the prediction of long-term soil salinity dynamics, western San Joaquin Valley, California, Hydrol. Process., 20, 2647–2668, https://doi.org/10.1002/hyp.6082, 2006.

Tavakoli-Kivi, S., Bailey, R. T., and Gates, T. K.: A salinity reactive transport and equilibrium chemistry model for regional scale agricultural groundwater systems, J. Hydrol., 572, 274– 293, https://doi.org/10.1016/j.jhydrol.2019.02.040, 2019.

Tiwari, P. and Goel, A., 2017. An overview of impact of subsurface drainage project studies on salinity management in developing countries. Applied Water Science, 7(2), pp.569-580.

Wei, X., Bailey, R.T. and Tasdighi, A., 2018. Using the SWAT model in intensively managed irrigated watersheds: model modification and application. Journal of Hydrologic Engineering, 23(10), p.04018044.

Wei, X., Bailey, R.T., Records, R.M., Wible, T.C. and Arabi, M., 2019. Comprehensive simulation of nitrate transport in coupled surface-subsurface hydrologic systems using the linked SWAT-MODFLOW-RT3D model. Environmental Modelling & Software, 122, p.104242.

Yao, R., Yang, J., Wu, D., Xie, W., Wang, X. and Zhang, X., 2017. Scenario Simulation of Field Soil Water and Salt Balances Using SahysMod for Salinity Management in a Coastal Rainfed Farmland. Irrigation and Drainage, 66(5), pp.872-883.

CHAPTER 3 – QUANTIFYING THE IMPACT OF TILE DRAINS ON SALINITY TRANSPORT IN IRRIGATED SEMI-ARID REGIONS

### 3.1 Introduction

Salinity in soils, groundwater, and surface waters is a critical issue for food security. To provide food for the world's population, which is expected to reach 9.7 billion people by 2050 (Rosegrant et al., 2002), the pressure to produce more with less water is intensifying. However, elevated soil salinity, which occurs in many arid and semi-arid regions due to low leaching potential, and waterlogging and evapo-concentration from shallow groundwater (Morway and Gates, 2012), impedes crop growth, decreasing overall production. Many regions experience this detrimental effect of salinity, including the western United States, eastern Australia, China, north and east Africa, and the Middle East (Abbas et al., 2013; Ivushkin et al., 2019), with approximately 33% of irrigated land affected (Ghassemi et al., 1995; Shirvastava et al., 2014). In response, many growers, cooperatives, and irrigation districts in these regions have installed artificial drainage systems to lower the water table (Hornbuckle et al., 2007; Hopkins et al., 2012; Feng et al., 2017). However, although these systems perform well in increasing crop production and ameliorating general soil health, they also are a major source of salt loading into receiving waters (Skaggs and Schilfgaarde 1999, Christen et al., 2001; Shrivastava and Kumar, 2015; Okuda et al., 2020; Addab et al., 2022), which affect nearby streams and downstream users, either for drinking water or irrigation needs. Because of these benefits and disadvantages, subsurface drainage can be regarded as a "double-edged sword" feature in agricultural landscapes. These benefits and disadvantages should be quantified under varying management and climatic conditions to determine optimal strategies for sustaining crop production while controlling downstream salinity pollution.

Recent studies have focused on the impact of drainage systems on in-system salinity (e.g. soil salinity) and drainage salt loading (i.e. salt that is conveyed by the drainage system to nearby surface water). These studies use field methods (Christen et al., 2001; Horbuckle et al., 2005; Jafari-Talukolaee et al., 2015; Okuda et al., 2020; El-Ghannam et al., 2021) and numerical modeling methods (Yao et al., 2017; Lu et al., 2019; Qian et al., 2021; Liu et al., 2021; Addab et al., 2022) to quantify the effect of drainage spacing, drain depth, and controlled drainage on soil salinity, crop yield, and salt loading in the drains.

*Field Methods*

Christen et al (2001) concluded that saline drainage water disposal is the key issue which may severely restrict future implementation of subsurface drainage in agriculture. Hornbuckle et al (2005) found that controlled drainage can reduce water drainage volumes and subsequently salt loads, decreasing negative downstream effects associated with subsurface drainage. Mehdi Jafari-Talukolaee et al. (2015) found that by increasing drain spacing decreased drainage water volume and salt load, and that increasing drain depth decreased electrical conductivity (EC) of drainage water. However, bi-level drainage systems increased EC in drainage water. Okuda et al. (2020) evaluated the effect of a low-cost shallow subsurface drainage system on salt removal and noted that the drainage system enhances salt removal from fields. El-Ghannam et al (2021) studied the influence of drain depth on drainage outflows, salinity buildup, irrigation system- and water use efficiencies, and seed yield of sunflower in field scale experiment.

*Modeling Methods*

Modeling studies for assessing impacts of subsurface drainage on system salinity and crop yield include a regional-scale water and salt balance approach using the SahysMod tool (Yao et al., 2017), field-scale experiments with HYDRUS and SWMS-2D (Yao et al., 2017; Lu et al., 2019; Qian et al., 2021; Liu et al., 2021), and watershed-wide (500 $km^2$) assessment using the SWAT-Salt (Bailey et al., 2019) model (Addab et al., 2022). Each of these approaches has benefits and disadvantages. Regional-scale water and salt balance modeling does not include important salt chemical processes (e.g. precipitation-dissolution of individual salt minerals and salt ions) and physically based groundwater-tile interactions; spatially refined, field-scale experiments elucidate key processes and outcomes for individual fields and drains, but do not assess impacts of a larger drainage system on crop yield and downstream water quality. Watershed-wide applications of SWAT-Salt allows rapid assessment of region-wide implementation of tile drains on salt yield (Addab et al., 2022), but is limited due to reliance on a lumped, linear reservoir, non physically based, spatially distributed approach to simulate groundwater flow and soil-drain interactions, the groundwater transport of salts and groundwater-drain interactions were only coarsely considered and not modeled in a physically based manner. There remains a need to investigate and quantify the impact of subsurface drains on crop yield, system salinity (soil, groundwater), and salt loads to receiving waters in a semi-arid, regional irrigated system using a spatially distributed, physically based approach.

The objective of this paper is to quantify the effect of tile drains on 1) system salinity and its impacts (i.e. groundwater salinity, soil salinity, crop yield, salt loading in drains) and 2) downstream salinity within the context of historical conditions. This objective is accomplished using a numerical groundwater flow and solute transport modeling system, MODFLOW and RT3D-Salt (Tavakoli-Kivi et al., 2019), applied to a 17 $km^2$ tile drained catchment in an irrigated region of the Arkansas River Valley, Colorado, USA. The RT3D-Salt model simulates the fate and transport of eight major ions ($SO_4$, Ca, Na, Cl, Mg, K, $CO_3$, and $HCO_3$) in a variably-saturated subsurface system, and is modified in this study to simulate the loading of salt ion mass from the aquifer to the tile drain system. The model is tested against groundwater levels, groundwater salt ion concentrations, tile drain flow volumes, and tile drain salt loadings. The tested model is used to determine the impact of the drainage system on crop yield (system benefit) and downstream water quality (system detriment) of receiving waters.

### 3.2 Methods

### 3.2.1 Study region

The study region, shown in Figure 3-1, is located in the Lower Arkansas River Valley (LARV) in southeastern Colorado, USA. The tile drain system, known locally as the Fairmont Drainage District (FDD) and one of 25 drainage districts located within the LARV that have been in operation since the early 20$^{th}$ century, is shown in red lines in Figure 3-1. The map shows the Arkansas River and two tributaries (Timpas Creek, Crooked Arroyo), irrigation canals (black lines), cultivated fields, and the location of groundwater monitoring wells (green dots). The outlet trunk of the drainage system is on the northern end of the system, and discharges to Timpas Creek, which then discharges to the Arkansas River, which flows from west to east. Main crop types in the area include wheat, sorghum, corn, alfalfa, legumes, melons and vegetables (Figure 3-2A). Irrigation is provided by either a system of canals (see Figure 3-1), which divert water upstream from the Arkansas River, or from a network of 35 pumping wells that extract water from the unconfined aquifer (see Figure 3-2A for well locations). Ground surface elevation (m) of the area ranges between 1241 m - 1289 m (Figure 3-2B).

The region is semi-arid in climate, with an average annual precipitation of 375 mm (14.5 in) and monthly average temperatures that range from -13 °C in January to 36 °C in July. The region has experienced high salinity in soils, groundwater, and streams (Arkansas River and tributaries) during the past few decades. Elevated salinity is due principally to the abundance of salt minerals (calcium carbonate $CaCO_3$, gypsum $CaSO_4$) in soils and aquifer materials (Konikow and Person, 1985; Gates et al., 2016) and the lack of adequate natural drainage, which, under conditions of irrigation, lead to shallow groundwater and consequent evapo-concentration of salts in the root zone and soil profile (< 2 m from ground surface). Soil salinities in the LARV range from 2 dS/m to 10 dS/m (average 4.1 dS/m), resulting in approximately 70% of the region experiencing a decline in crop yield in recent years (Morway and Gates, 2002). Due to salt leaching from the soil profile, groundwater salt concentrations are also high, averaging approximately 3,300 mg/L from $n$ = 443 samples taken between 2006 and 2010. High groundwater salt concentrations, coupled with high groundwater levels and a groundwater gradient that drive groundwater into the Arkansas River and its tributaries, particularly in the months following the irrigation season, have led to elevated salt concentrations in the Arkansas River, with an average of 1,145 mg/L (Gates et al., 2009).

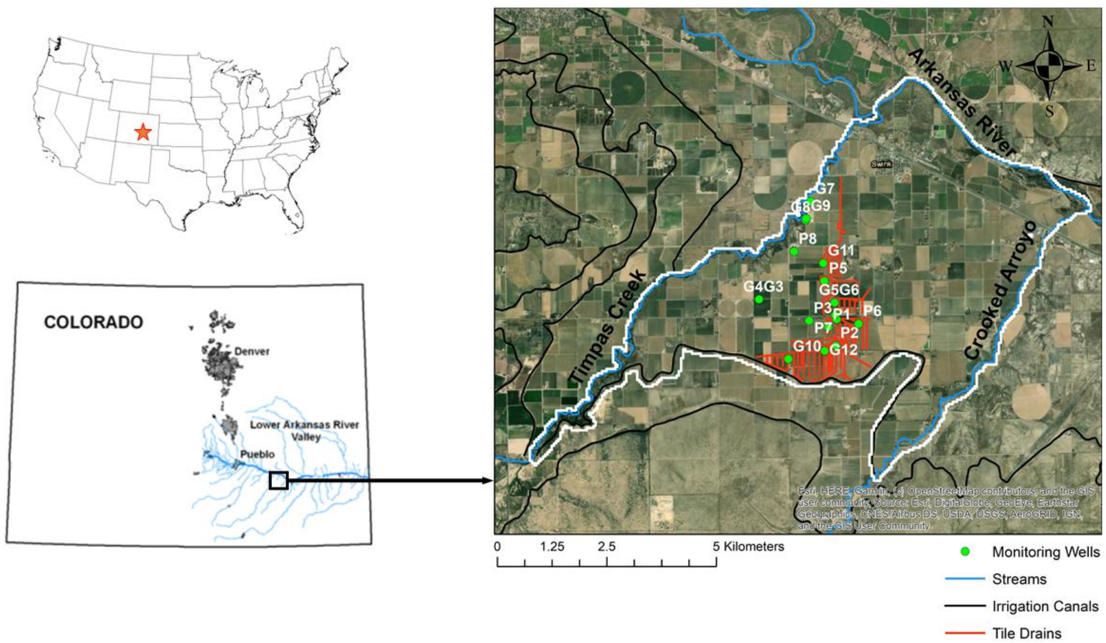


**Figure 3-1.** Map of the study region, located in the Lower Arkansas river Valley in southeastern Colorado. The map on the right shows the layout of the Fairmont Drainage District tile drains, irrigation canals, streams (Timpas Creek, Crooked Arroyo) and the Arkansas River, and groundwater monitoring wells for groundwater head and salt ion concentration measurements.

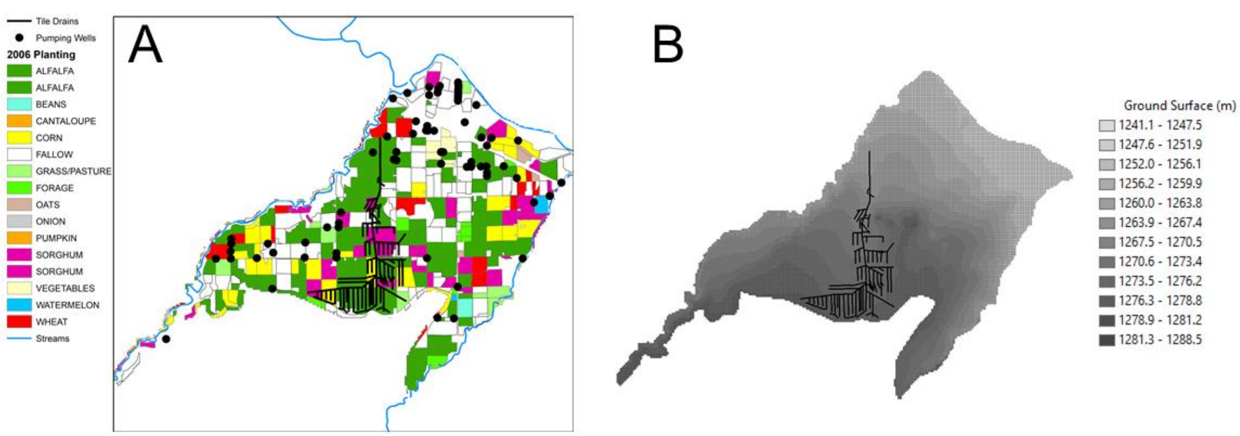


**Figure 3-2.** (A) 2006 crop types and (B) ground surface elevation (m) for the study region.

### 3.2.2 Field data collection

Field data were collected in this study to first, elucidate system conditions regarding groundwater levels, groundwater salinity, and tile drain salinity; and second, to provide data for model testing.

#### 3.2.2.1 Groundwater levels and salt concentration

A set of 15 groundwater monitoring wells (see Figure 3-1 for location) were installed during August 2014. The wells were completed in the unconfined aquifer (~10 m in depth for each well) as observation wells, using 2-inch PVC pipe, screened along its length to provide average groundwater head in the aquifer. A sand filter pack was used, with bentonite clay used as a surface seal. Each well was capped, with a lock. Each well was equipped with an Onset HOBO pressure transducer, to log pressure at 15-min intervals. An additional logger was placed in the open air within one of the wells to measure barometric pressure, which was subtracted from the transducer readings to obtain water pressure, which was converted to meters of pressure head. Readings were taken from May 2015 through November 2018.

Groundwater was sampled from each well for salt ion concentration measurement ($SO_4$, Ca, Na, Cl, Mg, K, $CO_3$, and $HCO_3$). Groundwater was extracted from the monitoring wells using a low-flow pumping technique with the Sample Pro® Portable MicroPurge Pump. The pump was placed into the well, situated at approximately the mid-point of the water column. Pumping continued until water quality parameters (pH, specific conductance, temperature, oxidation-reduction potential, dissolved oxygen) became stable to ensure groundwater came from the aquifer, at which point the sample was collected in a 1,000 mL plastic bottle. To prevent de-watering of the well and entrainment of air, the pumping rate was adjusted using a QED MicroPurge® Controller MP10 to ensure a flow rate of between 0.0001 to 0.0002 $m^3$ per minute, which allowed the water storage in the well column to remain constant. A unique tubing set was designated for each well, with the pump disassembled and washed with muriatic acid and a cation-free detergent solution between each well sample, and the tubing washed between sampling events (event = sampling from each of the 15 wells). The instruments were calibrated before each sample event. At the conclusion of each sampling event, the samples were shipped with ice to Ward Laboratories Inc. (Kearney, NE) for analysis. At each sampling event, at least one sample with distilled water was sent to the lab as a blank, as was a duplicate sample from one of the wells, for lab analysis verification. During the period of 2017-2018 each well was sampled 10 times (each year: 3 during the summer, 1 in October, and 1 in January), for a total of 150 groundwater samples.

#### 3.2.2.2 Tile drain outflow and concentration

Tile drain flow rate in the outlet drunk of the drainage system was estimated using the Stingray 2.0 Portable Level-Velocity Logger, which measures level and velocity in pipes. The watertight electronics enclosure, which includes a sealed ultrasonic sensor that mounts inside the pipe, was situated in the drainage pipe. The sensor was attached to a data logger via cords and enclosed in a water-tight box at the ground surface adjacent to the tile drain pipe. Unfortunately, the cords were repeatedly severed due to local wildlife activity, and data for only three months (May 24, 2018 to August 12, 2018) were recorded. Tile drain water samples were collected in the outlet trunk and analyzed for salt ion concentrations. Samples were collected using a peristaltic pump. Samples were shipped with ice to Ward Laboratories Inc. (Kearney, NE) for analysis. Thirteen samples were taken from May 24, 2017 to November 17, 2018.

### 3.2.3 Simulating salinity transport in an aquifer-drain system

This section provides an overview of RT3D-Salt (Tavakoli-Kivi et al., 2018), a numerical modeling code that couples the groundwater flow model MODFLOW and the groundwater solute reactive transport model RT3D to simulate salt ion concentration fate and transport in a stream-aquifer system, and how it was modified for application to the FDD study region. This section first provides details regarding MODFLOW, followed by RT3D-Salt. As an overview, Figure 3-3 shows a schematic of hydrologic and salinity transport processes simulated by the coupled MODFLOW/RT3D-Salt modeling system, with equilibrium chemistry reactions (precipitation-dissolution) simulated in the soil profile and unconfined aquifer. Some of the various processes that can be represented by the model are shown in the figure. Of note is the groundwater → drain water transfer, with accompanying salt ion mass loading.

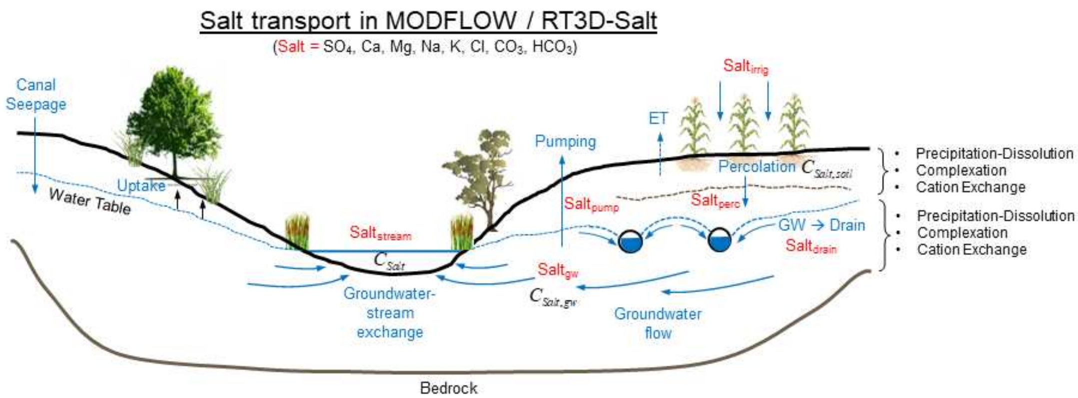


**Figure 3-3.** Watershed cross-section schematic showing the water (blue) and salt (red) processes simulated by the MODFLOW and RT3D-Salt numerical models. Salt consists of 8 major anions and cations, and salinity equilibrium processes (precipitation-dissolution, complexation, cation exchange) are simulated in both the soil and aquifer systems.

#### 3.2.3.1 Groundwater storage and interactions: MODFLOW

MODFLOW (McDonald and Harbaugh, 1988; Niswonger et al., 2011) is a three-dimensional, physical-based, distributed finite difference groundwater flow model for aquifer systems. The model combines conservation of mass with Darcy's Law and specified or calculated groundwater inflow/outflow volumetric flow rates to estimate groundwater storage and groundwater head throughout a specified aquifer domain. Inflow/outflow packages include recharge, vadose zone percolation, evapotranspiration, pumping (Well package), aquifer-river exchange (River package), and aquifer-drain exchange (Drain package). Flow rates for these various packages can be specified in space (per grid cell) and time (per stress period).

The MODFLOW grid used in this study uses 50 m by 50m grid cells, resulting resulting in 184 rows and 256 columns for a total of 47,104 cells. The model contains 6 layers to discretize the vertical distance between the ground surface and the bedrock. The topographical surface of each cell in the top layer of the model (see Figure 3-2B) was assigned using a 30-m Digital Elevation Model (DEM; USGS National Map System). Hydraulic conductivity $K$ and specific yield $S_y$ maps for the MODFLOW model are shown in Figure 3-4, with values obtained from the calibrated MODFLOW model of the larger region, reported in Morway et al. (2011).

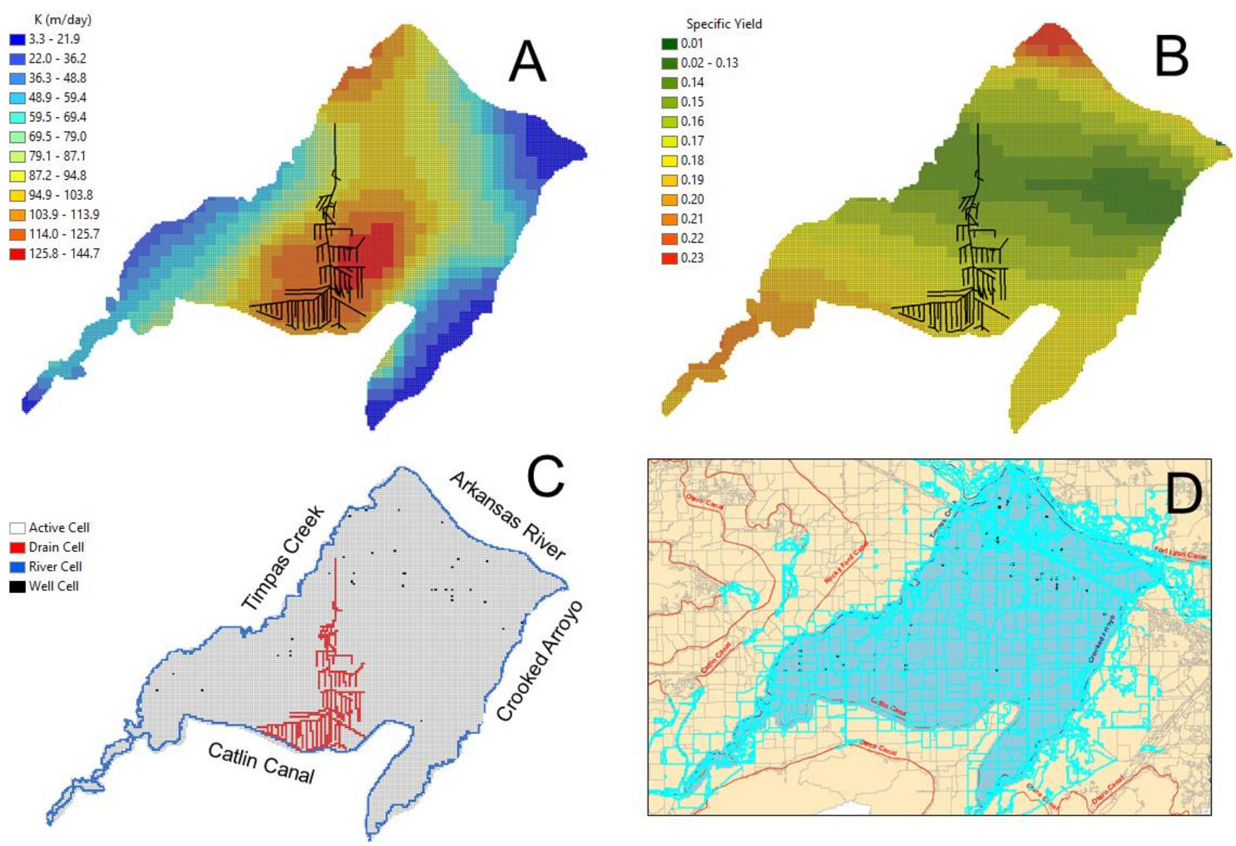


**Figure 3-4.** Maps of (A) hydraulic conductivity (K) (m/day), (B) specific yield, (C) MODFLOW cell types (drain, river, well), and (D) intersections between SWAT hydrologic response units (Wei et al., 2019) and MODFLOW grid cells.

Exchange rates of water between the aquifer and streams (Arkansas River, Timpas Creek, Crooked Arroyo, Catlin Canal) were simulated using the River Package of MODFLOW (1,315 blue cells in Figure 3-4C). Cell-by-cell stream bed elevation and stream stage were obtained from the DEM and stream gage data from the USGS (sites 07121500, 07120500). Exchange rates of water between the aquifer and drain network were simulated using the Drain package of MODFLOW (744 red cells in Figure 3-4C). For cells designated as Drain cells, groundwater is removed from the aquifer at a rate proportional to the difference between groundwater head and the drain elevation, so long as the head in the aquifer is above that elevation. Drain conductance is used to include the effect of tile drain material *K* on the rate of drain inflow. 744 drain cells are included in the model. A single conductance value is used for all Drain cells. Groundwater pumping is simulated using the Well package (37 black cells in Figure 3-4C). Daily pumping rates for the 37 pumping wells were obtained from the Colorado Division of Water Resources (CDWR). Percolation of infiltrating rainwater and irrigation in the vadose zone were simulated using the Unsaturated Zone Flow (UZF) package (Niswonger et al., 2006). Daily infiltration rates and potential evapotranspiration (PET) rates were provided to the UZF package using output from a calibrated SWAT model of the region (Wei et al., 2008), which for this study was extended through 2018. As SWAT uses hydrologic response units (HRUs), which are a geographic collection of polygons, as the computational unit, cell-by-cell rates of infiltration and PET were calculated by intersecting the HRU polygons and the MODFLOW grid cells, as shown in Figure 3-4D.

**3.2.3.2 Salt ion fate and transport: RT3D-salt**

RT3D is a three-dimensional groundwater contaminant and solute transport model that can simulate advection, dispersion, and chemical reactions of dissolved constituents in groundwater (Clement, 1997; Clement et al., 1998). The RT3D modeling code was modified by Bailey et al. (2013, UZF-RT3D) to simulate reactive transport of solutes in variably-saturated soil-aquifer systems, using percolation rates simulated by the UZF package of MODFLOW. The advection-dispersion-reaction equation of UZF-RT3D is:

$$\frac{\partial(C_k\theta)}{\partial t}R_k = -\frac{\partial}{\partial x_i}\left(\theta v_i C_k\right) + \frac{\partial}{\partial x_i}\left(\theta D_{ij}\frac{\partial C_k}{\partial x_j}\right) + q_f C_{f_k} + \theta r_f - \rho_b \frac{\partial \overline{c}_k}{\partial t} \qquad k = 1, 2, \ldots, m \quad (1)$$

where $C_k$ is the concentration of the $k^{th}$ dissolved-phase solute [$M_f L_f^{-3}$], with $f$ denoting the fluid phase; $D_{ij}$ is the hydrodynamic dispersion coefficient [$L^2T^{-1}$]; $v$ is the pore velocity [$L_bT^{-1}$] with $b$ denoting the bulk phase; $\theta$ is the volumetric water content [$L_f^3 L_b^{-3}$]; $q_f$ is the volumetric flux of water representing sources and sinks [$L_f^3 T^{-1} L_b^{-3}$] such as irrigation water, canal and seepage, groundwater discharge to the river, or pumped groundwater; $C_f$ is the concentration of solute in the source or sink water [$M_f L_f^{-3}$]; $r_f$ represents the rate of the reactions that occur in the dissolved phase [$M_f L_f^3 T^{-1}$]; $R_j$ is the retardation factor for species $j$ and is equal to $1+(\rho_b K_{d_j})/\theta$, where $\rho_b$ is the bulk density of the porous media [$M_b L_b^{-3}$] and $K_{d_j}$ is the partitioning coefficient for the $j$th species [$L_f^{-3} M_b$]; $\overline{c}_k$ is the total solid phase concentration of aqueous species $k$. UZF-RT3D uses output from a MODFLOW-NWT (Niswonger et al., 2011) that uses the UZF package for $v$ and $q_f$.

UZF-RT3D was further modified by Tavakoli-Kivi et al. (2018) to include salinity chemistry in soil water and groundwater. The salinity module simulates precipitation-dissolution of five major salt minerals ($CaSO_4$, NaCl, $MgSO_4$, $CaCO_3$, $MgCO_3$) in the soil and aquifer, and is linked within the code to standard RT3D subroutines to simulate the movement and transformation of major salt ions ($SO_4$, Ca, Na, Cl, Mg, K, $CO_3$, and $HCO_3$). Similar to other water chemistry models, the concentration of species at equilibrium is calculated using a stoichiometric algorithm for mass balance and mass action (Parkhurst and Appelo, 2013). The resulting modeling code, RT3D-Salt, simulates, for each time step of the simulation period, the change in concentration $C$ due to advection, dispersion, and kinetic reactions, with Equation (1) solved for $C$ for each of the eight salt ions, at each grid cell, followed by equilibrium chemistry for precipitation-dissolution mass exchange.

For this study, the RT3D-Salt model uses the same finite difference grid as MODFLOW and the simulated groundwater head, groundwater flow rates, and groundwater source/sink flux rates to simulate the fate and transport of salt ions. The following items are of importance when constructing the model:

*Crop type*: the yearly crop type must be specified for each grid cell. Seasonal crop growth effects crop ET, which effects soil water percolation, soil salinity, and resulting salt leaching to the water table. Yearly crop type was provided by USDA CropScape datasets for the region.

*Salt mineral fractions*: each grid cell must be provided an initial fraction of each of the 5 salt minerals. These fractions change throughout the simulation, as salt minerals dissolve into the soil water and groundwater, and then as salt ions precipitate back to solid form. The salt mineral fractions were provided by NRCS maps of the study region.

*Solubility constants*: the solubility of each of the 5 salt minerals is specified based on published literature values. These values do not change during the simulation.

*Salt mass in irrigation water*: irrigation is derived from either the Catlin Canal or the aquifer, via the 37 pumping wells. If irrigation water is from the Catlin Canal, the salt mass (g) added to the top layer of the model is calculated by multiplying the applied irrigation volume ($m^3$) by the measured concentration ($g/m^3$) of each salt ion in the canal water. If the irrigation water is from the aquifer, the salt mass (g) added to the top layer of the model is calculated by multiplying the measured pumping rate ($m^3$/day) by the simulated salt ion concentration of the groundwater ($g/m^3$).

*Salt mass in tributary/canal/stream seepage water*: The salt mass in surface water seeping into the aquifer is calculated by multiplying the flow rate simulated by MODFLOW ($m^3$/day) by the measured concentration ($g/m^3$) of each salt ion in the surface water.

#### 3.2.3.3 Aquifer-drain salt ion mass exchange

The RT3D-Salt modeling code was modified in this study to simulate the loading of salt ion mass from the aquifer to the tile drain system. For each of the 744 drain cells, MODFLOW simulates the volume ($m^3$) of groundwater removed from the aquifer by the drains, and within the RT3D-Salt code this volume is multiplied by the simulated concentration of each salt ion in the corresponding drain cell to calculate the salt ion mass that loads to the drains. This calculation is performed during each time step.

### 3.2.4 Simulation overview

The model was run for the 2008-2018 time period, using 0.5 day time steps for both the MODFLOW and RT3D-Salt models. MODFLOW was run first, with head and inflow/outflow flow rates saved and used by the RT3D-Salt model. Model output was compared to measured field data for modeling testing. Field data includes groundwater levels at the 15 monitoring wells during 2015-2018; tile drain outflow for the May-August 2018 period; tile drain salt ion loadings, estimated by multiplying tile drain outflow rate by salt ion concentration for 13 days in May-November 2018; and groundwater salt ion concentrations at the 15 monitoring wells during 2017-2018. Manual calibration was performed to achieve correct magnitudes of groundwater levels, tile drain outflow, and tile drain salt ion loading. For MODFLOW, only drain conductance (uniform for all drain cells) was adjusted. For RT3D-Salt, only the initial salt mineral fractions were adjusted, based on ranges provided in the NRCS soil map data.

### 3.2.5 System analysis and scenarios

A key objective of this study is to determine the impact of tile drains on two system responses: crop yield, as impacted by soil salinity; and downstream water quality, as impacted by tile drain loadings to Timpas Creek and then to the Arkansas River. As reported in other studies, we hypothesize that the presence of tile drains decreases soil salinity, thereby increasing crop yield, but also stresses downstream water systems due to salinity export. With temporally and spatially refined results from the MODFLOW/RT3D-Salt, we can quantify these impacts in a manner that has not yet been reported. To quantify the impact of tile drains on crop yield and downstream water quality, the MODFLOW/RT3D-Salt model was run with and without the Drain package in operation. The difference in crop yield was estimated using the relative yield $RY$ equation of Maas (1993):

$$RY = Str_{salt} = \left\{100 - \left[b * \left(EC_{sat} - a\right)\right]\right\} / 100 \qquad (2)$$

where *a* and *b* are the threshold (saturated electrical conductivity $EC_{sat}$, dS/m) and slope of salinity impact on yield decrease. $EC_{sat}$ is estimated by summing the salt ion concentrations in each grid cell to obtain total dissolved solids TDS (mg/L), multiplying by water content and then dividing by a TDS:EC conversion factor (1,020) obtained from an analysis of field data in the region (Gates et al., 2009). The parameters *a* and *b* are listed in Table 1 for the crop types in the study region, with the crop type for each grid cell obtained from the model input data.

The effect of tile drain salt ion export loadings on downstream water quality, i.e. the downstream in-stream salinity concentration, was estimated by performing a salt mass balance at the discharge point of the tile water into Timpas Creek, using measured flow from USGS gage site 07121500. As the gage site is located downstream of the tile drain discharge point, the flow upstream of the discharge point is estimated by adding the gage site flow volume to the simulated tile drain outflow volume. As Timpas Creek does not have measured salt ion concentrations upstream of the tile drain discharge point, we assumed several concentrations (0, 400, 800 mg/L) for the mass balance analysis. A similar analysis was performed for the Arkansas River, in the hypothetical scenario that it received the tile drain outflow and salt loading rather than Timpas Creek. This was performed to quantify tile drain effects on streams of disparate flow rates, the Arkansas River having a much higher discharge rate than Timpas Creek.

## 3.3. Results and discussion

### 3.3.1 Hydrologic results

#### 3.3.1.1 Groundwater levels

Spatially distributed groundwater results are shown in Figure 3-5. Figure 3-5A shows the cell-by-cell groundwater head (m) in July 2014 (middle of irrigation season), Figure 3-5B shows the increase in head (m) between April 2014 and July 2014, due to the application and recharge of irrigation water, and Figure

3-5C shows the depth to water table in July 2014. Flow patterns based on groundwater head equipotential lines (Figure 3-5A) show a general south→north flow direction, with local gradients toward Timpas Creek (on the west), Crooked Arroyo (on the east), and the Arkansas River (on northeast). Locations of groundwater level increase between April and July (Figure 3-5B) are moderate in and around the tile drain network, which experiences shallow water table conditions (Figure 3-5C), and hence the need for the drains to prevent waterlogging in these fields.

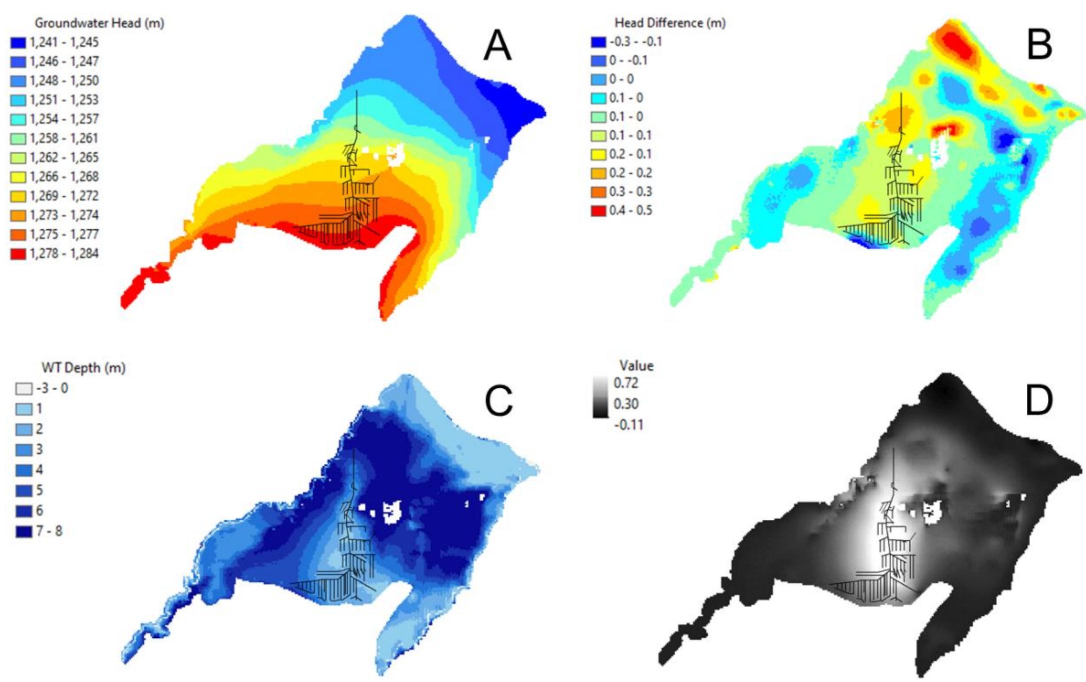


**Figure 3-5.** Spatial results of the MODFLOW simulation, showing (A) groundwater head (m) during July 2014, (B) the increase in groundwater head (m) between the late spring (April 2014) and summer (July 2014), (C) water table depth (m) during July 2014, and (D) the difference in groundwater head (m) in July 2014 if drains are not installed.

Temporal patterns at four monitoring wells, selected to represent area both without (well G4, well G7) and within (P5, G2) the drain network footprint, are shown in Figure 3-6, for both simulated results (blue line) and measured levels (red dots with hashed connecting lines). The ground surface at each location is also shown on the plots (black line), indicating the shallow nature of groundwater in this area. Simulated values represent well the magnitude and seasonal dynamics of groundwater levels in these wells. The comparison between observed and simulated groundwater head (m) at the locations of the monitoring wells is shown in Figure 3-7, using a 1:1 plot and a frequency distribution of head residuals. The mean absolute error (MAE) of the model values is 0.44 m, with only a few residuals greater than 1 m. From these results we conclude that the model is an adequate simulator of shallow water table conditions in the vicinity of tile drains.

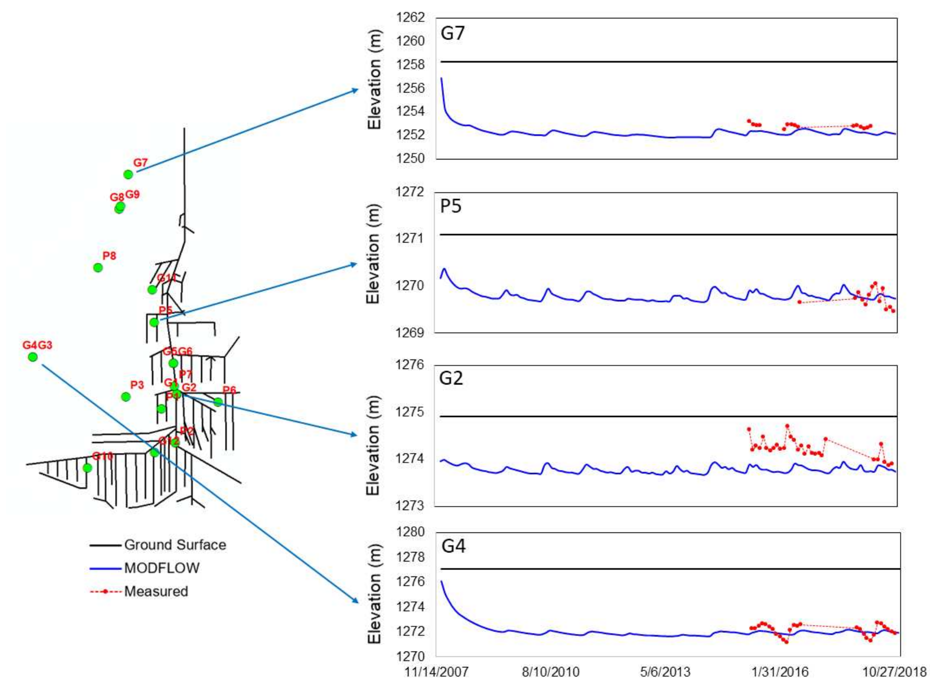


**Figure 3-6.** Times series of simulated (blue line) and measured (dashed red line) groundwater head at four selected groundwater monitoring wells within the tile drain area.

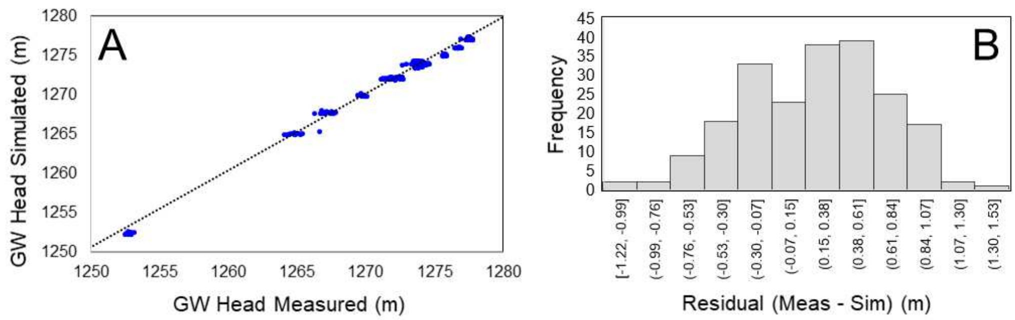


**Figure 3-7.** Results of MODFLOW simulation, showing (A) comparison between measured and simulated groundwater head at groundwater monitoring wells (see locations in Figure 3-1) and (B) residuals of the simulated groundwater head values.

### 3.3.1.2 Tile flow

Results of simulated aquifer-drain exchange are shown in Figure 3-8. These results are achieved based on manual calibration, with the fit between measured and simulated tile drain flows balanced by the fit with the groundwater levels (Section 3.1.1). Figure 3-8A shows the simulated (blue) ad measured (red) daily summation of tile flows, with the simulated values calculated by summing the groundwater-drain exchange for each of the 744 cells. Figure 3-8B shows the same results, but only for the period of 81 days in 2018 for which tile drain flow was measured. This comparison assumes that the groundwater flowing into each tile section (i.e. each 50 m grid cell) reaches the outlet trunk on the same day. Although the general magnitude and temporal pattern of tile flow is achieved by the model, in particular the general flow increase in June and steady flow in July and August, we are not able to capture the short-term temporal dynamics of tile flow as exhibited by the measured data. This could be due to the use of a single conductance value for all 744 Drain cells, rather than spatial-varying conductance, which could be a result of spatial-varying soil properties in the region. In total, 597,284 $m^3$ of water was measured as flowing through the tile outlet trunk during these 81 days, compared to a simulated value of 486,333 $m^3$/day (81%), for daily averages of 7,374 $m^3$/day and 6,004 $m^3$/day, respectively. The measured volume of 597,284 $m^3$, when compared to the geographic footprint of the tile drain network (~ 6 $km^2$), equates to a depth of 0.1 m. When compared to other groundwater budget terms (see Table 1), drainage flux is 53% of the value of recharge, 7.8 times that of pumping, and 45% of the value of groundwater ET.

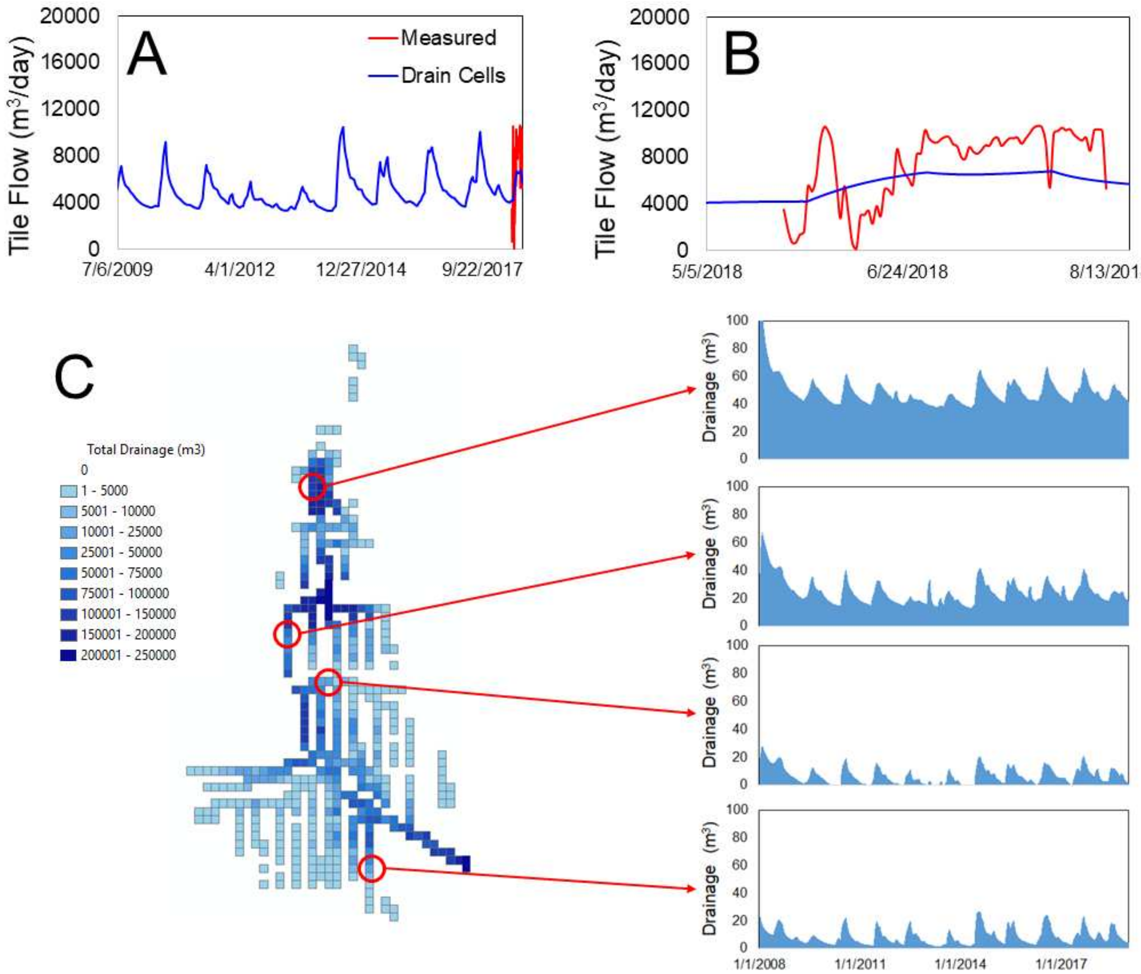


**Figure 3-8.** Spatial and temporal drainage results of the MODFLOW simulation. (A) shows the total daily volume of groundwater entering the drains during the simulation period. (B) shows the simulated daily volume of groundwater entering the drains during the 2018 growing season, as compared to the field-estimated tile drain flow in the main drainage trunk. (C) shows the total volume of groundwater ($m^3$) entering the drains for each drain cell during the 2010-2018 period, with time series of daily groundwater outflow for 4 selected drain cells.

**Table 3-1.** System-wide groundwater balance during the 2008-2018 MODFLOW simulation for the condition with drains and without drains. All values are in $m^3$.

| Groundwater Flux | With Drains | Without Drains | % Difference |
|---|---|---|---|
| Recharge | 2.99E+07 | 3.12E+07 | 4% |
| Canal Seepage | 4.28E+08 | 4.27E+08 | 0% |
| Groundwater ET | 3.52E+07 | 3.90E+07 | 11% |
| Drains | 1.59E+07 | 0.00E+00 | - |
| Groundwater Discharge | 7.71E+07 | 7.95E+07 | 3% |
| Pumping | 2.04E+06 | 2.22E+06 | 9% |
| Change in Storage | 3.27E+08 | 3.37E+08 | 3% |

Figure 3-8C shows the spatial variation of groundwater discharge to tiles, with flow rates (summed over 2008-2018 period) shown for each of the 744 Drain cells, highlighting the strong dependence of groundwater-tile discharge on location. Values range from 0 to 254,000 $m^3$ (daily average of 63 $m^3$). These differences are due to the local patterns of groundwater head in relation to the elevation of the drains, local variation in aquifer *K*, and localized groundwater gradients. These differences are highlighted by the time series of four drain cells shown in Figure 3-8. From top chart to bottom chart, total drainage outflows during the 2008-2018 period are 154,000 $m^3$, 74,000 $m^3$, 28,000 $m^3$, and 19,000 $m^3$, respectively.

#### 3.3.1.3 Comparison without drains

The simulation without tile drains (i.e. removing the Drain package from the MODFLOW solution) shows a 4% increase in recharge, an 11% increase in groundwater ET, and a 9% increase in pumping, all due to the additional groundwater available that was not removed by the tile drain network. The spatial distribution of groundwater head difference (m) is shown in Figure 3-5D, for July 2014, with cell values representing the increase in groundwater head due to the removal of tile drains. The increase can be up to 0.72 m within the immediate vicinity of the drain network. This difference is significant, as groundwater levels in this region typically are within a few meters of the ground surface (see time series plots in Figure 3-6).

### 3.3.2 Salt ion results

Simulated and measured tile drain salt ion loads are shown in the time series charts in Figure 3-9. As with the tile drain flow comparisons, we assume that the groundwater salt mass loading into each tile section reaches the outlet trunk on the same day. Temporal patterns of simulated daily salt ion loadings, as shown in Figure 3-9, are due to a combination of groundwater fluctuations (see Figure 3-8) and local salt ion transport and precipitation-dissolution reactions. From the results we conclude that, for several ions ($SO_4$, Ca, Mg, $CO_3$), the simulated loading values are close in magnitude to the measured loads during the 2018 growing season. Unfortunately, due to the lack of measurement data, we are not able to test the model for seasonal dynamics. For $SO_4$, the sum of the loads for the five days of measurements is 72,600 kg, compared to a simulated value of 67,400 kg (93%). Percent of measured for Ca and Mg is 125% and 90%, respectively. Results for Na, $HCO_3$, and Cl are poor, with percent of measured equal to 42%, 16%, and 223%. However, as the vast majority of salt is composed of $SO_4$ and Ca, the measured and simulated total salt loads are 127,900 kg and 109,300 kg, respectively, with the simulated value 85% of the measured value. The dominant salt ion in tile drainage water is $SO_4$, due to the prevalence of the salt mineral gypsum ($CaSO_4$) in the region's soils. This is true of soil water, groundwater, and surface water in the LARV in general (Gates et al., 2002; Gates et al., 2009).

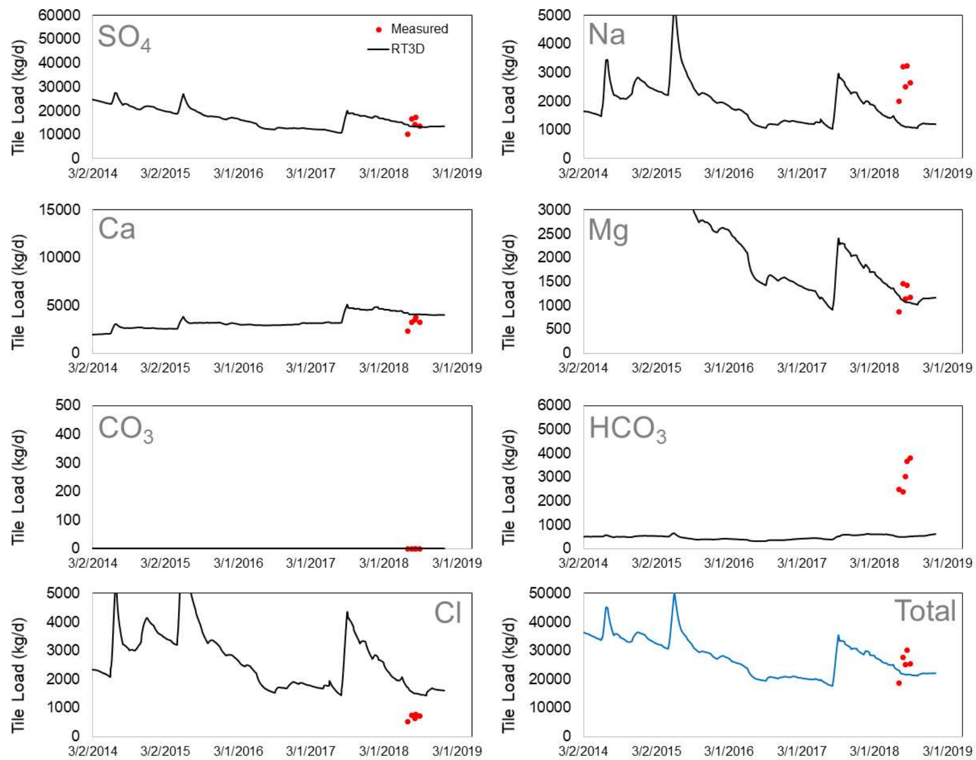


**Figure 3-9.** Simulated (black line) mass entering the drain system from groundwater, and field-estimated (red dots) tile load (kg/day) in the main drainage trunk, for 7 salt ions and for total salt.

Maps of cell-by-cell salt loading (kg) are shown in Figure 3-10, with two cells selected for time series plotting (charts below the maps). From these maps we conclude that spatial variation in loading is significant, with many areas exhibiting no loading of $SO_4$, Ca, or Na to the tile drain network. By comparing to the groundwater-drain discharge maps shown in Figure 3-8C, hotspots of tile drain salt loading often coincide with areas of high groundwater-drain flow rates, but not always, due to areas of low salt ion concentrations in the aquifer. These spatial variations in groundwater concentrations are shown in Figure 3-11 for $SO_4$, Ca, and Na, for the final day of the simulation (December 31, 2018). These maps show a strong spatial variation in simulated groundwater concentrations. Curiously, although tile drain (i.e. groundwater→drain) loads of $SO_4$ and Ca match the measured loads in magnitude (see Figure 3-9), there is a significant mismatch between simulated and measured groundwater concentrations, as indicated by the frequency distribution plots shown on the right in Figure 3-11. For these plots, simulated

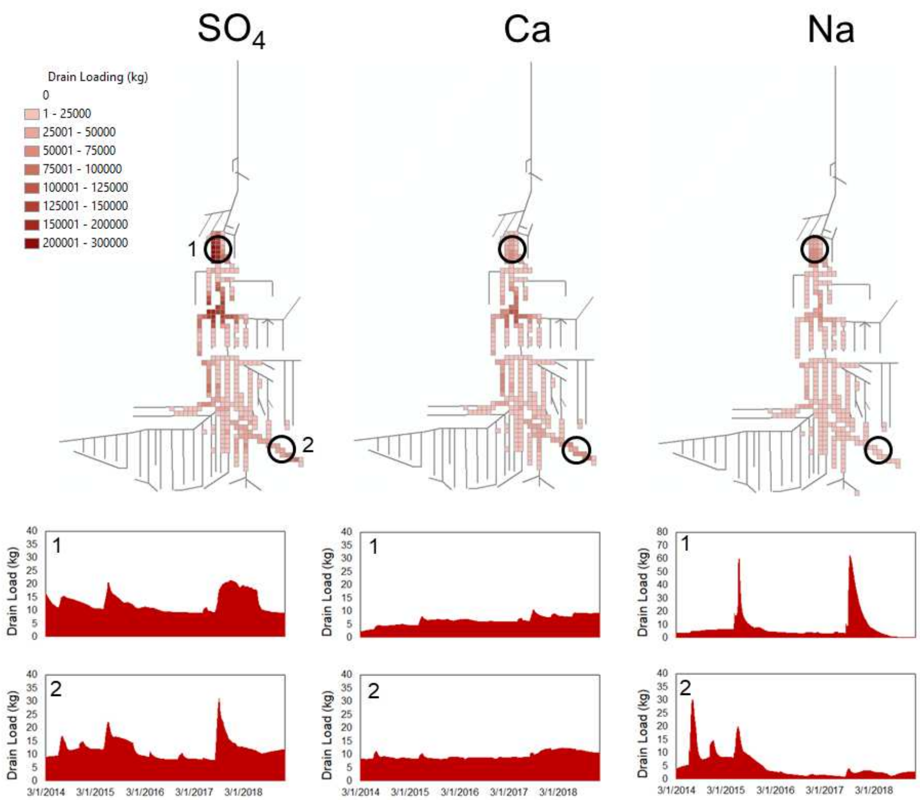


**Figure 3-10.** Maps showing total mass (kg) of $SO_4$, Ca, and Na entering the drains for each drain cell during the 2014-2018 period, with time series of daily groundwater mass loading for 2 selected drain cells.

values are retrieved from cells within the vicinity of the tile drain network. Simulated $SO_4$ concentrations are much higher (mean = 15,913 mg/L for 3,520 grid cells) than measured concentrations (mean = 1,911 mg/L for 159 samples), and simulated Ca concentrations are much lower (mean = 306 mg/L compared to mean = 394 mg/L), although for Ca the majority of cells have a concentration between 100-200 mg/L, whereas the measured data are generally evenly spread in number across 150-600 mg/L. For Na, although the simulated groundwater concentrations are much higher than the measured concentrations, the simulated tile drain loads are lower than the measured loads (see Figure 3-9, Na plot). Therefore, since groundwater→drain flow rates are reasonable as compared to measured rates (Figure 3-8B), and salt ion concentration data in the groundwater that discharges to the drains is reasonable, then we conclude that the measured groundwater concentrations do not capture the totality of groundwater salinity in the region, particularly adjacent to the tile drains.

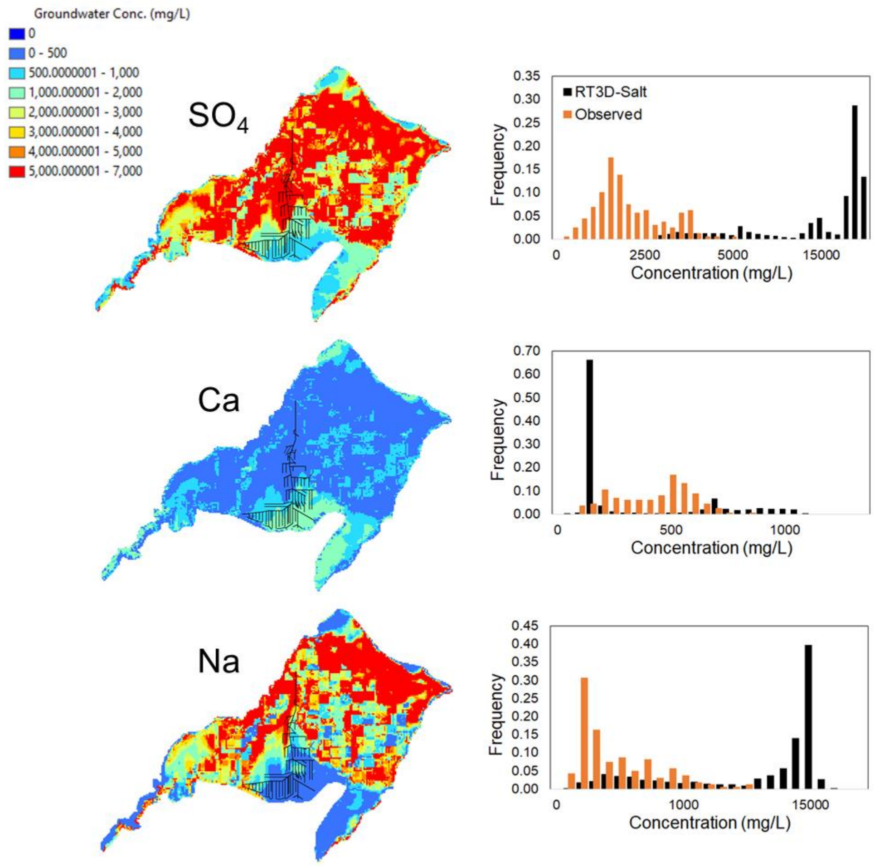


**Figure 3-11.** Maps showing simulated groundwater concentration of $SO_4$, Ca, and Na at the final day of the simulation (December 31, 2018), along with frequency distribution plots showing simulated and measured groundwater concentrations at locations of groundwater monitoring wells.

In general, the difficulty in matching tile drain salt loadings and groundwater salt ion concentrations is due to several factors: 1) measured loads are based on a grab sample of tile drain water, which we assume is constant throughout the day; and 2) the model is extremely sensitive to initial salt mineral fractions for the 5 salt minerals. For the latter, the NRCS soil maps were used to population spatial data for $CaSO_4$ and $CaCO_3$. Provided values often are given as ranges, with many soil types missing data. In addition, the soil maps do not contain information for content of NaCl, $MgSO_4$, and $MgCO_3$, resulting in values based on a literature review. However, when assessing the sensitivity of model output to NaCl soil fractions, we noticed that increases in fractions would yield an over-estimation of Cl tile drain loads (see Figure 3-9, Cl plot), but an underestimation of Na tile drain loads (Figure 3-9, Na plot), and no salt mineral fractions would achieve a balance between the two.

Results for both groundwater and salt ion loading point to the need for more comprehensive salinity data sets (groundwater, tile drain water) in areas directly adjacent to tile drains. In general, however, we conclude that the model performs adequately in simulating salt ion export from a subbasin that contains extensive tile drainage.

**3.3.3 The influence of tile drains**

**3.3.3.1 Within system: crop yield**

Results of estimating relative crop yield are shown in Figure 3-12 for the conditions of July 2012. Estimated $EC_{sat}$ for each grid cell is shown in Figure 3-12A, showing large spatial variations in ECsat throughout the model domain, particularly in the areas within and around the tile drain network. Due to the over-estimation of soil water and groundwater salt ion concentrations to match the tile salt ion loadings (see Section 3.2), $EC_{sat}$ values are very high (mean = 14.52 dS/m), leading to an average relative yield of 33%, with spatial distribution of relative yield shown in Figure 3-12C. Although these values are higher ($EC_{sat}$) and lower (relative yield) than in the real system, we can still make comparisons with the condition of no drainage. These results also are shown in Figure 3-12. The difference in $EC_{sat}$ between the drainage and no drainage conditions (drain – no drain) for each grid cell during July 2012 is shown in Figure 3-12B, and corresponding differences in relative yield are shown in Figure 3-12D. Of note is the variation in the tile drainage area, with the "downstream areas" experiencing much higher salinity concentrations under the scenario with no drains and therefore lower relative yield (black and purple color areas in Figures 3-12B and D, respectively), whereas the "upstream areas" experience the opposite effect. This is due to the downstream areas experiencing, under normal drainage conditions, a large outflow of groundwater (see the map in Figure 3-8C) and associated salt ion mass (see Figure 3-10, $SO_4$

map), with this groundwater and salt mass remaining in the subsurface and thereby increasing soil salinity and decreasing crop yield. In the upstream areas, soil salinity decreases in the condition with no drainage, leading to an increase in crop yield. This area (see Figure 3-11, $SO_4$ map and Na map) is an area of low groundwater salt ion concentration, and likely the incoming irrigation water has a higher salt concentration than the soil water and groundwater, leading to dilution if the groundwater remains in the subsurface rather than being removed via the drains.

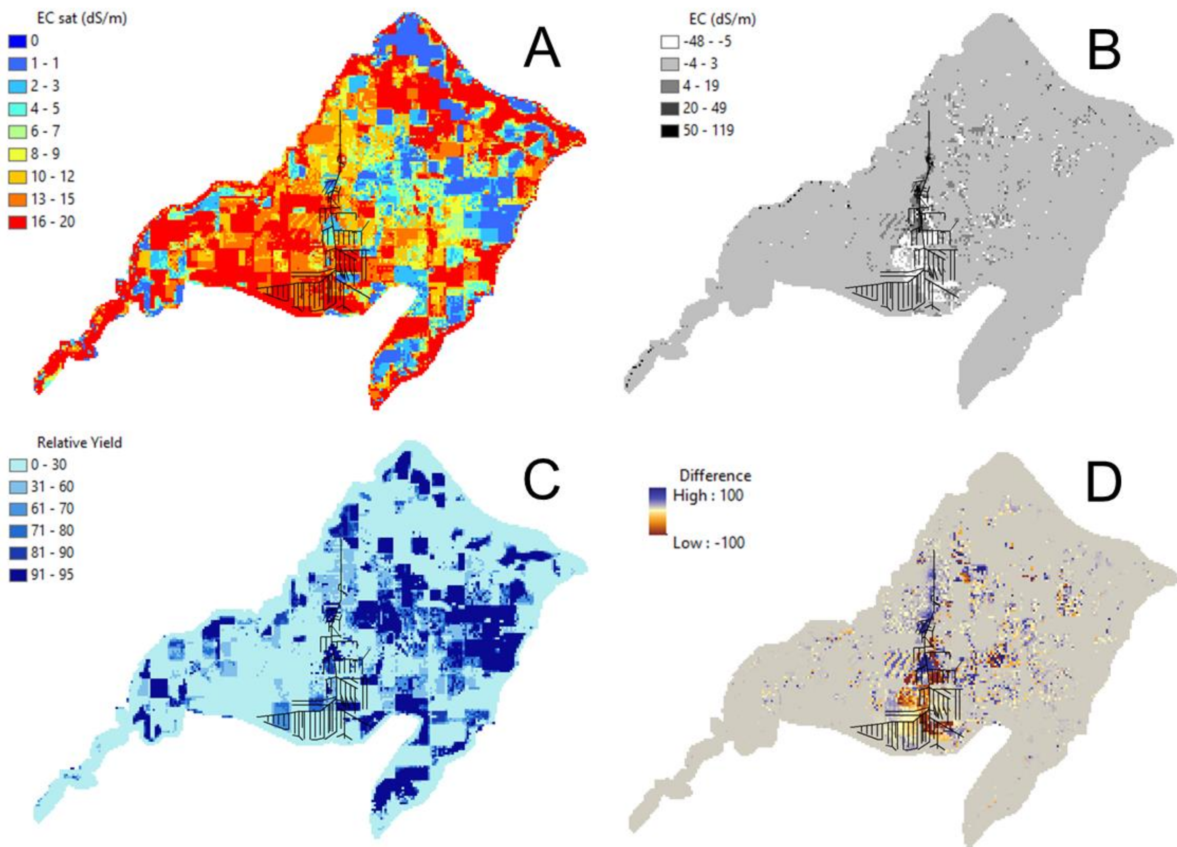


**Figure 3-12.** (A) Estimated saturated EC from model simulation salt ion results in layer 1, (B) the difference in EC between the "no drain" condition and the "drain" condition, (C) estimate relative yield based on model simulation salt ion results in layer 1, and (D) the difference in relative yield between the "drain" condition and the "no drain" condition.

### 3.3.3.2 Outside of system: impact on downstream water quality

The effect of tile drain salt loading on nearby receiving waters is summarized in the time series charts of Figure 3-13. Figure 3-13A shows the measured flow rate ($m^3$/sec) at the Timpas Creek USGS gage (located downstream of the tile drain inflow location) and the simulated volume of groundwater removed via tile drains (i.e. the volume of tile drain outflow) for each day during the 2014-2018 period. The chart shows the seasonal patterns, with higher flows during the summer and fall months. Figure 3-13C shows the corresponding estimated in-stream concentration of salt (TDS = summation of all salt ions) due to the simulated daily tile drain salt loading to Timpas Creek, with assumed upstream concentrations of 0 mg/L 400 mg/L, and 800 mg/L. For each of the three scenarios, the tile drain loading has a strong effect on Timpas Creek water quality. For the condition of 0 mg/L in upstream Timpas Creek water, the average concentration downstream of the tile drain outflow point is 220 mg/L; for 400 mg/L, the average is 606 mg/L, (i.e. 206 mg/L higher than the upstream concentration); and for 800 mg/L, the average is 991 mg/L, 191 mg/L higher than the upstream concentration.

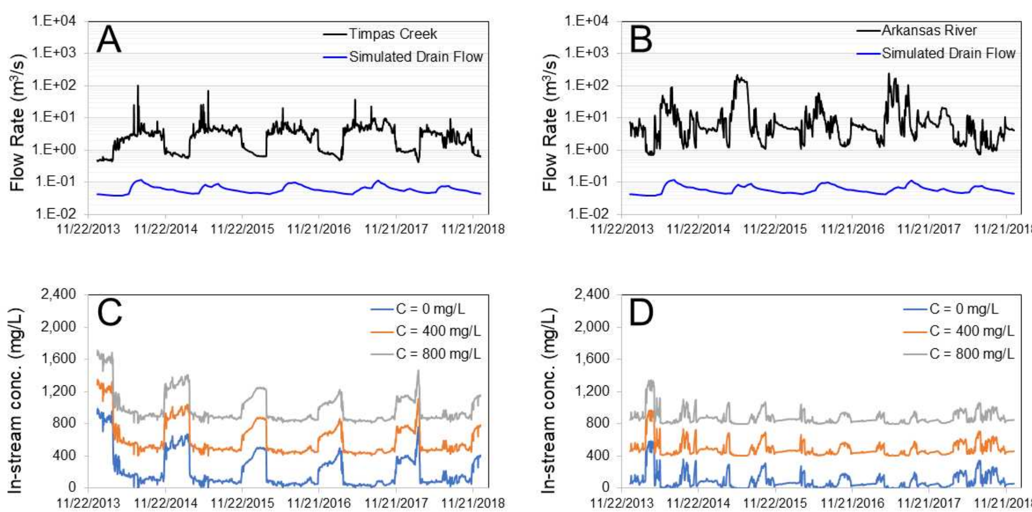


**Figure 3-13.** (A) measured flow rate at the Timpas Creek USGS gage site and simulated groundwater drain inflow, (B) measured flow rate the Arkansas River Las Animas USGS gage site and simulated groundwater drain inflow, (C) in-stream concentration of salt in Timpas Creek downstream of drainage point loading, based on upstream concentrations of 0, 400, and 800 mg/L, and (D) in-stream concentration of salt in the Arkansas River downstream of drainage point loading, based on upstream concentrations of 0, 400, and 800 mg/L.

Corresponding results are shown for the Arkansas River, in the hypothetical scenario that the tile drains discharge directly to the Arkansas River. The measured flow rate at the Las Animas gage site (USGS site 7124000), located downstream of the Timpas Creek confluence point with the Arkansas River, is shown in Figure 3-13B with the simulated tile drain outflow rate. Of course, the flow rate in the Arkansas River is higher than in Timpas Creek, a tributary. However, the effect on the in-stream concentration of salt in the Arkansas River is similar to the effect on Timpas Creek, although muted due to higher flow rates. For the condition of an upstream concentration of 0 mg/L, the average downstream concentration is 93 mg/L; and for 400 mg/L and 800 mg/L the downstream concentration is 486 mg/L and 879 mg/L, respectively. Therefore, in general the tile drain loadings increase the Timpas Creek salt concentration by approximately 200 mg/L, and increase the Arkansas River salt concentration by approximately 85 mg/L. These salinity increases can have significant effects on crop yield if downstream water is diverted for irrigation, and on overall ecosystem health if the water is received and accumulated in lakes or reservoirs.

Therefore, although installation of tile drains is beneficial for the tile area, leading to decreased groundwater levels, soil salinity, and increased crop yield, salt loads exported to receiving waters can lead to poor growing conditions downstream and decreased ecosystem health (Gill et al., 2015). These benefits and negative effects should be balanced in region-wide assessments of salinity control.

### 3.3.4 Limitations of this study

The approach presented in this paper uses a physically based spatially distributed groundwater flow and solute transport model, MODFLOW/RT3D-Salt, to quantify groundwater storage, groundwater movement, salt ion mass storage, and salt ion mass transport in a coupled soil-aquifer irrigation system under the influence of tile drains. The model performs well in simulating groundwater levels, but the extent to which the model is good simulator of tile drain outflow and salt ion loading is limited, due to limited measurement data (summer months of 2018) as a consequent of equipment problems. Simulated flow and loadings during 2018 match measured values to a reasonable degree, but additional years of data are required to attach a strong degree of confidence to model results, and therefore the results of model scenarios for relative crop yield and downstream water quality effects. In addition, although groundwater levels, tile flow, and tile drain loadings are matched in terms of magnitude and temporal patterns, the simulated groundwater salt ion concentrations are much too high compared to samples taken from the network of 15 monitoring wells during the 2017-2018 period. Therefore, we have more confidence in the results for downstream water quality (Figure 3-13) than for changes in crop relative yield (Figure 3-12), although conclusions can still be made using comparisons between "drainage" and "no drainage" scenarios can still be made, even if the base model over-predicts soil salinity and groundwater salinity.

These study limitations speak to the difficulty in quantifying, in a spatially distributed manner, groundwater discharge and groundwater salt ion loadings to a network of tile drains. 15 monitoring wells were installed, at a considerable cost in terms of time and funding, but likely more wells are needed to accurately depict the true spatial variation of groundwater salt ion concentrations. Having a flow-meter and taking grab samples at the tile drain outlet trunk is helpful for system-wide model testing, but placing these at several locations throughout the tile drain pipe network would allow for additional model testing, particularly since results (Figure 3-8C, Figure 3-10) indicate a strong spatial disparity in groundwater inflows and salt ion loadings. However, these needs must be balanced by available funding, as monitoring well drilling and the purchase and installation of flow-meters, e.g. Stingray level-velocity meters are costly.

However, we feel that this study represents an important step in representing salt fate and transport in a tile drained stream-aquifer system, using a combination of physically based spatially distributed models. Next steps include including more instrumentation to the study site, for several years, to provide robust data sets that can be used for additional model testing.

### 3.3.5 Comparison between swat-salt and rt3d -salt

This dissertation used two disparate models to analyze tile drain flow and salt transport. SWAT-Salt is a process-based, lumped hydro-chemical transport model that is ideal for large-scale applications, using a hydrologic response unit (HRU) as the computational unit for water balance and salt mass balance. Conversely, MODFLOW/RT3D-Salt is a physically based spatially distributed model that operates at the level of individual grid cells for groundwater and salt mass balance, and often requires small-scale applications for convergence and application. The movement of salinity in SWAT-Salt in the groundwater system is simulated in a simplistic manner at the HRU level, due to the use of steady-state and lumped equations in SWAT's groundwater module. However, MODFLOW/RT3D-Salt uses physically based spatially distributed flow and reactive transport modeling for groundwater and associated solutes. Within SWAT-Salt, tile drain water flow, and associated salt mass, is simulated as pulse loadings, often large in magnitude but infrequent in time. In contrast, in MODFLOW/RT3D-Salt, flow is simulated as diffuse transport of water from the soil/aquifer into individual tile drains, based on groundwater gradients and aquifer-drain interactions.

Results from Chapter 4 indicate that deeper tile drains, while yielding a large quantity of salt mass, can yield lower concentrations in receiving waters due to the higher tile drain outflow volume. Ideally, the modeling framework of MODFLOW/RT3D-Salt could be used to explore the relationship between salt yield in upstream tile drain networks vs. salt concentration in downstream receiving waters, as this downstream water is used for irrigation and/or drinking water supply. However, due to the complexity of MODFLOW/RT3D-Salt and the overall difficulty in its application at large scales, this is unfeasible currently. In contrast, SWAT-Salt, due to its lighter computational burden, could be used at the large spatial (i.e. regional, river basin) scale to explore these tradeoffs. Results from Chapter 2 suggest that tile drain loads provide short-term, large-magnitude pulses into the river, but that these do not change the overall salt balance in the watershed. Further research could investigate the resulting in-river salt concentrations downstream due to these tile drain salt loading pulses, and then apply the model to investigate and quantify regional tradeoffs of tile drain salt yield.

### 3.4. Summary and Conclusions

This paper introduces a new version of RT3D-Salt that simulates the fate and transport of salt ions ($SO_4$, Ca, Na, Cl, Mg, K, $CO_3$, and $HCO_3$) in irrigated watersheds drained by artificial subsurface tile drains. The model uses output from a MODFLOW model that uses the Drain package, with simulated groundwater-drain discharge rates multiplied by simulated salt ion groundwater concentrations to estimate salt ion loadings to tile drains. The model is run for the 2008-2018 period for the Fairmont Drainage District in the Lower Arkansas River Valley, Colorado, USA, and accounts for major hydrologic fluxes (infiltration, ET, vadose zone percolation, canal seepage, pumping, groundwater-surface water exchange, groundwater-drain discharge) and salinity processes (transport with all hydrologic fluxes, precipitation-dissolution reactions). Model results are tested against groundwater levels, tile drain outflow rates, groundwater salt ion concentrations, and tile drain salt ion loadings, whereupon the model is used to assess the impact of salinity on crop yield and the salinity concentrations of waters that receive the tile drain effluent. From results of the testing and scenario analysis we conclude the following:

- The model tracks groundwater levels and tile drain outflow well; however, groundwater levels were available for 2015-2018 whereas tile drain outflow rates were available only for 3 months during the 2018 growing season, due to equipment failure. Additional tile drain outflow rate measurements are needed to perform a thorough audit of the MODFLOW model.
- For most salt ions, the model estimates the correct magnitude of tile drain salt loading during the 2018 growing season. However, this came at a cost of over-estimating groundwater salt ion concentrations. Like the flow results, additional sampling of tile drain effluent is needed to further test the RT3D-Salt model. More monitoring wells should be installed to clarify spatial variation and magnitude of groundwater salt ion concentrations.

- Including tile drainage in this area only slightly improved soil salinity and crop yield conditions; however, export loading from the drains has a strong negative impact on the water quality of receiving waters. Timpas Creek, a tributary to the Arkansas River, experiences an overall increase of approximately 200 mg/L in the areas immediately downstream of the tile drain outflow point. If the tile drains loaded to the Arkansas River, the downstream concentration increase would be approximately 85 mg/L. These increases can have detrimental impacts on downstream crop yield, if river water is diverted and used as irrigation water, and ecosystem health.

In general, this study adds to the literature on balancing the positive and negative aspects of tile drainage in regards to salinity. Tile drains remove excess groundwater and salinity, leading to improved soil conditions and crop yield, but at a price, as the removed salinity is passed on to downstream stakeholders. The model introduced in this study, and the methods presented herein, can be used to assist in salinity management schemes in saline-affected regions, to balance crop yield sustainability and downstream water quality needs.

REFERENCES


Abbas, G., Saqib, M., Rafique, Q., Rahman, A. U., Akhtar, J., Haq, M. A. U., & Nasim, M. (2013). Effect of salinity on grain yield and grain quality of wheat (Triticum aestivum L.). Pak J Bot, 50, 185-189.

Ayars JE, Christen EW, Hornbuckle JW. Controlled drainage for improved water management in arid regions irrigated agriculture. Agricultural water management. 2006 Nov 16;86(1-2):128-39.

Bailey, R.T., Morway, E.D., Niswonger, R., and Gates, T.K., 2013b, Modeling variably saturated multispecies reactive groundwater solute transport with MODFLOW-UZF and RT3D. Groundwater, 51(5), 752-761.

Bailey, R.: SWAT-Salt: Source code for original SWAT model and new salt transport subroutines, available at: https://github.com/ rtbailey8/SWAT_Salinity, last access: 22 July 2019.

Christen EW, Ayars JE, Hornbuckle JW. Subsurface drainage design and management in irrigated areas of Australia. Irrigation Science. 2001 Dec 1;21(1):35-43.

Clement, TP. A Modular Computer Code for Simulating Reactive Multi-Species Transport in 3-Dimensional Groundwater Systems, report, June 24, 1999; Richland, Washington.

El-Ghannam, M., Aiad, M. and Abdallah, A., 2021. Irrigation efficiency, drain outflow and yield responses to drain depth in the Nile delta clay soil, Egypt. Agricultural Water Management, 246, p.106674.

Feng, G., Zhang, Z., Wan, C., Lu, P. and Bakour, A., 2017. Effects of saline water irrigation on soil salinity and yield of summer maize (Zea mays L.) in subsurface drainage system. Agricultural water management, 193, pp.205-213.

Gates, T. K., Burkhalter, J. P., Labadie, J. W., Valliant, J. C., and Broner, I.: Monitoring and modeling flow and salt transport in a salinity-threatened irrigated valley, J. Irrig. Drain. E., 128, 88– 99, https://doi.org/10.1061/(ASCE)0733-9437(2002)128:2(87), 2002.

Gill BC, Terry AD. ‘Keeping salt on the farm’—Evaluation of an on-farm salinity management system in the Shepparton irrigation region of South-East Australia. Agricultural Water Management. 2016 Jan 31;164:291-303.

https://greyline.com/index.php/products/irrigation/open-channel-flow/stingray-2-0-portable-level-velocity-logger-detail#description.

Hornbuckle JW, Christen EW, Ayars JE, Faulkner RD. Controlled water table management as a strategy for reducing salt loads from subsurface drainage under perennial agriculture in semi-arid Australia. Irrigation and Drainage Systems. 2005 May 1;19(2):145-59.

Jafari-Talukolaee M, Shahnazari A, Ahmadi MZ, Darzi-Naftchali A. Drain discharge and salt load in response to subsurface drain depth and spacing in paddy fields. Journal of Irrigation and Drainage Engineering. 2015 Nov 1;141(11):04015017.

Liu, Y., Ao, C., Zeng, W., Kumar Srivastava, A., Gaiser, T., Wu, J. and Huang, J., 2021. Simulating water and salt transport in subsurface pipe drainage systems with HYDRUS-2D. Journal of Hydrology, 592, p.125823.

Mass, E. V., and Hoffman, G.,J. 1977 ‘’Crop Salt Tolerance-current Assessment .’” Irrigation and Drainage Division 103:115-34

Mass, E. V. 1993” Testing Crops for Salinity Tolerance” Proceedings of workshop on adaption of plants to soil stresses,1-4 August 1993,University of Nebraska ,Lincoln, NE USA :234-47

Morway, E. D. and Gates, T. K.: Regional assessment of soil water salinity across an intensively irrigated river valley, J. Irrig. Drain. E., 138, 5, 393–405, https://doi.org/10.1061/(ASCE)IR.1943-4774.0000411, 2012.

McDonald, M.G. and Harbaugh, A.W., 1988. A modular three-dimensional finite-difference ground-water flow model (Vol. 6, p. A1). Reston, VA: US Geological Survey.

Niswonger, R. & Prudic, D. & Regan, R.. (2006). Documentation of the Unsaturated-Zone Flow (UZF1) Package for modeling unsaturated flow between the land surface and the water table with MODFLOW-2005: U.S. Geological Survey Techniques and Methods 6-A19, Niswonger, Richard G.; Prudic, David E.; Regan, R. Steven.

Okuda, Y., Onishi, J., Shirokova, Y., Kitagawa, I., Kitamura, Y. and Fujimaki, H., 2020. Water and Salt Balance in Agricultural Lands under Leaching with Shallow Subsurface Drainage Used in Combination with Cut-Drains. Water, 12(11), p.3207.

Qian, Y., Zhu, Y., Ye, M., Huang, J. and Wu, J., 2021. Experiment and numerical simulation for designing layout parameters of subsurface drainage pipes in arid agricultural areas. Agricultural Water Management, 243, p.106455.

Rosegrant, M.W., et al. (2002) The Role of Rainfed Agriculture in the Future of Global Food Production. Environment and Production Technology Division, International Food Policy Research Institute. - References - Scientific Research Publishing. (2022).

Rozemeijer, J., van der Velde, Y., McLaren, R., van Geer, F., Broers, H., & Bierkens, M. (2010). Integrated modeling of groundwater-surface water interactions in a tile-drained agricultural field: The importance of directly measured flow route contributions. Water Resources Research, 46(11). https://doi.org/10.1029/2010wr009155.

Skaggs, R.W., and Schilfgaarde, J.V. 1999. Agricultural drainage. Am. Soc. Agron. Madison.

Shrivastava, P., & Kumar, R. (2015). Soil salinity: A serious environmental issue and plant growth promoting bacteria as one of the tools for its alleviation. Saudi journal of biological sciences, 22(2), 123–131. https://doi.org/10.1016/j.sjbs.2014.12.001

Tavakoli-Kivi, S., Bailey, R. T., and Gates, T. K.: A salinity reactive transport and equilibrium chemistry model for regional scale agricultural groundwater systems, J. Hydrol., 572, 274– 293, https://doi.org/10.1016/j.jhydrol.2019.02.040, 2019.

Wei, X., Bailey, R.T. and Tasdighi, A., 2018. Using the SWAT model in intensively managed irrigated watersheds: model modification and application. Journal of Hydrologic Engineering, 23(10), p.04018044.

Yao, R., Yang, J., Wu, D., Xie, W., Wang, X. and Zhang, X., 2017. Scenario Simulation of Field Soil Water and Salt Balances Using SahysMod for Salinity Management in a Coastal Rainfed Farmland. Irrigation and Drainage, 66(5), pp.872-883.

# CHAPTER 4 - QUANTIFYING THE IMPACT OF CLIMATE EXTREMES AND LAND MANAGEMENT PRACTICES ON CROP YIELD AND SALT LOADING WITHIN A TILE DRAINED CATCHMENT

## 4.1 Introduction

Whereas subsurface drainage systems are implemented to remove excess water and salinity from soil profiles and shallow groundwater systems, they also provide quick transport routes of salinity to downstream receiving waters (Christen et al., 2001; Okuda et al., 2020). While salt removal is beneficial for the tiled area, salt loads exported via the tile drains to streams can lead to poor growing conditions downstream, as downstream users divert the saline water for irrigation purposes (Christen et al., 2001; Gill et al., 2015). Regarding this interplay of potential benefits (decreased soil salinity, leading to increase in crop growth) and drawbacks (increased salt export and loading, leading to adverse effects on downstream water quality), the following questions should be addressed regarding salinity transport and management:

1) What is the baseline relationship between system improvements (increase in crop yield) and downstream conditions (change in salinity concentration of receiving waters)? How can this relationship be simulated using spatially distributed flow and transport groundwater models?
2) How is this relationship affected by drain system management, e.g., choice of drainage depth, drainage material conductance?
3) How is this relationship affected by climate extremes, e.g., drought and wet conditions?

Many field (Christen et al., 2001; Hornbuckle et al., 2005; Jafari-Talukolaee et al., 2015; Okuda et al., 2020; El-Ghannam et al., 2021) and modeling studies (Yao et al., 2017; Lu et al., 2019; Qian et al., 2021; Liu et al., 2021) have focused on system improvements for single fields, i.e., affects on soil salinity and crop yield due to tile drain installation configurations, with several of these studies also quantifying salt loading from the tiled field. However, a systematic assessment for a large drained area over a long period (e.g. decadal) has not been undertaken. In addition, climate impacts on tile drain loads have been estimated for nutrients (Dayyani et al., 2012; Wang et al., 2015; Eimers et al., 2020; Golmohammadi et al., 2020; Jiang et al., 2020), but not yet for salinity.

The objective of the study summarized in this chapter is to address these three questions, by quantifying the impact of climate extremes and drain management practices on salt loading and overall salt balance in a semi-arid tile drained catchment that has experienced significant water quality issues in recent decades. To do so, the calibrated and tested MODFLOW and RT3D-Salt models, presented in Chapter 3, are applied to a number of climate scenarios and management strategies over an 11-year period. Results are summarized based on impact on crop yield and downstream water quality, with the latter quantified by salt loading and salt concentration in a receiving stream.

**4.2 Methods**

The modeling system of MODFLOW and RT3D-Salt presented in Chapter 3 is used in this chapter to quantify the impacts of climate extremes and management strategies on salt transport and consequent system variables in the Fairmont Drainage District, Colorado, USA. These impacts include direct model results: water table depth, groundwater discharge to tile drains, groundwater salt loading to tile drains, and soil salinity; and impacts derived from model output: 1) relative yield and 2) the salt concentration of waters receiving tile outflow. Characteristics of the study region will be presented first, followed by an explanation of climate and management scenarios.

**4.3 Quantifying impact of climate extremes and management strategies**

This study uses the calibrated and tested MODFLOW and RT3D-Salt models of the Fairmont Drainage District tile-aquifer-stream system, presented in Chapter 3. The model simulates groundwater flow, groundwater storage, and salt ion transport in a tile-drained irrigated stream-aquifer system. The scenarios investigated in this study for impact on salt loading and crop yield are summarized in Table 4-1. In total, there are 13 scenarios, with the first scenario designated as the Baseline scenario. Each scenario simulation is run for 11 years. The Baseline scenario uses the 2009 weather data, repeated for each year. Scenarios 2-6 investigate the impact of climate extremes; Scenarios 7-10 investigate the impact of drain managements; and Scenarios 11-13 investigate the impact of drain management subject to climate extreme conditions. For Scenarios 2-10, only a single feature is modified from the Baseline values.

**Table 4-1.** Summary of land management and climate scenarios. 2009 weather = 291 mm. Drought year = 97 mm. Wet year = 496 mm.

| Scenario | Description | Weather | Drain Conduct. ($m^2$/day) | Drain Depth (m) |
|---|---|---|---|---|
| **1** | **Baseline** | **2009** | **100** | **1.22** |
| **2** | **Dry 1** | 2 droughts | 100 | 1.22 |
| **3** | **Dry 2** | 4 droughts | 100 | 1.22 |
| **4** | **Wet 1** | 1 year wet | 100 | 1.22 |
| **5** | **Wet 2** | 2 years wet | 100 | 1.22 |
| **6** | **Wet 3** | 3 years wet | 100 | 1.22 |
| **7** | **Cond High** | 2009 | 120 | 1.22 |
| **8** | **Cond Low** | 2009 | 80 | 1.22 |
| **9** | **Deep** | 2009 | 100 | 1.52 |
| **10** | **Shallow** | 2009 | 100 | 0.92 |
| **11** | **Combo 1** | 3 years wet | 120 | 1.52 |
| **12** | **Combo 2** | 4 yrs dry | 80 | 0.92 |
| **13** | **Combo 3** | 2 yrs dry | 120 | 1.52 |

The climate extremes consist of drought, with either 2 droughts or 4 droughts, using the 2003 historical precipitation data (97 mm total) for the drought years; and wet periods, with an annual precipitation of 496 mm, the highest annual rainfall recorded during the 2008-2018 time period (CoAgMet data; CSU Arkansas Valley Research Center; https://coagmet.colostate.edu/). "Cond" refers to the conductance ($m^2$/day) of the material surrounding the perimeter of the drainage pipes, i.e. the interface between the aquifer material and the drain. The values of drainage conductance depends on the characteristics of the drain itself and its immediate environment, and also on the convergent flow path toward the drain (Zaidelman et al., 2009), with large values indicating low resistance to flow (Batelaan et al., 2004). Based on MODFLOW simulation runs (see Chapter 3 for MODFLOW set-up and simulation), a conductance value of 100 $m^2$/day provided the best match between measured and simulated drainage flow. In this study, the baseline value of 100 $m^2$/day is increased and decreased by 20% for each Drain cell (see Figure 3-4C for location of the 744 Drain cells), to provide values of 120 $m^2$/day ("Cond High") and 80 $m^2$/day ("Cond Low"). Higher and lower values were attempted, but convergence issues occurred in the MODFLOW simulation. The impact of the tile drain depth also was quantified, using the "Deep" and "Shallow" scenarios, increasing and decreasing the depth of the drain in each Drain cell by 0.3 m (~ 1 ft), respectively. The final four scenarios (11-13) uses a combination of climate and drain management, for the scenario with the highest potential outflow and salt loading (Scenario 11, with high drainage conductance and deep depth, wet conditions), the lowest potential outflow and salt loading (Scenario 12, with low drainage conductance and shallow depth), and a final scenario that (Scenario 13) that investigates the impact of climate on the high outflow scenario (same as Scenario 11, but changing wet conditions to drought conditions).

Scenario results are contrasted with the Baseline results to determine the impact of each climate and drain management feature. Key indicators of impact are:

- *Groundwater discharge to tile drains* ($m^3$) (total over 11-year simulation period)
- *Percent change in soil salinity and crop relative yield*, with soil electrical conductivity and crop relative yield calculated using the method presented in Chapter 3 (Section 3.2.5, Equation 2).
- *Groundwater salt loading to tile drains* (kg) (total over 11-year simulation period)
- *Salt concentration in receiving waters* (mg/L) due to tile salt loading (average over the final 5 years of the simulation), calculated for each day during the 2014-2018 period. Conditions for both Timpas Creek and the Arkansas River are assessed. Although tile flow and salt loading does not feed directly into the Arkansas River, this assessment is provided to contrast the impact of salt

loading on a tributary (Timpas Creek) and on a large river (Arkansas River). For both receiving waters, the upstream concentration (i.e. before tile inflow) is assumed to be 500 mg/L, and total flow downstream of the tile inflow is equal to the summation of the measured flow in the stream and the tile inflow. For Timpas Creek, daily measured flow is provided by the USGS gage site 07121500 near Swink, Colorado; for the Arkansas River, flow is provided by the USGS gage site 07124000 at Las Animas, Colorado.

In addition, two metrics are used to provide further analysis of climate and drain management impacts. These are:

- **Metric #1**: total tile salt loading (kg) / total tile drainage flow ($m^3$) (i.e. concentration of salt in tile outflow); and
- **Metric #2**: average crop relative yield (-) / average salt concentration in Timpas Creek (mg/L).

Metric #1 provides an overall assessment of salt concentration in water that loads to Timpas Creek, with lower values desired. Metric #2 provides the ratio of positive impact to negative impact, with higher values desired, thereby providing a simple method of ranking the 12 scenarios.

### 4.4 Results and Discussion

Results of the 12 climate and management scenarios are presented in Table 4-2. Results consist of total groundwater fluxes (shown in millions of $m^3$), average water table depth (m) at locations of groundwater monitoring wells, percent change in soil salinity (electrical conductivity) and relative yield, groundwater salt loading to drains (million kg), and average concentration of receiving waters (Timpas Creek, Arkansas River). Results are compared between the scenarios and to the Baseline scenario. The following sections provide details regarding these results.

**Table 4-2.** Summary of climate and management scenarios on groundwater fluxes, groundwater salt ion loads, crop relative yield, and concentration of receiving waters (Timpas Creek, Arkansas River).

| | | | | MODFLOW | | | | | RT3D | | | | |
|---|---|---|---|---|---|---|---|---|---|---|---|---|---|
| | | *m²/day* | *m* | *Million m³* | | | | *m* | | | *Million kg* | *mg/L* | *mg/L* |
| Scenario | Weather | Cond. | Depth | Canal Seep. | Rech. | Tile Flow | ET | WT Depth | % Decr. Soil EC | % Incr. Rel. Yield | Tile Salt Loading | Timp. Creek Salt Conc. | Ark. River Salt Conc. |
| **Baseline** | **2009** | **100** | **1.22** | **417** | **36** | **56** | **57** | **1.88** | **-** | **-** | **1207** | **988** | **719** |
| **Dry 1** | 2 yrs dry | 100 | 1.22 | 417 | 36 | 56 | 57 | 1.88 | 0.1% | 0.5% | 1207 | 987 | 718 |
| **Dry 2** | 4 yrs dry | 100 | 1.22 | 417 | 34 | 56 | 57 | 1.88 | -5.4% | -4.3% | 1197 | 1004 | 728 |
| **Wet 1** | 1 year wet | 100 | 1.22 | 417 | 39 | 56 | 58 | 1.90 | 8.8% | 9.4% | 1196 | 988 | 719 |
| **Wet 2** | 2 years wet | 100 | 1.22 | 417 | 41 | 58 | 58 | 1.88 | 8.8% | 9.4% | 1206 | 1012 | 733 |
| **Wet 3** | 3 years wet | 100 | 1.22 | 417 | 43 | 58 | 59 | 1.88 | 8.8% | 9.4% | 1206 | 1011 | 732 |
| **Cond High** | 2009 | 120 | 1.22 | 417 | 36 | 58 | 57 | 1.92 | -0.1% | -0.1% | 1224 | 973 | 713 |
| **Cond Low** | 2009 | 80 | 1.22 | 417 | 36 | 53 | 58 | 1.84 | 0.2% | 0.3% | 1170 | 1002 | 725 |
| **Deep** | 2009 | 100 | 1.52 | 418 | 36 | 66 | 56 | 2.08 | -1.0% | -1.7% | 1293 | 1001 | 729 |
| **Shallow** | 2009 | 100 | 0.92 | 417 | 37 | 44 | 60 | 1.71 | 0.4% | 1.1% | 1070 | 1028 | 737 |
| **Combo 1** | 3 years wet | 120 | 1.52 | 418 | 42 | 69 | 57 | 2.11 | 7.6% | 7.5% | 1314 | 1019 | 741 |
| **Combo 2** | 4 yrs dry | 80 | 0.92 | 417 | 35 | 40 | 61 | 1.68 | -5.7% | -3.3% | 982 | 1057 | 750 |
| **Combo 3** | 2 yrs dry | 120 | 1.52 | 418 | 35 | 67 | 56 | 2.12 | -0.9% | -1.2% | 1305 | 997 | 728 |

WT Depth = average water table depth at locations of groundwater monitoring wells

Timp. Creek Salt Conc. = average temporal concentration downstream of tile drain loading, assuming upstream conc. = 500 mg/L

Ark. River Salt Conc. = average temporal concentration downstream of tile drain loading, assuming upstream conc. = 500 mg/L

## 4.5 Groundwater discharge and salt loading to tile drains

*Groundwater discharge to tile drains*

Figure 4-1 shows the daily groundwater discharge rates ($m^3$/day) for (A) climate scenarios, (B) drain management scenarios, and (C) climate-drain management combinations. Daily discharge rates are a sum for all 744 Drain cells in the MODFLOW model. The temporal summation of groundwater discharge for scenario is shown in Table 2, in the column “Tile Flow”, with units of million $m^3$. From Table 2, we see that the scenarios with the highest drainage flow rates are “Deep”, “Combo 1”, and “Combo 3”, with 66 million $m^3$, 69, and 67, respectively, increases of 18%, 22%, and 18%. As the common feature of these three scenarios is the depth of 1.52 m, we conclude that drainage depth has a strong effect on drainage outflow. This is also seen in the time series charts of Figure 4-1. Whereas the climate scenarios (Figure 4-1A) and conductance scenarios (Figure 4-1B) show a minimal impact on drainage outflow, the depth scenarios (Figure 4-1B) show a large difference from the Baseline scenario. In Figure 4-1C, the large difference in

Combos 1 and 3 are due to installing the drains at a deeper depth, with the only difference in Combo 1 a jump in the summer of 2012 due to wet conditions. The "Deep" scenario is also shown in Figure 4-1C, to show that implementing this feature alone provides most of the difference from the Baseline scenario. This result is also seen in Figure 4-2. From the "Deep" scenario to the "Combo 1" scenario, with the latter including high drainage conductance and wet conditions, the increase is only 4% (3 million $m^3$). Even with drought conditions (Combo 3), the deep depth of the drains causes a high drainage outflow of 67 million $m^3$, again indicating the minimal impact of climate compared to drain depth. In conclusion, drainage depth has a much stronger impact on drainage outflow than extreme climate conditions or drainage conductance.

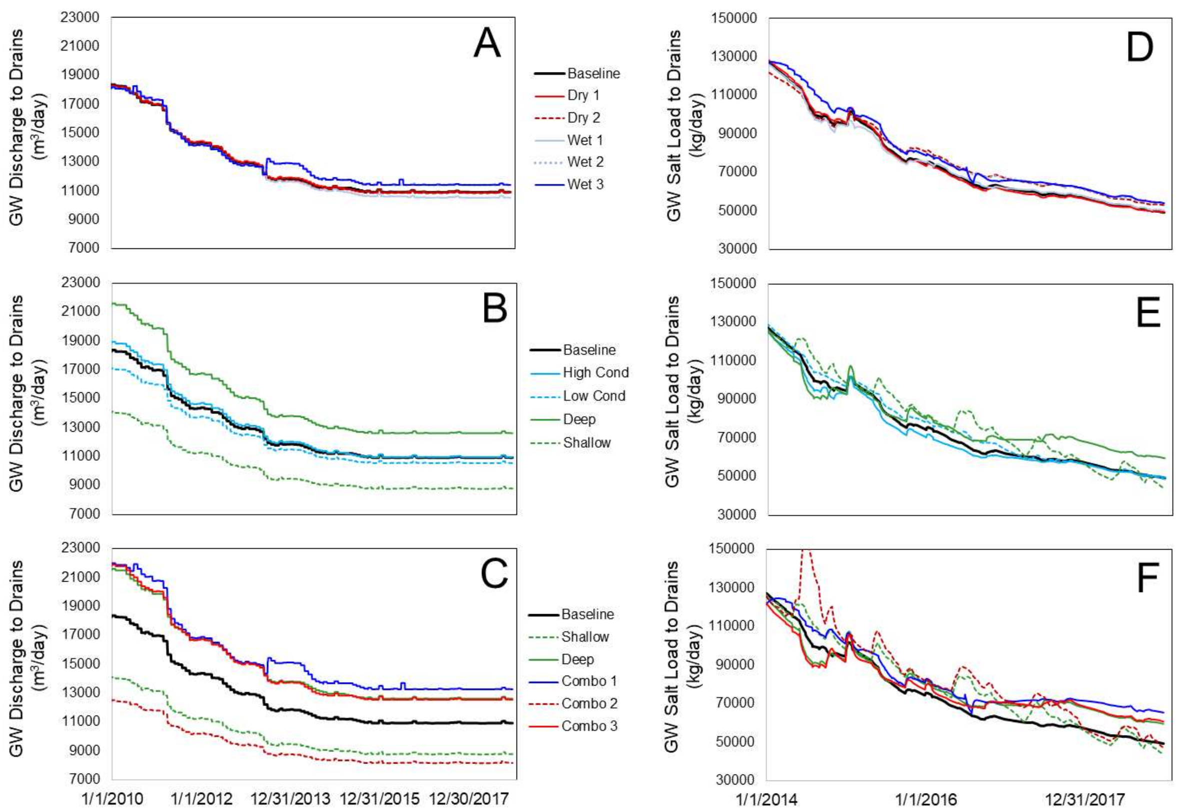


**Figure 4-1.** Daily groundwater discharge ($m^3$) and salt loads (kg) to drains, for the 2010-2018 period (discharge) and the 2014-2018 period (loads). (A) and (D) show results of the climate scenarios, (B) and (E) show the results of the management scenarios, and (C) and (F) show results of the combination scenarios and the depth scenarios.

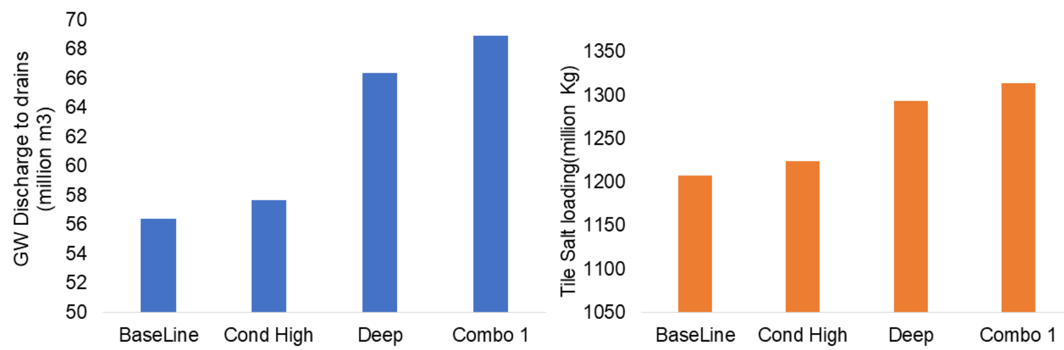


**Figure 4-2.** Groundwater discharge (left) and salt loading (right) results for the Baseline, High Conductance, Deep, and Combo 1 scenarios.

*Groundwater salt loading to tile drains*

Groundwater salt loading simulated by the scenarios is summarized in Table 2 (total loadings, column "Tile Salt Loading") and the daily time series charts of Figure 4-1 (D, E, F). Similar to groundwater discharge, although to a lesser degree, the depth scenarios have a stronger impact on salt loading to the tile drains than the climate scenarios or the drainage conductance scenarios. Whereas climate scenarios change salt loading by 0-1% from the Baseline and conductance scenarios change loading by 1-3%, depth scenarios change the loading by 7-11%. Again similar to the flow results, the results of the combination scenarios (Scenarios 11-13, Figure 4-1F) are influenced mainly by the depth to the drains, with the same temporal patterns shown in the depth scenarios in Figure 4-1E. Figure 4-2 shows the tile salt loading (million kg) listed in Table 4-1, with the "Deep" scenario yielding an increase in loading of 7% from the Baseline, and the "Combo 1" scenario yielding an increase of 9%, indicating that including wet conditions and high drainage conductance only provides slightly more loading than if a deeper drainage depth is the only feature change in the drainage system. The "Combo 2" scenario, with is designed to provide the least amount of groundwater salt loading to the tile drains, yields 982 million kg over the 11-year period, a decrease of 19% from the Baseline. This decrease is due mainly to the shallow depth (0.92 m) of the drains, as implementing the shallow depth solely ("Shallow" scenario) yields a decrease of 11% from the Baseline. It is interesting to note that results are not additive: Combo 2 results in a decrease of 225 million kg (19% decrease) from the Baseline, but the individual features of this combination (4 years drought, low conductance, shallow depth) results in decreases of 10, 37, and 137, which provides a sum of only 184 million kg. Therefore, implementing these three distinct features yields interactive effects.

### 4.6 System effects: relative yield, concentration of receiving waters

*Impact on Soil Salinity and Relative Yield*

Model results are analyzed for soil salinity, with electrical conductivity of saturated soil, $EC_{sat}$, computed using the summation of salt ion concentration in the soil water and then, and crop relative yield, which uses $EC_{sat}$ in crop-specific linear relationships (see Chapter 3). As expected, wet conditions in Scenarios "Wet 1", "Wet 2", "Wet 3", and "Combo 1" yield a decrease in $EC_{sat}$ (8.8%, 7.6% in the "% Decr. Soil EC" column in Table 4-1). Conversely, dry conditions in Scenarios "Dry 2" and "Combo 2" yield an increase (5.4%, 5.7%) in $EC_{sat}$. These results are shown spatially in the maps of Figure 4-3, which show the cell-by-cell values for the Baseline scenario, and then cell-by-cell differences in $EC_{sat}$ for selected scenarios. In these maps, red colors indicate a decrease in soil salinity, and blue colors indicate an increase in soil salinity, from the Baseline scenario. For the "Wet 3" and "Combo 1" scenarios, the decrease in soil salinity occurs throughout the study region. For the "Deep" and "Shallow" drainage depth scenarios, the effects on soil salinity occur principally near the drains. The "Deep" scenario results in a slight increase in soil salinity (1%; Table 4-1), whereas the "Shallow" scenario results in a slight decrease (0.4%). Although the "Deep" scenario loads more salt to the tile drains (1,293 million kg vs. 1,207 million kg in the Baseline scenario), the high amount of groundwater discharge to the drains (66 vs. 56 million m$^3$) leaves a lower water content in the soil, resulting in higher salt ion concentrations.

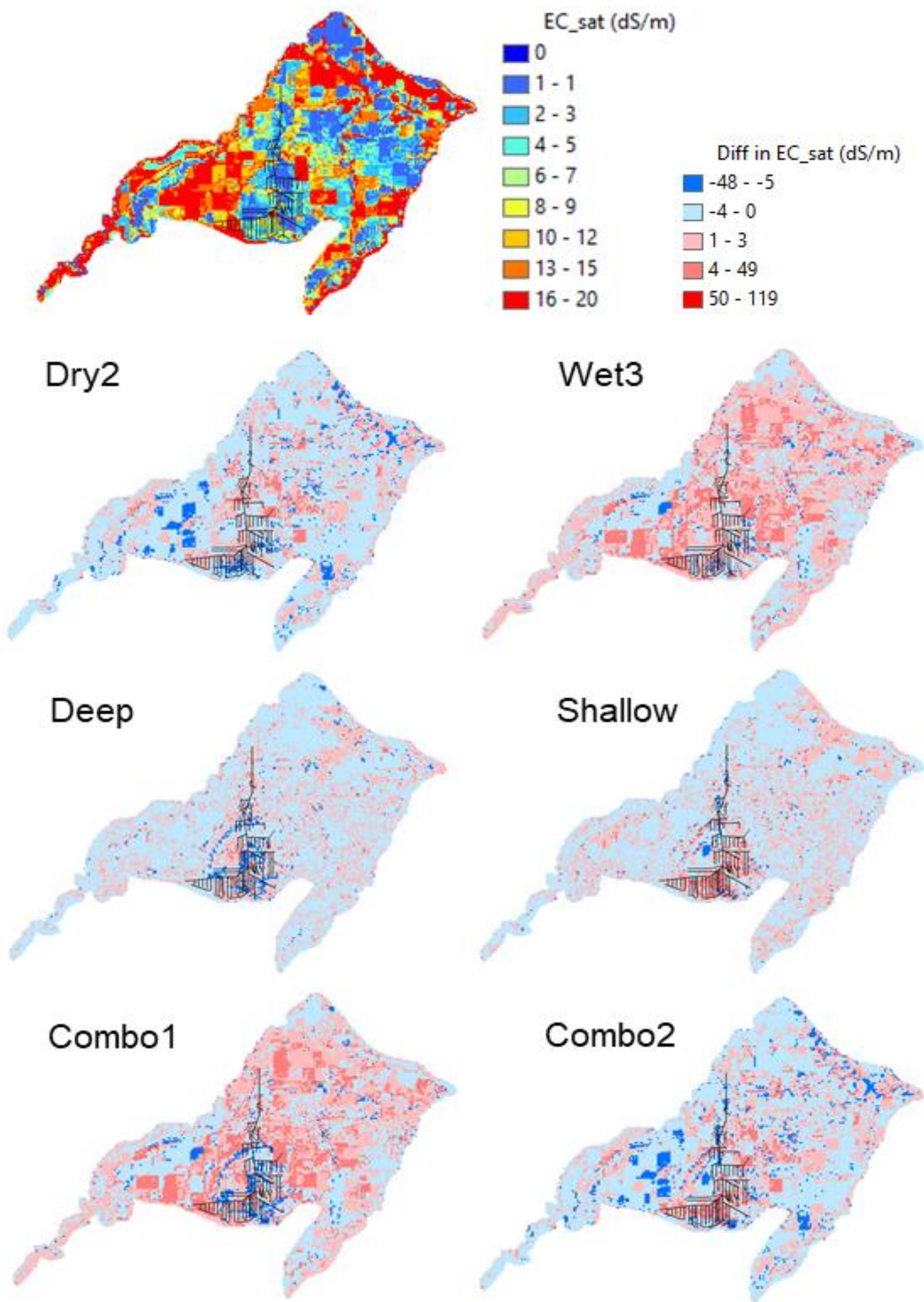


**Figure 4-3.** (Top map) Estimated soil EC from the Baseline simulation (layer 1), and (Bottom maps) the difference in soil EC between the Baseline scenario and other scenarios.

The change in soil salinity results in changes in crop relative yield (see "% Incr. Rel. Yield" column in Table 4-1). The decrease in soil salinity in the wet condition scenarios results in an increase in relative yield: 9.4% for the "Wet" scenarios and 7.5% for the "Combo 1" scenario, with the latter value lower due to the deep (1.52 m) installation of the tile drains. The increase in soil salinity in the dry condition scenarios results in a decrease in relative yield: 4.3% for the "Dry 2" scenario, and 3.3% for the "Combo 2" scenario, which assumed four years of drought during the 11-year period. In general, and conversely to tile outflow volumes, the drainage management schemes (drainage conductance, drainage depth) to not have a strong impact on soil salinity and crop yield, whereas climate conditions have a strong influence. This is due to climate conditions having an immediate impact on near-surface moisture conditions and associated leaching events in the root zone and soil profile.

*Impact on Water Quality of Receiving Waters*

Removing salt from the soil profile and aquifer is an important step in improving soil and crop growth conditions. However, the salt removed is eventually loaded to downstream receiving waters, which can have adverse effects on ecosystem health, irrigation practices, and wildlife. Table 4-1 lists the estimated average concentrations (mg/L) during the 2014-2018 in both Timpas Creek (column "Timp. Creek Salt Conc.") and the Arkansas River (column "Ark. River Salt Conc."), downstream of the tile inflow site. These results are shown in the bar charts of Figure 4-4 for visualization.

Of note is the decrease in concentration of Timpas Creek in the "Cond High" scenario (988 mg/L to 973 mg/L, decrease of 1.5%) as compared to the Baseline scenario, even though this scenario has higher tile salt loading (1,224 million kg) than the Baseline scenario (1,207 million kg). The reason for this is the increased tile drainage outflow (58 million $m^3$) as compared to the Baseline (56 million $m^3$), which acts to dilute the salt mass to a lower concentration. The same effect occurs for other scenarios. For "Combo 1", for example, the tile salt loading is 9% higher than in the Baseline, but the Timpas Creek salt concentration only increases by 3%, owing to the large increase in tile drain outflow (69 vs. 56).

Conversely, the highest increase in Timpas Creek concentration is the "Combo 2" scenario (see Figure 4-4): the tile salt loading is lower than in the Baseline by 19%, the lowest of all scenarios, but due to the low tile drainage outflow (40 compared to 56), the concentration is higher in the receiving waters. The same patterns occur for the Arkansas River (Table 4-1, Figure 4-4), although changes in concentration are dampened due to the larger measured flow in the river as compared to Timpas Creek (see Figure 3-13 in Chapter 3 for a time series chart of flow rates in Timpas Creek and the Arkansas River).

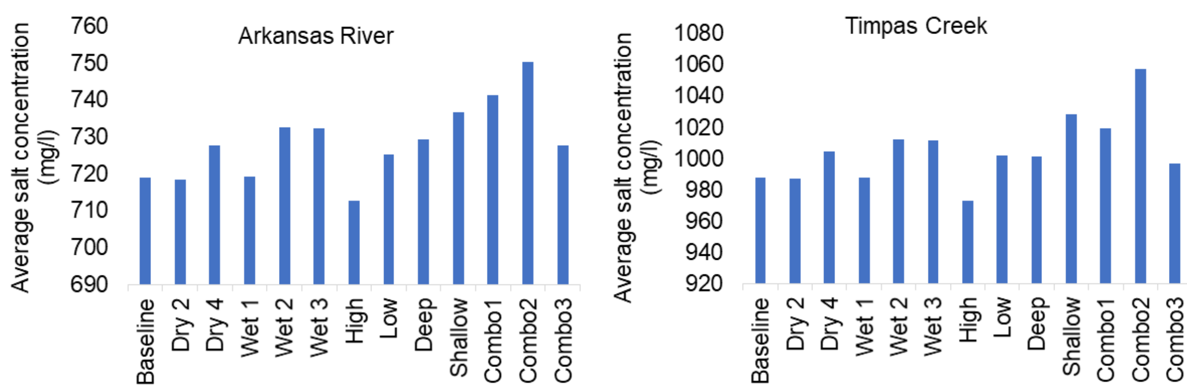


**Figure 4-4.** Temporal average (2014-2018) concentration in Timpas Creek and Arkansas River, downstream of the tile salt loading site, assuming an upstream concentration of 500 mg/L.

More detailed temporal results are provided in Figure 4-5, which shows time series charts of simulated daily downstream concentration (mg/L) in Timpas Creek for the depth scenarios, "Combo 1", and "Combo 2" (Figure 4-5A). Again, "Combo 1" yields the highest salt loading to Timpas Creek, whereas "Combo 2" yields the lowest salt loading (see Table 4-1, column "Tile Salt Loading"). Figure 4-5B shows the difference in downstream concentration between each of the two combination scenarios and the Baseline scenario, showing the much higher concentrations in the "Combo 2" scenario, despite significantly lower overall tile salt loading. The time series chart in Figure 4-5B demonstrates that there is much temporal variability in these results: whereas "Combo 2" has higher concentrations during the 2014-2016 period, the "Combo 3" scenario has higher concentrations during 2018. This is due to the first few years being governed by wet conditions (years of annual rainfall = 496 mm), from which we conclude that weather conditions play an important role in year-to-year tile drain outflow volumes and dilution of salt mass in the tile drain water.

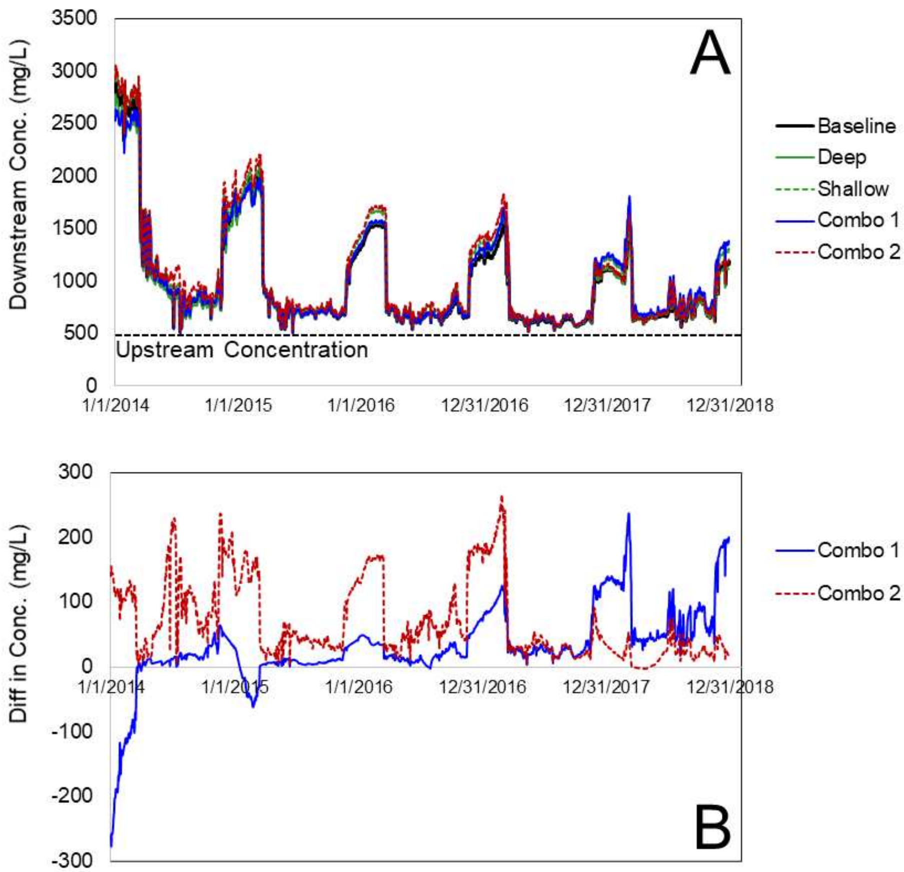


**Figure 4-5.** (A) Estimated salt concentration in Timpas Creek, downstream of the tile loading site, assuming a constant upstream concentration of 500 mg/L, for the Baseline scenario, the depth scenarios, and two combination scenarios; (B) the difference in downstream concentration between the two combination scenarios and the Baseline scenario.

*Downstream salinity: which scenarios are most favorable?*

A key discussion point is the impact of salt loading to receiving waters. Although salt loadings are higher in the scenarios of higher drainage outflow (e.g. high drainage conductance, deep drainage depth, wet conditions), concentrations are relatively low due to high outflow volumes. The degree of severity of these loadings and concentrations is based on 1) intended use of downstream water and 2) existing fish populations and diversity. Typically, the influence of salinity on crop yield is based on the quality of irrigation water, in terms of Total Dissolved Solids (TDS) concentration (mg/L). Similarly, the influence of salinity on fish egg fertilization, larval growth, and body metabolism also depends on salinity concentration in the river water (Boefu and Payan, 2001; Evans and Kültz, 2020). Therefore, although certain scenarios yield the most salt mass to downstream areas, the water has a resultant lower salinity concentration than scenarios with less salt loading, and therefore the high-yield scenarios may in fact be more desirable and provide a dual benefit: decrease soil salinity and increase in crop yield in the tile drained area, and provide a lower downstream river concentration. These results are in contrast to previous tile drain salinity studies, which treat salt export as an automatic negative aspect of the system (Christen et al., 2001; Gill et al., 2015; Okuda et al., 2020). These results assume, of course, that tile drain loading is a mainstay in the watershed system (i.e. removal of tile drains is not an option), and management decisions are therefore focused on best practices for the existing tile drain network. The interplay between within-system benefits (crop yield) and downstream effects (concentration of receiving waters) is explored in more detail in the following section.

### 4.7 Summary of climate and management impacts: assessment of metrics

Results for Metric #1 are presented in Figure 4-6A. The “Deep” and “Combo 1”, and “Combo 3” scenarios, although having the highest tile salt loading, have the lowest values of Metric #1 (red circles in Figure 4-6A) due to the dilution effect of the high drainage outflow rates. In fact, “Combo 3” was included in the list of scenarios due to these results for “Combo 1”. The low tile drainwater concentration could be due to the wet periods included in the “Combo 1” scenario, and therefore the “Combo 3” scenario was included with a drought period, to determine which system features were controlling the results of “Combo 1”. From a comparison between the results of “Combo 1” (Metric #1 = 19.1 $kg/m^3$) and “Combo 3” (Metric #1 = 19.5 $kg/m^3$), as compared to the Baseline scenario (Metric #1 = 21.4 $kg/m^3$), we conclude that results are due mainly to the deep depth (1.52 m) of the drains. Conversely, the highest (i.e.

worst) values of Metric #1 are for the two scenarios with the lowest tile salt loadings, “Shallow” and “Combo 2” (black circles in Figure 4-6A), due to the low drainage outflow volumes. These results point to the strong effect of drainage depth on flow and loadings, and on the dilution effect of high drainage outflow volumes.

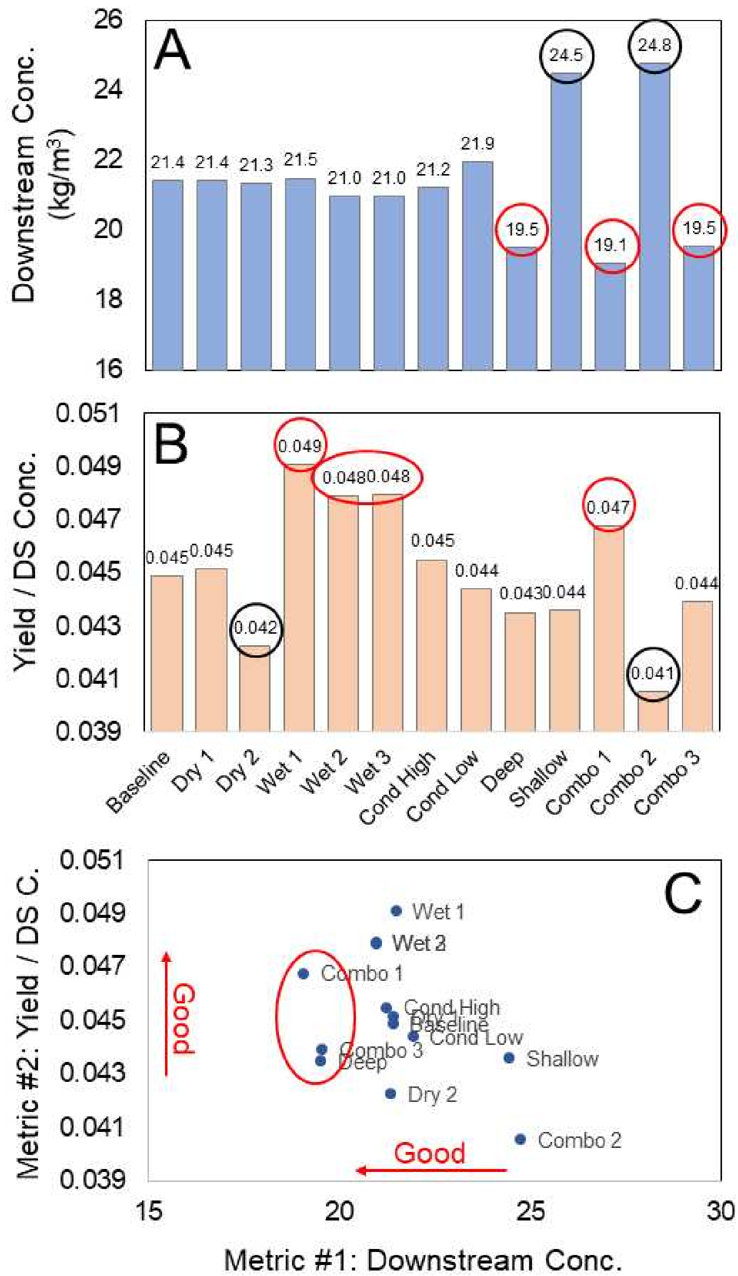


**Figure 4-6.** (A) results of Metric #1, tile salt loading (million kg) divided by tile flow (million m$^3$); (B) results of Metric #2, relative yield / downstream concentration of Timpas Creek; (B) Metric #1 plotted vs. Metric #2, to identify scenarios with most beneficial system effects.

Results of Metric #2, which is the ratio between relative yield and Timpas Creek downstream concentration, are shown in Figure 4-6B. The wet condition scenarios (Wet 1, Wet 2, Wet 3, Combo 1) have the highest values (red circles: 0.049, 0.048, 0.048, 0.047) due to increase soil moisture and leaching due to higher rainfall rates and slight impact on Timpas Creek downstream concentration (see Table 4-1). The "Combo 1" scenario produces an increase in Timpas Creek concentration by 3%, but this is balance by the 7.5% in crop relative yield. However, if dry conditions occur for a deep drainage depth ("Combo 3"), the metric is only 0.044, due to the decrease in relative yield (1.2%, Table 4-1) as a result of less soil moisture and soil leaching. The lowest values (0.042, 0.041, black circles in Figure 4-6B) are for scenarios with drought conditions, again due to less soil moisture and soil leaching, leading to increases in soil salinity and decreased in crop yield. In general, high values for Metric #2 are obtained only if wet conditions occur during the 11-year period, with drainage practices (drainage depth, drainage conductance) not having an influence.

Between Metric #1 and Metric #2, results indicate that 1) drainage practices, particularly drainage depth, play a key role in controlling salinity concentration of tile drain outflow water, whereas 2) climate is the deciding factor in whether soil salinity and crop yield improve. When plotted against each other (Figure 4-6C), we conclude once again that a deep drainage depth (1.52 m, compared to the Baseline depth of 1.22 m), which is the common feature amongst the circled scenarios ("Deep", "Combo 1", "Combo 3"), is a system feature that produces desirable outcomes for both within-system conditions (soil salinity, crop yield) and downstream conditions (salinity concentration in tile drain outflow water).

### 4.8 Study limitations

Limitations of the modeling approach are detailed and discussed in Section 3.3.4 (see Chapter 3). In addition to these, we note that the results presented in this chapter are based on an 11-year simulation. Different results might occur if the modeling tool is run for longer (multi-decadal) periods.

### 4.9 Summary and Conclusions

This chapter presents the use of the calibrated and tested MODFLOW/RT3D-Salt modeling system (see Chapter 3) to quantify the impact of climate extremes (drought, wet conditions) and drainage management features (drainage depth, drain material conductance) on within-system conditions (soil salinity, crop yield) and water quality of receiving waters, with the aim of identifying viable drainage management strategies for salinity in tile-drained landscapes. The model is applied to the stream-aquifer system that contains the tile drain network of the Fairmont Drainage District, near Swink, Colorado, within the Lower Arkansas River Valley. A total of 13 scenarios were considered, with the first representing a Baseline condition. Model outputs analyzed include soil salinity (used to estimate changes in relative crop yield), total tile drainage outflow volumes, total tile salt loadings, and the salinity concentration in downstream receiving waters (Timpas Creek, Arkansas River). The major findings of this study include:

1. Drainage depth has a much stronger impact on drainage outflow volumes and salt loading mass than extreme climate conditions or drain material conductance.
2. Climate conditions (drought, wet conditions) have a much stronger impact on soil salinity and crop yield than drainage management schemes (drainage depth, drain material conductance). Therefore, future climate extremes likely will play a larger role in the viability of tile drain systems than will the specific characteristics (e.g., depth) of the tile drain network.
3. Scenarios with high drainage outflow volumes and salt loading mass (e.g. deep drains, deep drains + wet conditions) result in lower downstream salinity concentrations than scenarios with low outflow volumes and salt loading mass, due to the dilution effect of higher water volumes on salt mass in the tile drainage water. Therefore, if new tile drain networks are being installed, we recommend using a deep drainage scheme (1.52 m) as opposed to the regular depth of 1.22 m, to minimize the effect on downstream salinity concentration.

Finding #3 has important implications for salinity management in tile drained areas: high salt export from tile drained landscapes typically is seen as a negative aspect of the system. However, if accompanied by high drainage outflows, such as with the scenario of deep drains, the overall impact can be beneficial for the system (lower water tables → decreased soil salinity → increased crop yield) without causing harm to downstream areas in terms of salinity concentration and its effects on downstream irrigation and fish populations, as compared to scenarios of low drainage outflow. Results of this study can be used in other tile drained landscapes to guide tile network design. Methods used herein can be adopted for other tile drain studies that use numerical models as experimental tools.

REFERENCES


Batelaan, O. and De Smedt, F., 2004. SEEPAGE, a new MODFLOW DRAIN package. *Groundwater*, *42*(4), pp.576-588.

Bœuf, G. and Payan, P., 2001. How should salinity influence fish growth?. Comparative Biochemistry and Physiology Part C: Toxicology & Pharmacology, 130(4), pp.411-423.

Christen EW, Ayars JE, Hornbuckle JW. Subsurface drainage design and management in irrigated areas of Australia. Irrigation Science. 2001 Dec 1;21(1):35-43.

Dayyani, S., Prasher, S.O., Madani, A. and Madramootoo, C.A., 2012. Impact of climate change on the hydrology and nitrogen pollution in a tile-drained agricultural watershed in eastern Canada. Transactions of the ASABE, 55(2), pp.389-401.

Eimers, M.C., Liu, F. and Bontje, J., 2020. Land use, land cover, and climate change in southern Ontario: implications for nutrient delivery to the lower Great Lakes. In Contaminants of the Great Lakes (pp. 235-249). Springer, Cham.

El-Ghannam, M., Aiad, M. and Abdallah, A., 2021. Irrigation efficiency, drain outflow and yield responses to drain depth in the Nile delta clay soil, Egypt. Agricultural Water Management, 246, p.106674.

Evans, T.G. and Kültz, D., 2020. The cellular stress response in fish exposed to salinity fluctuations. Journal of Experimental Zoology Part A: Ecological and Integrative Physiology, 333(6), pp.421-435.

Golmohammadi, G., Rudra, R.P., Parkin, G.W., Kulasekera, P.B., Macrae, M. and Goel, P.K., 2020. Assessment of impacts of climate change on tile discharge and nitrogen yield using the DRAINMOD model. Hydrology, 8(1), p.1.

Hornbuckle JW, Christen EW, Ayars JE, Faulkner RD. Controlled water table management as a strategy for reducing salt loads from subsurface drainage under perennial agriculture in semi-arid Australia. Irrigation and Drainage Systems. 2005 May 1;19(2):145-59.

Gill BC, Terry AD. 'Keeping salt on the farm'—Evaluation of an on-farm salinity management system in the Shepparton irrigation region of South-East Australia. Agricultural Water Management. 2016 Jan 31;164:291-303.

Jafari-Talukolaee M, Shahnazari A, Ahmadi MZ, Darzi-Naftchali A. Drain discharge and salt load in response to subsurface drain depth and spacing in paddy fields. Journal of Irrigation and Drainage Engineering. 2015 Nov 1;141(11):04015017.

Jiang, Q., Qi, Z., Xue, L., Bukovsky, M., Madramootoo, C.A. and Smith, W., 2020. Assessing climate change impacts on greenhouse gas emissions, N losses in drainage and crop production in a subsurface drained field. Science of The Total Environment, 705, p.135969.

Liu, Y., Ao, C., Zeng, W., Kumar Srivastava, A., Gaiser, T., Wu, J. and Huang, J., 2021. Simulating water and salt transport in subsurface pipe drainage systems with HYDRUS-2D. Journal of Hydrology, 592, p.125823.

Lu et al., 2019

Okuda, Y., Onishi, J., Shirokova, Y., Kitagawa, I., Kitamura, Y. and Fujimaki, H., 2020. Water and Salt Balance in Agricultural Lands under Leaching with Shallow Subsurface Drainage Used in Combination with Cut-Drains. Water, 12(11), p.3207.

Qian, Y., Zhu, Y., Ye, M., Huang, J. and Wu, J., 2021. Experiment and numerical simulation for designing layout parameters of subsurface drainage pipes in arid agricultural areas. Agricultural Water Management, 243, p.106455.

Wang, Z., Qi, Z., Xue, L., Bukovsky, M. and Helmers, M.J., 2015. Modeling the impacts of climate change on nitrogen losses and crop yield in a subsurface drained field. Climatic Change, 129(1), pp.323-335.

Yao, R., Yang, J., Wu, D., Xie, W., Wang, X. and Zhang, X., 2017. Scenario Simulation of Field Soil Water and Salt Balances Using SahysMod for Salinity Management in a Coastal Rainfed Farmland. Irrigation and Drainage, 66(5), pp.872-883.

Zaidel’man, F.R., 2009. Degradation of soils as a result of human-induced transformation of their water regime and soil-protective practice. *Eurasian Soil Science*, *42*(1), pp.82-92.

# CHAPTER 5 – SUMMARY AND CONCLUSIONS

## 5.1 Summary and major findings

The overall objective of this dissertation is to understand the impact of subsurface drainage systems on salt movement and loading in an irrigated, drained stream-aquifer system. This objective is accomplished by a suite of numerical modeling experiments applied to the stream-aquifer system that encompasses the Fairmont Drainage District (FDD; 385-ha) tile drain network within the Lower Arkansas River Valley, Colorado, USA. The numerical models used in this dissertation simulate the reactive transport of major salt ions ($SO_4$, Ca, Na, Cl, Mg, K, $CO_3$, and $HCO_3$) in soils, groundwater, tile drain water, and streams.

This dissertation first presents the use of the SWAT-Salt model, a new version of the SWAT model that includes a salinity reactive transport module and modified in this study to include salt ion transport in tile drain water, applied it to a 732 $km^2$ salinity-impaired irrigated region within the Lower Arkansas River Valley. The tool, once tested against tile drain salt ion concentrations in the FDD, is used to assess the impact of region-wide implementation of subsurface tile drainage on in-stream salt ion concentrations, in-stream salt ion loading, and total salt export from the watershed. The model can be a useful tool in simulating salinity transport in tile drained watershed and investigating the effect of salinity management practices at a variety of spatial and temporal scales. Major findings from this first study include:

1. Implementing region-wide tile drainage increases total salt yield from the watershed by only 1% during a long simulation period (2000-2018). The increase in salt loaded from the landscape to stream via tile drains is balanced by the decrease in groundwater loading, as the salt mass that would be transported in the aquifer is instead intercepted by the tile drains.

2. Even with tile drains installed in every cultivated field in the region, groundwater discharge is still the dominant pathway for salt to load to streams, with annual salt fluxes of 1,280 kg ha-1 and 360 kg ha-1 for groundwater and tile drains, respectively (see Figure 2-7B).
3. Although the long-term watershed salt yield is approximately the same under tile drained conditions, the timing of salt loading to streams changes to higher daily pulse loadings as opposed to long-term diffuse loading from groundwater (see Figure 2-8). These higher daily loadings result in high in-stream concentrations (see Figure 2-9D,E,F), which can lead to negative impacts on crop growth and overall soil health in downstream irrigated areas.
4. Groundwater salt ion concentrations can be decreased significantly in tile drained areas (see Figures 2-10 and 2-11), resulting in improved crop yield for areas that pump groundwater for irrigation. See Figure 2-2B for the locations of pumping wells in the study region.

However, for more accurate interactions between tile drains and groundwater, other models that include physically based groundwater flow and transport modeling were employed in the second part of the dissertation. The modeling system consists of the groundwater flow model MODFLOW and the groundwater reactive transport model RT3D-Salt, modified in this study to include salt ion mass exchange between the aquifer and the tile drains, at grid cells designated as drainage cells. Specific for this model, the modeling system simulates groundwater head, groundwater-tile drain inflows, soil salt ion concentration, groundwater salt ion concentrations, and salt ion loading to tile drains. The model is applied to the FDD. The model results are tested against measured groundwater levels, groundwater salt ion concentrations, and estimated tile outflow and tile salt ion loading. Spatial results (cell-by-cell groundwater-tile flows and salt ion loads) also are analyzed. The model is then used to quantify the effect of tile drains on relative crop yield and salt loading in Timpas Creek and the Arkansas River, which receive outflow from the tile drain network. Major findings from this second study include:

1. The model tracks groundwater levels and tile drain outflow well; however, groundwater levels were available for 2015-2018 whereas tile drain outflow rates were available only for 3 months during the 2018 growing season, due to equipment failure. Additional tile drain outflow rate measurements are needed to perform a thorough audit of the MODFLOW model.
2. For most salt ions, the model estimates the correct magnitude of tile drain salt loading during the 2018 growing season. However, this came at a cost of over-estimating groundwater salt ion concentrations. Like the flow results, additional sampling of tile drain effluent is needed to further test the RT3D-Salt model. More monitoring wells should be installed to clarify spatial variation and magnitude of groundwater salt ion concentrations.
3. Including tile drainage in this area only slightly improved soil salinity and crop yield conditions; however, export loading from the drains has a strong negative impact on the water quality of receiving waters. Timpas Creek, a tributary to the Arkansas River, experiences an overall increase of approximately 200 mg/L in the areas immediately downstream of the tile drain outflow point. If the tile drains loaded to the Arkansas River, the downstream concentration increase would be approximately 85 mg/L. These increases can have detrimental impacts on downstream crop yield, if river water is diverted and used as irrigation water, and ecosystem health.

In general, this study adds to the literature on balancing the positive and negative aspects of tile drainage in regards to salinity. Tile drains remove excess groundwater and salinity, leading to improved soil conditions and crop yield, but at a price, as the removed salinity is passed on to downstream stakeholders. However, as is shown in the findings of the third study, these negative aspects can be tempered in areas that will continue with tile drainage into future decades. In general, the modeling system (MODFLOW/RT3D-Salt) introduced in this study can be used to assist in salinity management schemes in saline-affected regions, to balance crop yield sustainability and downstream water quality needs.

Lastly, this dissertation used the calibrated and tested MODFLOW/RT3D-Salt modeling system from the second study to quantify the impacts of climate extremes and management strategies on salt transport and consequent system variables in the FDD. These impacts include direct model results: water table depth, groundwater discharge to tile drains, groundwater salt loading to tile drains, and soil salinity; and impacts derived from model output: 1) relative yield and 2) the salt concentration of waters receiving tile outflow. Climate extremes include periodic drought and periodic wet conditions; drainage management features include drainage depth (shallow, deep) and drain material conductance (high, low). Combined climate-management scenarios also are run. Major findings of this third study are:

1. Drainage depth has a much stronger impact on drainage outflow volumes and salt loading mass than extreme climate conditions or drain material conductance.
2. Climate conditions (drought, wet conditions) have a much stronger impact on soil salinity and crop yield than drainage management schemes (drainage depth, drain material conductance). Therefore, future climate extremes likely will play a larger role in the viability of tile drain systems than will the specific characteristics (e.g., depth) of the tile drain network.
3. Scenarios with high drainage outflow volumes and salt loading mass (e.g. deep drains, deep drains + wet conditions) result in lower downstream salinity concentrations than scenarios with low outflow volumes and salt loading mass, due to the dilution effect of higher water volumes on salt mass in the tile drainage water. Therefore, if new tile drain networks are being installed, we recommend using a deep drainage scheme (1.52 m) as opposed to the regular depth of 1.22 m, to minimize the effect on downstream salinity concentration.

High salt export from tile drained landscapes typically is seen as a negative aspect of the system. However, if accompanied by high drainage outflows, such as with the scenario of deep drains, the overall impact can be beneficial for the system (lower water tables → decreased soil salinity → increased crop yield) without causing harm to downstream areas in terms of salinity concentration and its effects on downstream irrigation and fish populations, as compared to scenarios of low drainage outflow. These results of course assume that existing tile drain systems will remain in place, and that the aim is to minimize impact on downstream water quality. Results of this study can be used in other tile drained landscapes to guide tile network design. Methods used herein can be adopted for other tile drain studies that use numerical models as experimental tools.

**5.2 Filling method gaps and future research**

Study results can be improved if the following procedures are followed:

- For Study #1 (Chapter 2), SWAT-Salt should be linked with a physically based spatially distributed groundwater model for groundwater flow and salt transport. This will provide more accurate results for water table elevation and groundwater salt ion concentrations, in addition to a physically based procedure for simulating groundwater and salt ion loading from the aquifer to the drainage pipes.
- For all studies, a more accurate soil map of salt mineral fractions ($CaSO_4$, $MgSO_4$, $MgCO_3$, $CaCO_3$, $NaCl$) will be helpful to initialize model factors.
- For Studies #2 and #3: implement a tile drain transport algorithm into MODFLOW/RT3D-Salt. As implemented, these models only simulate the exchange of groundwater and salt ion mass from the aquifer to the tile drains, with the assumption that all water and salt mass leave the tile drain system on the same day (i.e in the comparison between model results and field-measured tile drain outflow rates and salt loadings).
- Conduct a more thorough survey of soil water salt ion concentration and groundwater salt ion concentration within the immediate vicinity of tile drains. This will provide more thorough model testing, and provide insights into the transport of salt from the soil profile, to groundwater, to tile drain water.

- Perform additional drain management scenarios for drain spacing. As we studied an existing tile drain network (FDD), this feature was not included in scenario analysis.
- Implement a socio-economic feature to the modeling system, that accounts for farmer crop type decisions within the context of a saline soil environment. The model could predict farmer's planting decisions based on climate conditions and soil salinity conditions.